Electronic Supplementary Material (ESI) for RSC Advances.

Design, synthesis and biological evaluation of benzo [*d*]imidazo [2,1-*b*] thiazole and imidazo [2,1-*b*]thiazole carboxamide triazole derivatives as anti-mycobacterial agents

Surendar Chitti[a], Kevin Van Calster[b], Davie Cappoen[b1], Adinarayana Nandikolla[a], Yogesh Mahadu Khetmalis[a], Paul Cos[b], Banoth Karan Kumar[c], Sankaranarayanan Murugesan[c], and Kondapalli Venkata Gowri Chandra Sekhar[a2]

[a]*Department of Chemistry, Birla Institute of Technology and Science, Pilani, Hyderabad Campus, Jawahar Nagar, Hyderabad – 500 078, Telangana, India.*

[b]*Laboratory of Microbiology, Parasitology and Hygiene, Department of Pharmaceutical Sciences, University of Antwerp, Universiteitsplein 1, 2610, Wilrijk, Belgium.*

[c]*Medicinal Chemistry Research Laboratory, Department of Pharmacy, Birla Institute of Technology and Science Pilani, Pilani Campus, Pilani-333031, Rajasthan. India.*

[1] Corresponding author: Davie Cappoen (davie.cappoen@uantwerpen.be)

[2] Corresponding author: Kondapalli Venkata Gowri Chandra Sekhar (Tel.: +91 40 66303527; E-mail: kvgc@hyderabad.bits-pilani.ac.in; kvgcs.bits@gmail.com)

Table of Contents

1.0. Experimental

1.1. Chemistry

All the reagents were procured from commercial available sources and used with further purification wherever necessary. All reactions were monitored by thin layer chromatography (TLC) performed on E-Merck 0.25 mm precoated silica gel aluminum plates (60 F254) using mixture of pet ether and ethyl acetate. Visualization of the spots on TLC was achieved by exposure to UV light. Column chromatography was performed using silica gel (Acme, 100-200mesh). Solvents were dried and purified by distillation prior to use. Solvents for chromatography (pet ether and ethyl acetate) were distilled prior to use. Evaporations were carried out under reduced pressure on Heidolf rotary evaporator. ^{1}H and ^{13}C NMR spectra were recorded on Bruker (400 MHz for ^{1}H, 101 MHz for ^{13}C), DMSO-d6. Chemical shifts have been expressed in parts per million (δ) relative to tetramethylsilane (δ = 0.0) as an internal standard and coupling constants (*J*) in Hertz. Low-resolution mass spectra (ESI-MS) were recorded on LC/MS-2020 Agilent.

1.2 General procedure for synthesis of ethyl 6-methylimidazo-[2,1-b]-thiazole-5-carboxylate (3a) & ethyl 2-methylbenzo-[d]-imidazo-[2,1-b]-thiazole-3-carboxylate (3b): A solution of (**1a)** (10.0 g, 99.86 mmol, 1.0 eq) and ethyl-2-chloroacetoacetate (32.87 g, 199.72 mmol, 2 eq) were dissolved in 10 V of 1,4-dioxane and heated for 24 h at reflux. The reaction progress was monitored by TLC; after completion of reaction, as indicated by TLC. The reaction mixture wash extracted with EtOAc. The organic layer wash dried over anhydrous sodium sulfate. The obtained organic layer wash evaporated under reduced pressure. The Crude material was purified by silica gel column chromatography with 20% ethyl acetate: petroleum ether solvent system. The compounds **3a** to be yielded 80% (16.79g). Same procedure followed for the synthesis of **3b** and yielded 91% (15.77 g).

ethyl 2-methylbenzo-[d]-imidazo-[2,1-b]-thiazole-3-carboxylate (3b): ^{1}HNMR (400 MHz, DMSO- d_6): δ 8.28 (d, *J* = 7.8 Hz, 1H), 8.15 (dd, *J* = 8.0, 1.0 Hz, 1H), 7.99 (dd, *J* = 8.2, 1.0 Hz, 1H), 7.69 (d, *J* = 8.5 Hz, 1H), 4.15 (q, *J* = 3.5 Hz, 2H), 2.28 (s, 3H), 1.35 (t, *J* = 3.5 Hz, 3H).

1.2.1 synthesis of 6-methylimidazo-[2,1-b]-thiazole-5-carboxylic acid (4a) & 2-methylbenzo-[d]-imidazo-[2,1-b]-thiazole-3-carboxylic acid (4b):

Compound **3a** (9.5 g, 4.52 mmol, 1.0 eq) was taken in mixture of THF-MeOH and LiOH (monohydrate) (0.570 g, 13.55 mmol, 3.0 eq) was added at 0 ℃ and allowed to rt stirred for 16 h. The reaction was monitored by using TLC, after completion of reaction evaporated under reduced pressure. The crude was dissolved in water and adjusted the pH ≈ 4-5 by the addition of 4N HCl solution. The precipitated compound was filtered and dried. Compound **4a** yielded 82% (6.75g). Same procedure followed for the synthesis of compound **4b** and yielded 85% (11.37 g).

2-methylbenzo-[d]-imidazo-[2,1-b]-thiazole-3-carboxylic acid (4b): ^{1}HNMR (400 MHz, DMSO- d_6): δ 12.08 (s, 1H), 8.32 (d, J = 7.9 Hz, 1H), 8.20 (dd, J = 8.2, 1.5 Hz, 1H), 8.05 (dd, J = 8.2, 1.5 Hz, 1H), 7.72 (d, J = 8.5 Hz, 1H), 2.29 (s, 3H) .

1.2.2. General procedure for synthesis of tert-butyl 4-(6-methylimidazo-[2,1-b]-thiazole-5-carbonyl)-piperazine-1-carboxylate (5a) & tert-butyl 4-(2-methylbenzo-[d]-imidazo-[2,1-b]-thiazole-3-carbonyl)-piperazine-1-carboxylate (5b):

Compound **4a** (6.7 g, 36.81 mmol, 1.0 eq) was taken in DMF, then HATU (27.99 g, 73.62 mmol, 2.0 eq), DIPEA (14.27 g, 110.44 mmol, 3.0 eq) and 1-Boc-Piperazine (7.533g, 40.45 mmol, 1.1 eq) was added at rt. The reaction was stirred for 12 h. The reaction was monitored by using TLC, after completion of reaction extracted with EtOAc. The organic was washed with the brine solution and dried over anhydrous sodium sulfate. The organic layer was evaporated under reduced pressure. The crude material was purified by column by using 25 % Ethyl acetate in hexane as eluents. The compound **5a** was yielded 76% (9.79 g). Same procedure followed for the synthesis of **5b** and yielded 79% (14.98 g).

tert-butyl 4-(2-methylbenzo-[d]-imidazo-[2,1-b]-thiazole-3-carbonyl)-piperazine-1-carboxylate (5b): ^{1}HNMR (400 MHz, DMSO- d_6): δ 8.32 (d, J = 7.9 Hz, 1H), 8.20 (dd, J = 8.2, 1.0 Hz, 1H), 8.05 (dd, J = 8.3, 1.0 Hz, 1H), 7.75 (d, J = 8.7 Hz, 1H), 3.65 (t, J = 4.2 Hz, 4H), 3.35 (t, J = 4.2 Hz, 4H), 2.28 (s, 3H), 1.49 (s, 9H).

1.2.3. General procedure for synthesis of (6-methylimidazo-[2,1-b]-thiazol-5-yl)(piperazin-1-yl)-methanone hydrochloride (6a) & (2-methylbenzo-[d]-imidazo-[2,1-b]-thiazol-3-yl)(piperazin-1-yl)-methanone hydrochloride (6b):

Compound **5a** (9.5 g, 27.10 mmol, 1.0 eq) was taken in DCM (10 V) and 4.0 M HCl in Dioxane (5 V) was added at 0 ℃ and allowed to rt and stirred for 4h. The reaction was monitored by checking TLC. After completion of reaction, the reaction was evaporated under

reduced pressure. The crude compound was washed with EtOAc. The obtained compound **6a** was yielded 92% (6.24 g). Same procedure followed for the synthesis of compound **6b** and yielded 90% (9.45g).

(2-methylbenzo-[d]-imidazo-[2,1-b]-thiazol-3-yl)(piperazin-1-yl)-methanone (6b): ^{1}HNMR (400 MHz, DMSO- d_6): δ 8.35 (d, J = 8.1 Hz, 1H), 8.23 (dd, J = 8.1, 1.2 Hz, 1H), 8.12 (dd, J = 8.1, 1.2 Hz, 1H), 7.81 (d, J = 8.5 Hz, 1H), 4.12 (s, 1H), 3.59 (t, J = 4.5 Hz, 4H), 3.32 (t, J = 4.5 Hz, 4H), 2.31 (s, 3H).

1.2.4. General procedure for synthesis of (4-(2-hydroxyethyl)-piperazin-1-yl)(6-methylimidazo-[2,1-b]-thiazol-5-yl)-methanone (8a) & (4-(2-hydroxyethyl)-piperazin-1-yl)(2-methylbenzo-[d]-imidazo-[2,1-b]-thiazol-3-yl)-methanone (8b):

Compound **6a** (3.1 g, 12.38 mmol, 1.0 eq) was taken in ACN (10 V), then K_2CO_3 (5.13 g, 37.15 mmol, 3.0 eq), 2-Boromo ethanol (1.7 g, 13.62 mmol, 1.1 eq) was added at rt and stirred for 6 h. The reaction was monitored by using TLC. After completion of reaction extracted with EtOAc. The organic layer was washed with brine solution, later dried over the anhydrous sodium sulfate, evaporated under reduced pressure. The crude compound was purified by silica gel column by using 35 % Ethyl acetate in hexane as eluents. The obtained compound **8a** was yielded 86% (3.135 g). Same procedure followed for the compound **8b** and yielded 92% (4.95 g).

(4-(2-hydroxyethyl)-piperazin-1-yl)(2-methylbenzo-[d]-imidazo-[2,1-b]-thiazol-3-yl)-methanone (8b): ^{1}HNMR (400 MHz, DMSO- d_6): δ 8.30 (d, J = 8.5 Hz, 1H), 8.26 (dd, J = 8.1, 1.5 Hz, 1H), 8.12 (dd, J = 8.5, 1.2 Hz, 1H), 7.81 (d, J = 8.1 Hz, 1H), 4.25 (s, 1H), 3.65 (t, J = 5.2 Hz, 2H), 3.59 (t, J = 4.5 Hz, 4H), 3.32 (m, 6H), 2.28 (s, 3H).

1.2.5. General procedure for synthesis of (4-(2-azidoethyl)-piperazin-1-yl)(6-methylimidazo-[2,1-b]-thiazol-5-yl)-methanone (9a) & (4-(2-azidoethyl)-piperazin-1-yl)(2-methylbenzo-[d]-imidazo-[2,1-b]-thiazol-3-yl)-methanone (9b):

Compound **8a** (3.1 g, 1.053 mmol, 1.0 eq) was taken in DCM (10 V), then Et_3N (3.19 g, 31.59 mmol, 3.0 eq), tertiary methyl silyl chloride (1.37 g, 12.63 mmol, 1.2 eq) was added at 0 ℃ and allowed to rt, stirred for 2 h. The reaction was monitored by using TLC. After completion of reaction extracted with EtOAc. The organic layer was dried over anhydrous sodium sulfate, evaporated under reduced pressure. The crude compound was dissolved in DMSO, to this sodium azide (1.2 eq) was added. The reaction was stirred for

5 h at 70 °C. The reaction was monitored by using TLC. After completion of reaction extracted with EtOAc. The organic layer was washed with brine solution, later dried over the anhydrous sodium sulfate. The organic layer was evaporated under reduced pressure. The obtained crude compound was purified by silica gel column by using 25 % Ethyl acetate in hexane as eluents. The obtained compound **9a** was yielded 90% (3.02 g). Same procedure followed for the compound **9b** and yielded 86% (4.57 g).

(4-(2-azidoethyl)-piperazin-1-yl)(2-methylbenzo-[d]-imidazo-[2,1-b]-thiazol-3-yl)-methanone (9b): ^{1}HNMR (400 MHz, DMSO-d_6): δ 8.32 (d, J = 8.2 Hz, 1H), 8.21 (dd, J = 7.9, 1.1 Hz, 1H), 8.12 (dd, J = 7.9, 1.1 Hz, 1H), 7.86 (d, J = 8.2 Hz, 1H), 3.69 (t, J = 5.2 Hz, 2H), 3.56 (t, J = 4.5 Hz, 4H), 3.29 (m, 6H), 2.29 (s, 3H).

1.2.6. General procedure for synthesis of (6-methylimidazo-[2,1-b]-thiazol-5-yl)(4-(prop-2-yn-1-yl)-piperazin-1-yl)-methanone (11a) & (2-methylbenzo-[d]-imidazo-[2,1-b]-thiazol-3-yl)(4-(prop-2-yn-1-yl)-piperazin-1-yl)-methanone (11b):

Compound **6a** (3.1 g, 12.38 mmol, 1.0 eq) was taken in ACN (10 V), then K_2CO_3 (5.12 g, 37.15 mmol, 3.0 eq), Propargyl bromide (2.21 g, 18.57 mmol, 1.5 eq) was added at rt and stirred for 6 h. The reaction was monitored by using TLC. After completion of reaction extracted with EtOAc. The organic layer was washed with brine solution, later dried over the anhydrous sodium sulfate, evaporated under reduced pressure. The crude compound was purified by silica gel column by using 25 % Ethyl acetate in hexane as eluents. The obtained compound **11a** was yielded 95% (3.39 g). Same procedure followed for the compound **11b** and yielded 85% (4.5 g).

(2-methylbenzo-[d]-imidazo-[2,1-b]-thiazol-3-yl)(4-(prop-2-yn-1-yl)-piperazin-1-yl)-methanone (11b): ^{1}HNMR (400 MHz, DMSO- d_6): δ 8.39 (d, J = 7.5 Hz, 1H), 8.25 (dd, J = 6.5, 0.8 Hz, 1H), 8.19 (dd, J = 6.5, 0.8 Hz, 1H), 7.86 (d, J = 7.5 Hz, 1H), 3.69 (s, 2H), 3.55 (t, J = 4.7Hz, 4H), 3.35 (t, J = 4.7 Hz, 4H), 2.29 (s, 3H), 1.25 (s, 1H).

1.2.7. General procedure for synthesis of (4-(2-(4-substituted phenyl / aliphatic groups-*1H*-1,2,3-triazol-1-yl)-ethyl)-piperazin-1-yl)(6-methylimidazo-[2,1-b]-thiazol-5-yl)-methanone (IT01-IT05, IT19 and IT20) and **(4-(2-(4- substituted phenyl / aliphatic groups-*1H*-1,2,3-triazol-1-yl)-ethyl)-piperazin-1-yl)(2-methylbenzo-[d]-imidazo-[2,1-b]-thiazol-3-yl)-methanone (IT12-IT18):**

A solution of azide **9a**/**9b** (1.0 equiv.) in DMF: *t*-BuOH: H_2O (5:3:2) is reacted with various substituted acetylenes (1.5 equiv.) in the presence of sodium ascorbate (0.01 equiv.) and $CuSO_4 \cdot 5H_2O$ (0.02 equiv.) and catalytic amount of CuI. The reaction mixture is stirred at rt for 12-14h. Once completion of the reaction, as indicated by TLC, the reaction was diluted with EtOAc. The organic layer washed with brine solution. The organic layer was dried over anhydrous sodium sulfate and concentrated under reduced pressure. The crude was purified by column chromatography using 70-90% ethyl acetate in hexane as eluent to get title compounds **IT01-IT05**, and **IT12-IT20**.

1.2.8. General procedure for synthesis of (4-((1-substituted phenyl-*1H*-1,2,3-triazol-4-yl)-methyl)-piperazin-1-yl)(6-methylimidazo-[2,1-b]-thiazol-5-yl)-methanone (IT21-IT27), and (4-((1-substituted phenyl-*1H*-1,2,3-triazol-4-yl)-methyl)-piperazin-1-yl)(2-methylbenzo-[d]-imidazo-[2,1-b]-thiazol-3-yl)-methanone (**IT06- IT11**):

A solution of the alkyne **(11a**/**11b)** (1.0 equiv.) in DMF: *t*-BuOH: H2O (5:3:2) was reacted with different substituted azides (1.5 equiv.) in the presence of sodium ascorbate (0.01 equiv.) and $CuSO_4 \cdot 5H_2O$ (0.02 equiv.) and catalytic amount of CuI. The reaction mixture was stirred at rt for 12-14h. The reaction mixture was monitored by TLC. Once completion of the reaction, the reaction was diluted with ethyl acetate. The organic layer was washed with brine solution and dried over anhydrous sodium sulfate. The organic layer was concentrated under reduced pressure and the crude was purified by column chromatography by using 70-90% ethyl acetate in hexane as eluent to get title compounds **IT21-27** and **IT06-11**.

2. Biology Experimental procedures:

2.1. Material

Unless stated differently, the reagents used were purchased from the manufactures listed in this section. All synthesized test compounds and the assay specific reference compounds were dissolved in DMSO (Sigma-Aldrich) at 20mM. After verification of solubility, compounds were stored in 5 mL opaque glass bottles at room temperature, shielded from direct sunlight for max 1 month.

2.2. *In silico* prediction of drug-likeness properties

In silico ADMET properties of the titled compounds were predicted using the knowledge-based FAF Drugs4 [1] and Swiss ADME software tools [2] to enable the selection of designed analogues that are suitable for further biological evaluation.

2.3. Molecular docking studies

Computational sources: Xenon W3565 processor, Ubuntu 18.04

Software and version: Schrodinger software, version 2019-1[3] (Glide module for docking)

Retrieval of the protein: RCSB protein data bank [4]

(PDB-1P44, https://www.rcsb.org/structure/3IUB)[5]

Docking method: Extra precession mode

Results analysis: XP visualizer (Schrodinger)

2.3.1. Molecular dynamics studies

Computational sources: Tyrone workstation (NVIDIA RTX 2040), Ubuntu 18.04 OS

Software and version: Desmond software, D.E Shaw research group (Academic license, Version 2020-1) [6]

2.3.2. Docking workflow: To produce docking studies, ChemDraw 16.0 was used to sketch the ligand. Then, Ligprep module of the software (Version 2019-1, Schrodinger) [7] was used to minimize the energy with OPLS3e (Optimized Potentials for Liquid Simulations) force field. The minimization process enables the allocation of bond orders, addition of hydrogens to ligands and the conversion of 2D into 3D structures to improve docking. Further docking studies were conducted using the output file (Best conformations of the ligands) [7]. In Schrodinger, the protein preparation wizard (version 2019-1, Schrodinger) [8] is the primary application for preparing proteins and minimizing their energy content. It adds hydrogen atoms to proteins and assigns charges to them. The Het states were generated using Epik at pH 7.0 ± 2.0. Using workspace analysis, the protein was refined, modified and the heteroatoms in the water were removed. The crucial water molecules stayed the same, but all other molecules apart from water were removed except the co-crystal ligand. The OPLS3 force field was then used to minimize the protein. An active site grid was generated by considering co-crystal ligands, which are included

in the active site of the selected protein target (PDB-3IUB). To validate the protein, root mean square deviation (RMSD) was calculated after docking with the co-crystal ligand in XP mode. [9].

2.3.3. Molecular dynamics workflow: Simulation of Molecular Dynamics (MD) helps visualize the action of Protein-Ligand complexes (PLC) at the target's binding site region under physiological conditions. MD was performed using Desmond module of Schrödinger developed by D.E Shaw research group (Academic license, Version 2020-1) [6] through the system's builder panel; the orthorhombic simulation box was prepared with the Simple Point-Charge (SPC) explicit water model in such a way that the minimum distance between the protein surface and the solvent surface was 10 Å. Complexes docked with receptors were solvated with orthorhombic TIP3P water model [9]. Neutralization of the solvated system was accomplished by using counterions and limiting the salt concentration in the physiological system to 0.15 M. The receptor-ligand complex system was designated with OPLS AA force field [10].

Two seconds of relaxation time were used for the Reversible reference system Propagator Algorithms (RESPA) integrator [11], Nose-Hoover chain thermostat [12] and Martyna-Tobias-Klein barostat. The final production of MD simulation was performed using the equilibrated system. This MD simulation was set to run for 100 ns with 310 K temperatures at 1.0 bar pressure with the NPT (Isothermal-Isobaric ensemble, constant temperature, constant pressure, constant number of particles) ensemble at default settings [13] for relaxation before simulation. The MD simulation was performed with the MD simulation tool, with the simulation time set to 100 ns. Furthermore, the _out file was used to view the trajectories and create a movie. The out.cms file was imported and the movie was exported at higher resolution (1280x1024) with better quality. The trajectory was written with 1000 frames during the MD simulation. The protein backbone frames were aligned to the backbone of the initial frame in order to better understand the complex's stability during MD simulation. Finally, after loading the .out file and selected Root Mean Square Deviation (RMSD) and Root Mean Square Fluctuation (RMSF) in the analysis type to oblique, the simulation interaction diagram and the results was analyzed [14,15].

2.4. Cellular strains and culture conditions

Mycobacterium tuberculosis H37Ra ATCC 25177, *Mycobacterium avium* subsp. *avium* Chester ATCC 25291, *Mycobacterium intracellulare* ATCC 13950, *Mycolicibacterium smegmatis* MC(2) ATCC 700084, *Mycobacterium abscessus* ATCC 19977 were

selected for this study. All strains were transformed with pSMT -1 Hyg^R harboring the luxAB operon from the Gram-negative, bioluminescent, marine bacterium Vibrio Harvey, encoding the procaryotic luciferase. The growth kinetics, correlation relative light unit (RLU)/CFU and MICs towards first- and second-line drugs are routinely verified and standardized for all the bioluminescent enabled strains above with $1 \geq z' \geq 0.5$. All strains were grown in 7H9 (Becton Dickinson) supplemented with 10% Oleic Albumin Dextrose Catalase (OADC, Becton Dickinson), 0.5% tyloxapol (Sigma-Aldrich), 0.2% glycerol (Sigma-Aldrich) supplemented with 50 µg/ml hygromycin (Roche) at 37°C, static at 5% CO_2. MRC-5 ATCC CCL-171 were cultivated in Dulbecco's modified Eagle's medium (DMEM) supplemented with 10% (v/v) heat-inactivated fetal calf serum (iFCS), 1% (v/v) GlutaMAX™, 1% Non-Essential Amino Acids Solution, 1% (v/v) Penicillin-Streptomycin (10,000 U/mL) and 1% (v/v) Sodium Pyruvate (100 mM) at 37°C under an atmosphere of 5% CO_2. DMEM and all supplements used for the cultivation of the MRC-5 cells were purchased from Thermo Fisher. Cells were maintained in culture until a maximum passage number of 20 after which they are replaced by a cryo-stock culture preserved in liquid nitrogen.

2.5. *In vitro* activity against *Mycobacterium tuberculosis* by bioluminescence

Mtb H37Ra was transformed with pSMT-1 *HygR* harbouring *luxAB*, to create the *Mtb* $H37Ra^{luxAB}$ strain as previously described [16,17]. The strain was grown to mid-log phase in 7H9 + 10% OADC, glycerol, 0.05% tyloxapol, 0.2% glycerol supplemented with 50 µg/ml hygromycin and subsequently aliquoted at an RLU of 10^6 / 10^8 CFU for long time storage in 10% glycerol at 80°C. Prior inoculation with the compounds, the *Mtb* $H37Ra^{luxAB}$ culture was resuscitated in 7H9 + 10% OADC at 37°C, 5% CO_2 for 1 to 3 hours. Compound ½ dilution series and single shot dilutions of the synthesized test compounds as well as the reference compounds were spotted in a black 96 well plate in 7H9 with a Biomek 4000 Automated Liquid Handler (Coulter) in a volume of 10µL. The created dilutions resulranging from 128 µM to 0.125 µM in triplicate. The spotted compounds were inoculated with 190µL of *Mtb* $H37Ra^{luxAB}$ in 200µL of 7H9 + 10% OADC total to create a final dilution concentration ranging from 128 µM to 0.125 µM and an inoculum of 10^3 RLU/ 10^5 CFU. The negative control, without test compound was supplemented with 1% DMSO. After the inoculation of *Mtb* $H37Ra^{luxAB}$, the plates were sealed with parafilm and stored in a humidified incubator (Coulter) at 37°C with 5% CO_2 for 7 days. After incubation, the parafilm seal

and lid was removed and followed by 15 minutes of vigorous orbital shaking of the plates to obtain homogenised cultures in a dark room. To each well, 25 µL of 1% decanal in EtOH (Sigma) was added to act as a substrate for the bacterial luciferase. Light emission was enumerated as RLU with a Discover multi well plate reader (Promega) at wavelength 495nM. The growth inhibition induced by exposure to the test compound dilution was calculated as reduction in RLU, compared to the negative control inoculated to in 1% DMSO in 7H9 + 10% OADC. The results were reproduced in at least three independent repeats. Triplicate measurements with a Standard deviation exceeding 10% were repeated.

2.6. *In vitro* activity against *the panel of non-tuberculous Mycobacteria (NTM), Mycobacterium bovis and Mycolicibacterium smegmatis* by bioluminescence

The members of the NTM panel *(M. avium* subsp. *avium, M. intracellulare, M. abscessus)* as well as *Mycobacterium bovis and Mycolicibacterium smegmatis* were transformed with pSMT-1 *HygR* harbouring *luxAB*, to create the respective luminescent mycobacterial strains as previously described (Cappoen et al). All strains were grown in 7H9 + 10% OADC, glycerol, 0.05% tyloxapol, 0.2% glycerol supplemented with 50 µg/ml to mid-log phase and subsequently aliquoted at an RLU of 10^6 / 10^8 CFU for long time storage in 10% glycerol at 80°C. Prior inoculation with the compounds, the luminescent cultures were resuscitated in 7H9 + 10% OADC at 37°C, 5% CO_2 for 1 to 3 hours. Compound ½ dilution series and single shot dilutions of the synthesized test compounds were produced as outlined above. The spotted compounds were inoculated with 190µL of the panel of mycobacteria in 200µL of 7H9 + 10% OADC total to create a final dilution concentration ranging from 128 µM to 0.125 µM and an inoculum of 10^3 RLU/ 10^5 CFU. The negative control, without test compound was supplemented with 1% DMSO. After the inoculation of *Mtb* H37Ra^{luxAB}, the plates were sealed with parafilm and stored in a humidified incubator (Coulter) at 37°C with 5% CO_2. For the slow-growing mycobacteria (*M. bovis*, *M. avium* subspp. *avium*, *M. intracellulare*) compound activity was evaluated after 7 days. For the fast-growing mycobacteria, *M. abscessus* and *Mycolicibacterium smegmatis,* compound activity was accessed after 3 days of incubation. Following incubation, inhibition was measured as detailed in section 2.4.

2.7. Acute cellular toxicity towards the MRC-5 lung fibroblast cell line

Acute cellular cytotoxicity was investigated Growth on MRC-5 ATCC CCL-171 lung fibroblasts was studied by a resazurin (Sigma-Aldrich) viability assay. MRC-5 cells were grown at 37°C, 5% CO_2 in 75cm^2 culture flasks with filter cap (Greiner) until a semi confluent layer was obtained. After which, the cells were rinsed with PBS and detached from the culture flask with 1% trypsin (GIBCO), washed and after count seeded in a 96-well plate at 4x10^4 cells per well. The cells were left to recover for 24h after which 2-fold compound dilutions ranging from 128 µM to 0.125 µM were spotted into the wells. In the negative control wells, complete medium was added without test compound. In the positive control wells, Tamoxifen (Sigma-Aldrich) was used as a reference drug for cytotoxicity. The cells were exposed for 24h to the compounds at 37°C, 5% CO_2 in a humidified incubator. After drug exposure, 0.15% resazurin solution (Sigma Aldrich) was added to each well and the plates were further incubated for 4 h. Cell viability was determined by a fluorescence reading (excitation 550 nm, emission 590 nm) (Tecan®, GENios, Männedorf, Switzerland).

3.0. ^{1}H NMR and ^{13}C NMR spectra of IT series compounds

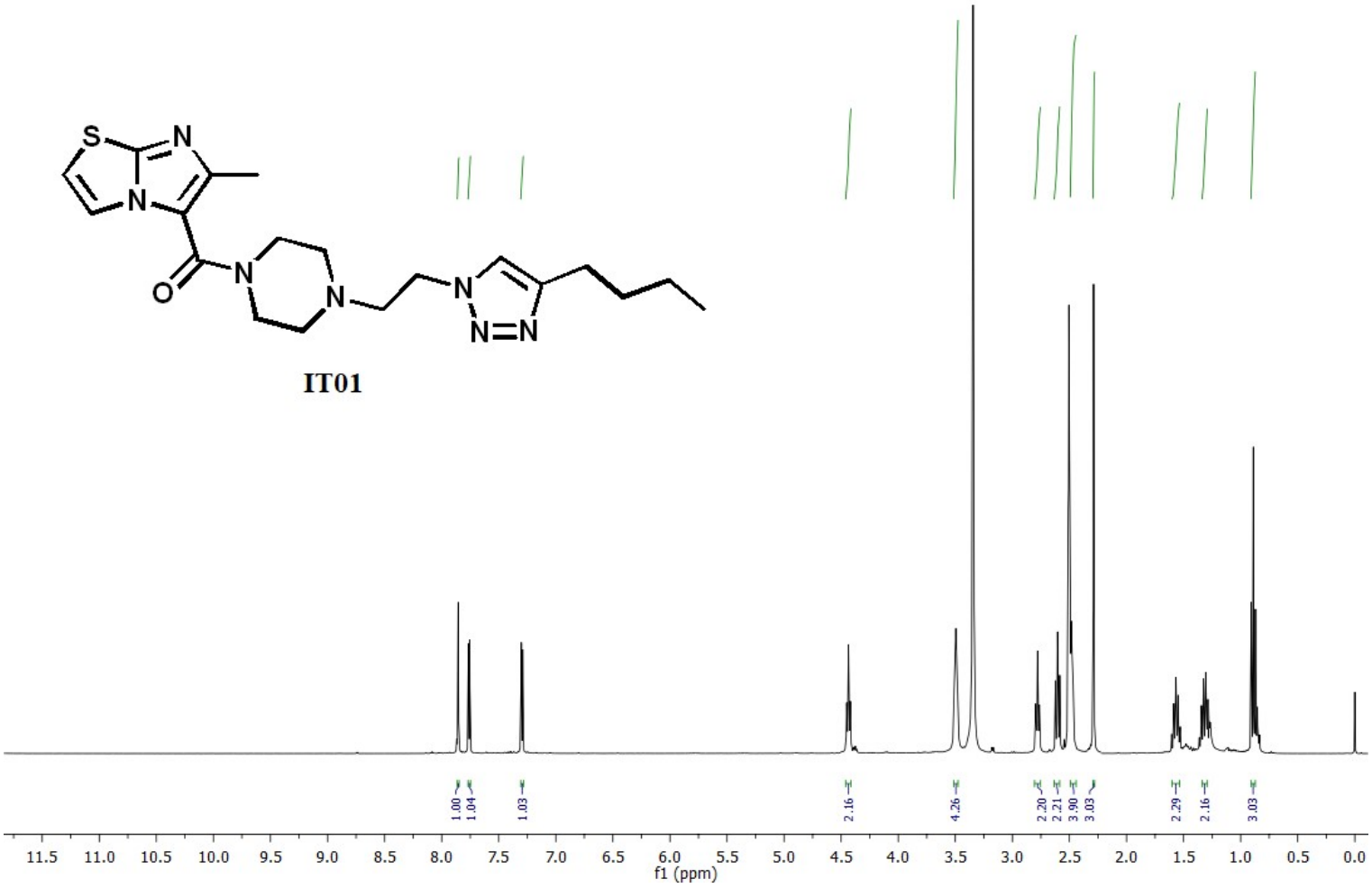

^{1}H NMR spectrum of compound **IT01 (**DMSO-d_6 400 MHz)

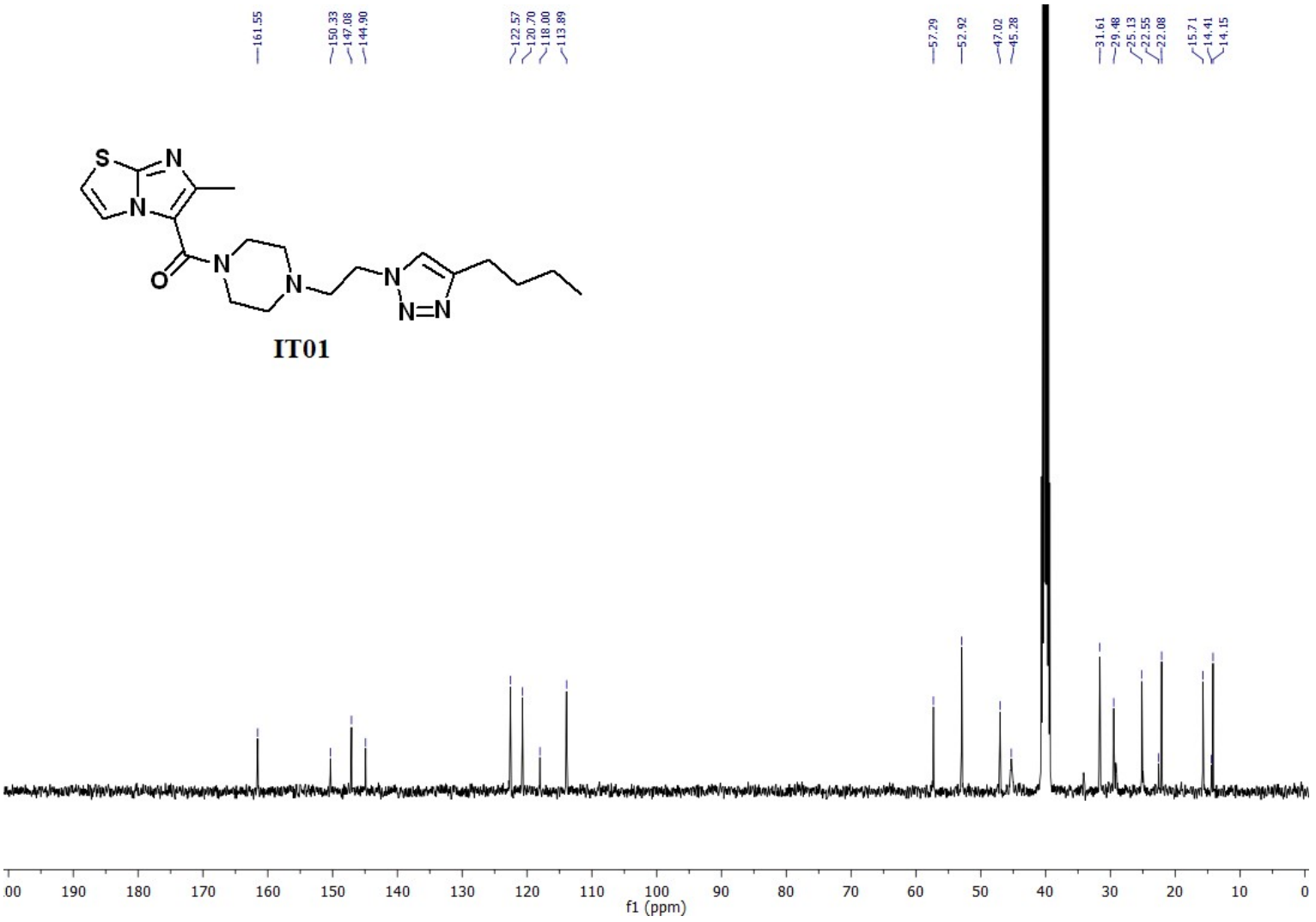

^{13}C NMR spectrum of compound **IT01** (DMSO-d_6 101 MHz)

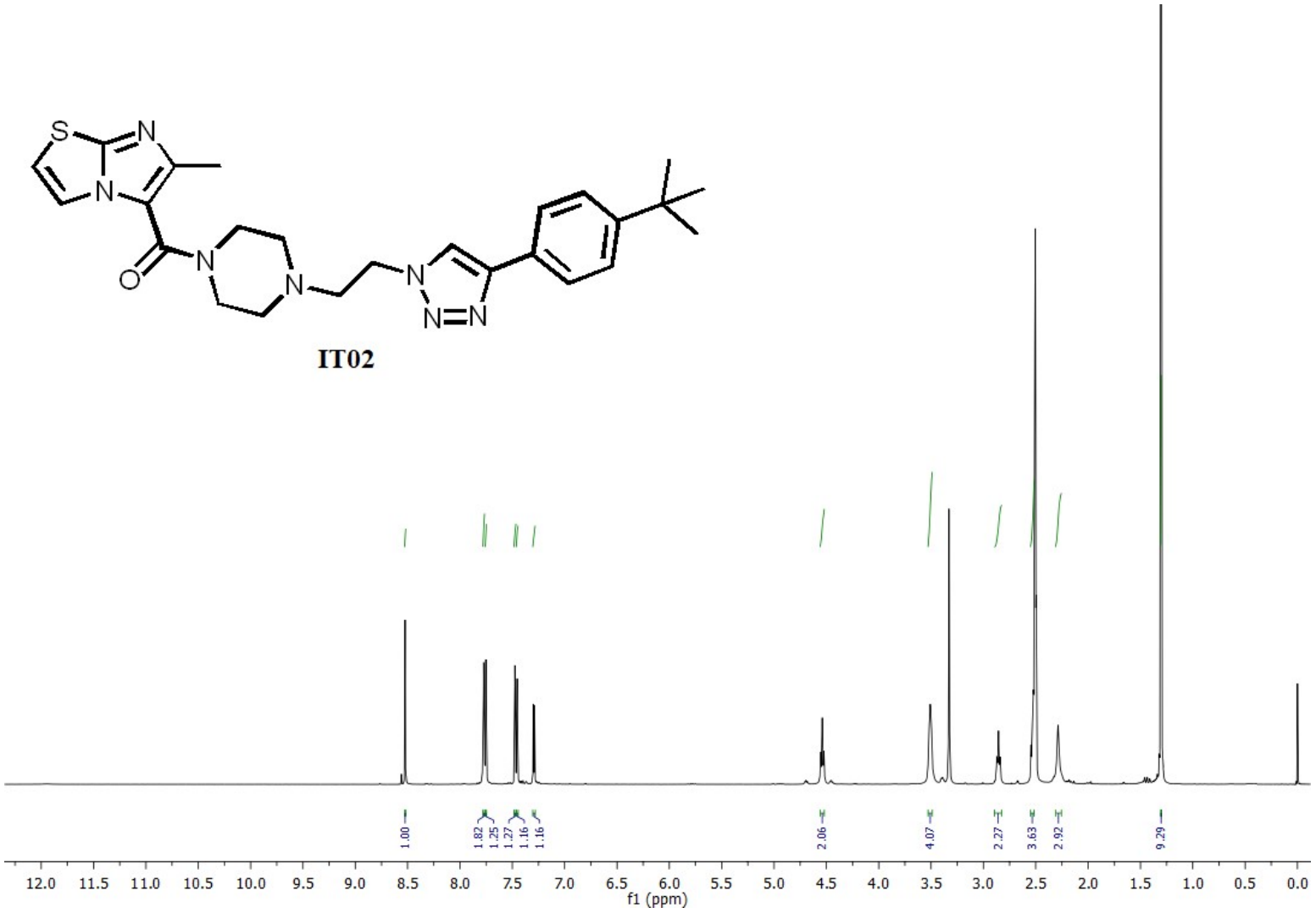

^{1}H NMR spectrum of compound **IT02 (**DMSO-d_6 400 MHz)

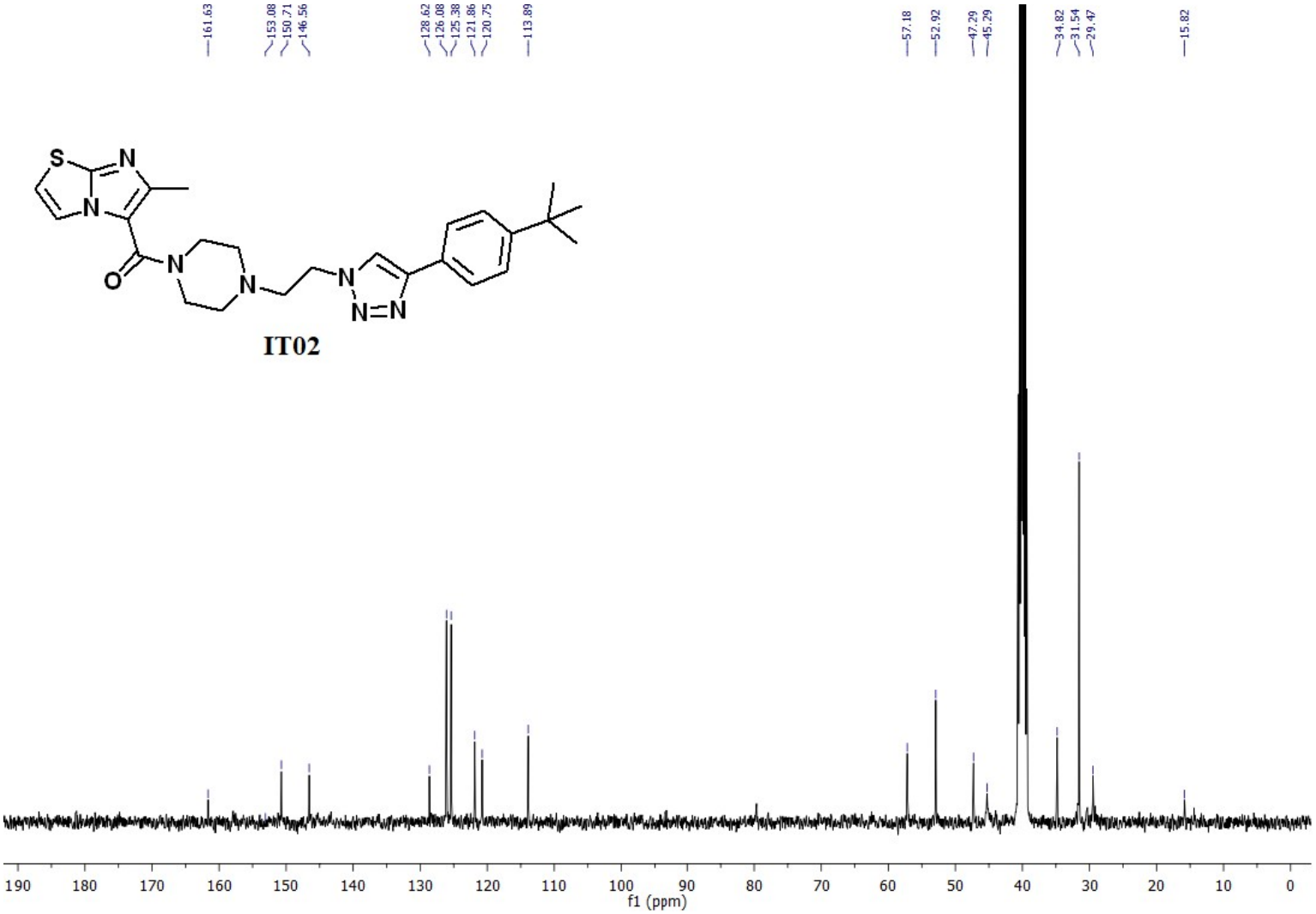

^{13}C NMR spectrum of compound **IT02** (DMSO-d_6 101 MHz)

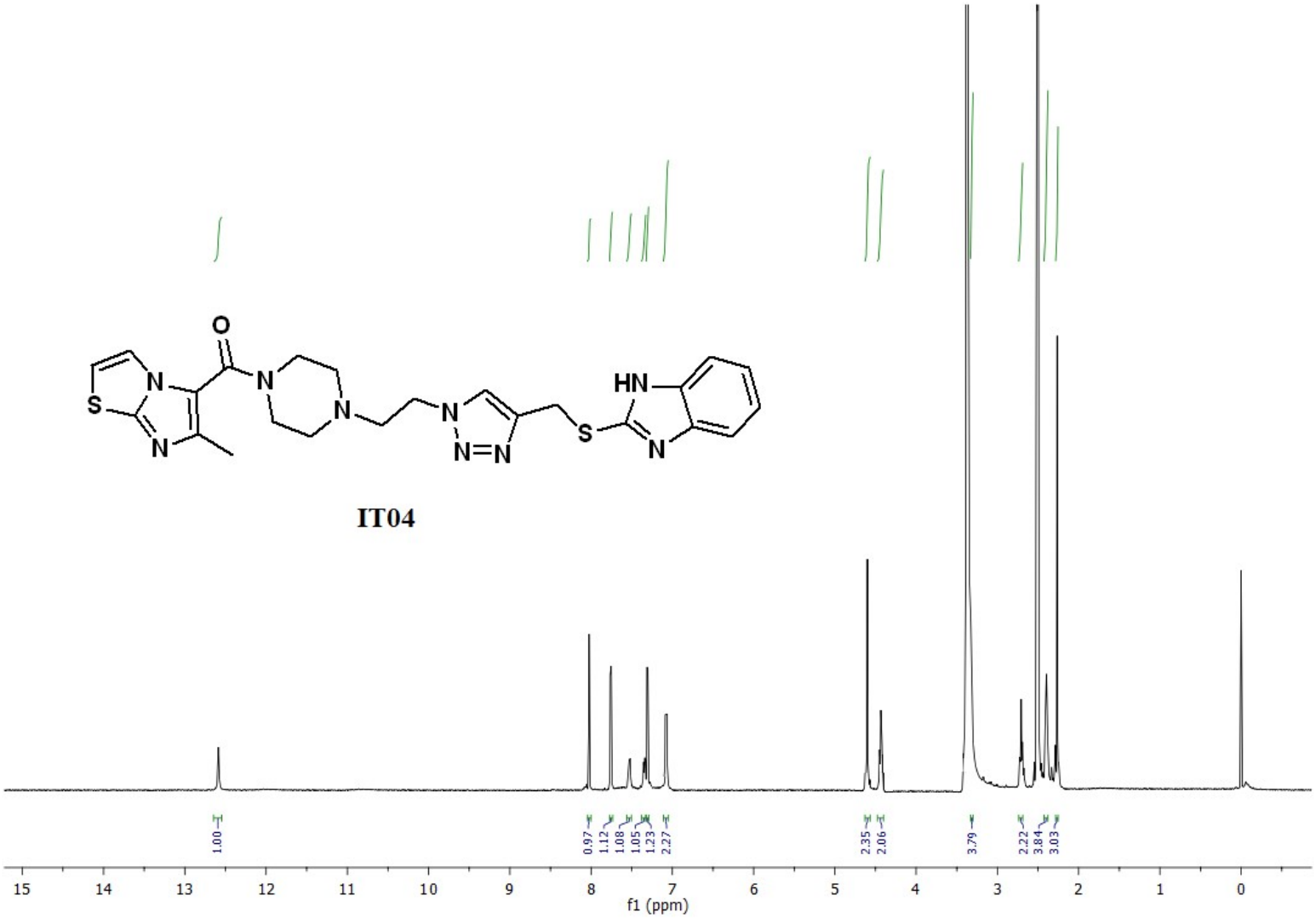

^{1}H NMR spectrum of compound **IT04 (**DMSO-d_6 400 MHz)

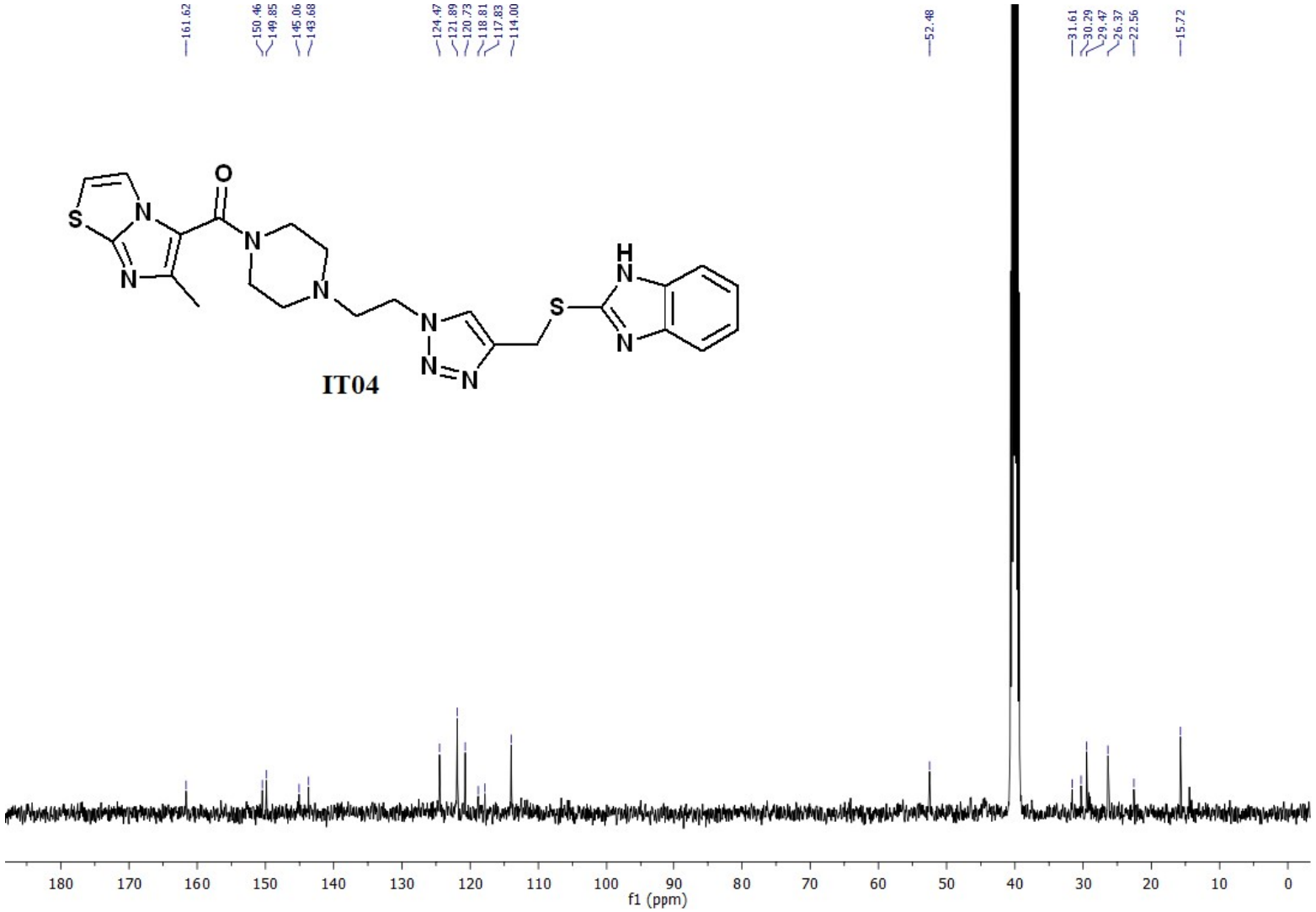

^{13}C NMR spectrum of compound **IT04** (DMSO-d_6 101 MHz)

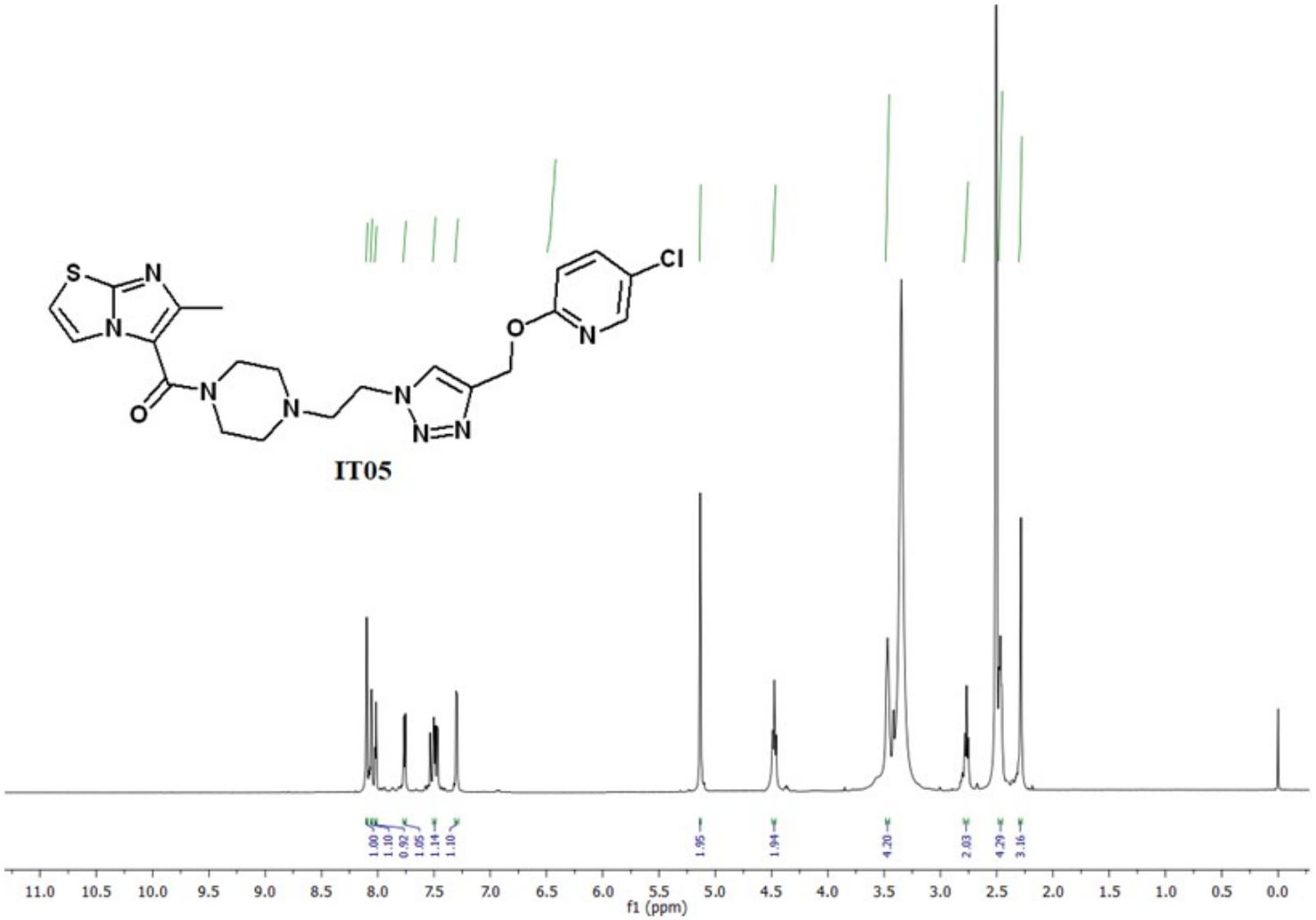

^{1}H NMR spectrum of compound **IT05 (**DMSO-d_6 400 MHz)

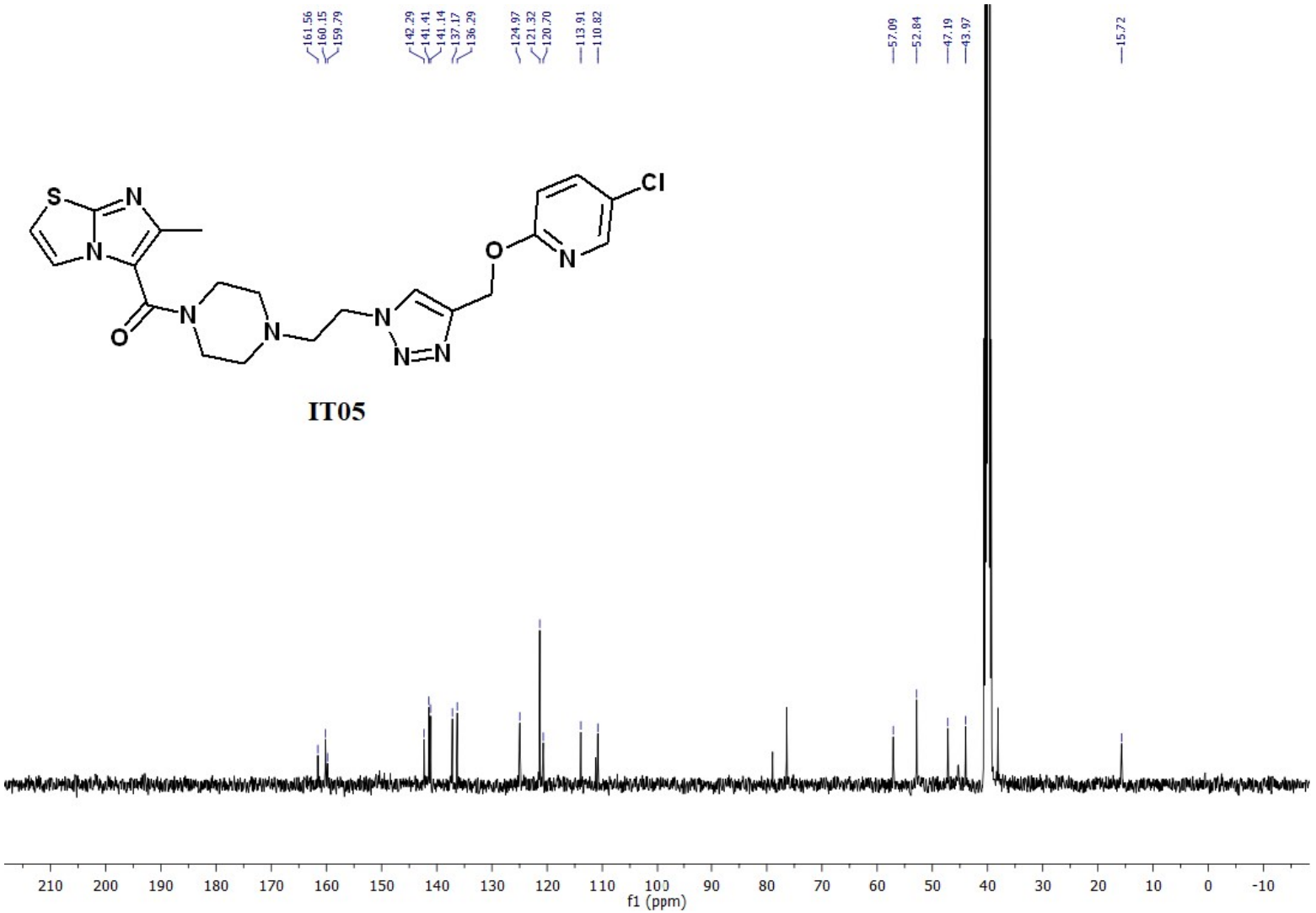

^{13}C NMR spectrum of compound **IT05** (DMSO-d_6 101 MHz)

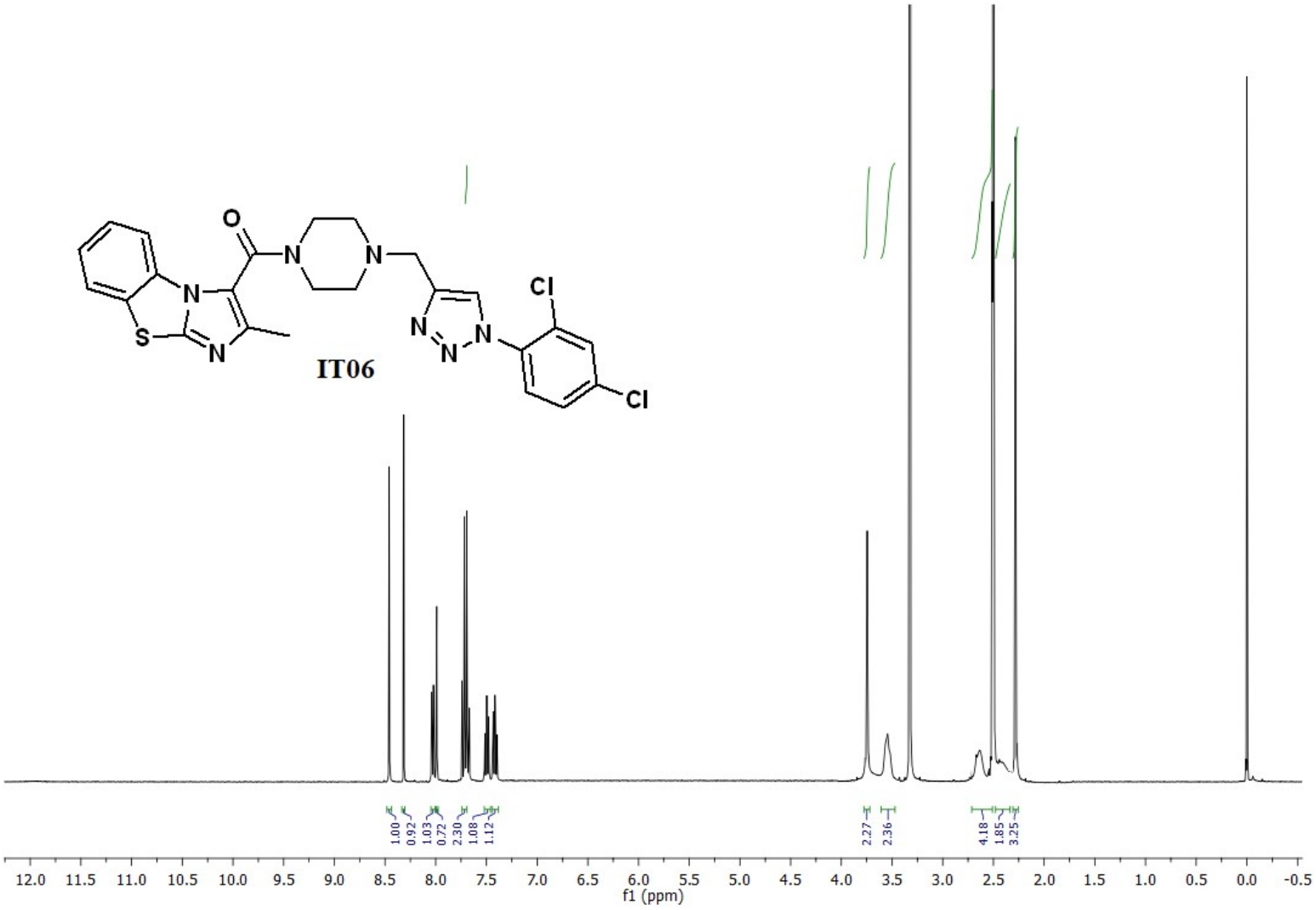

^{1}H NMR spectrum of compound **IT06 (**DMSO-d_6 400 MHz)

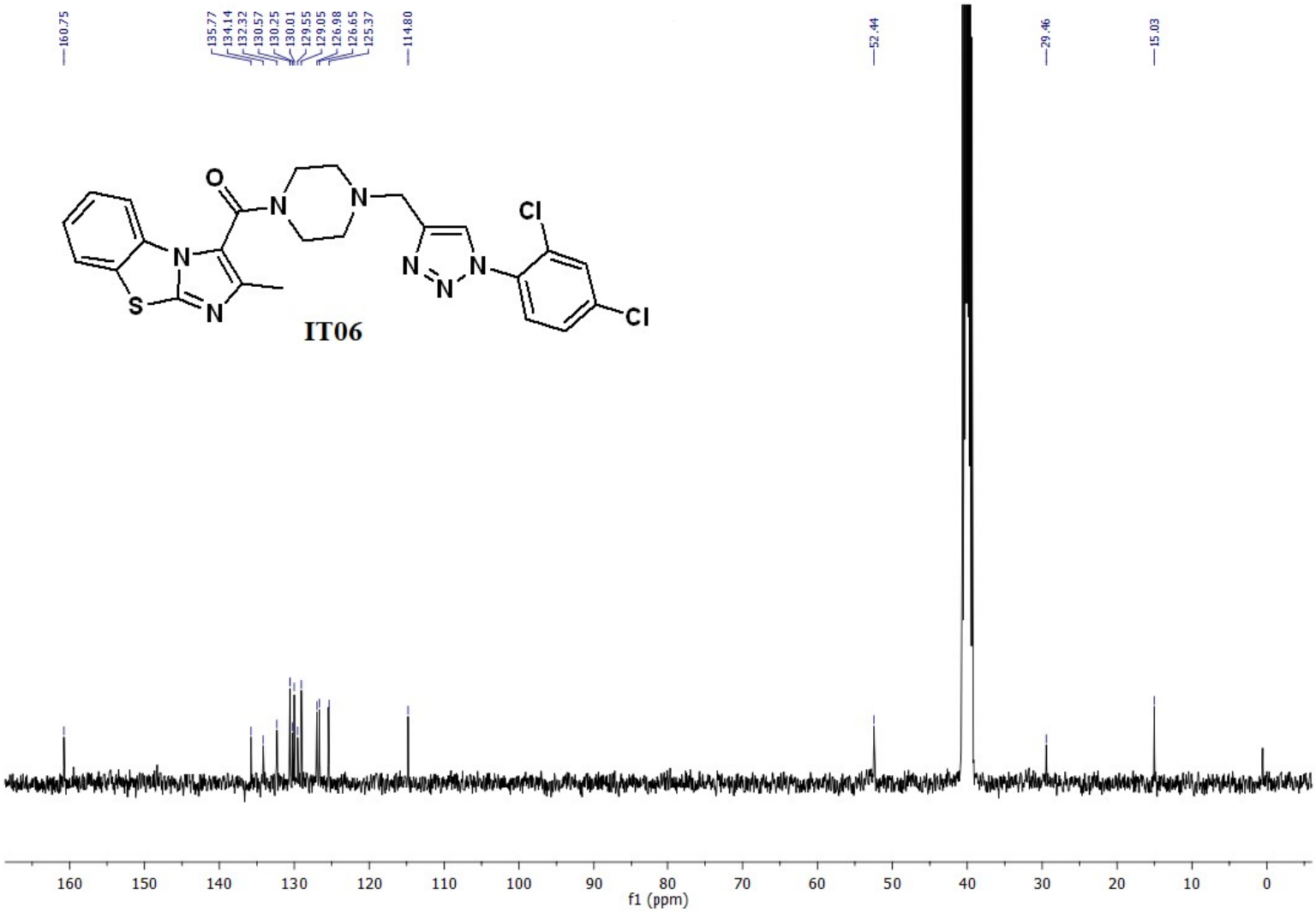

^{13}C NMR spectrum of compound **IT06** (DMSO-d_6 101 MHz)

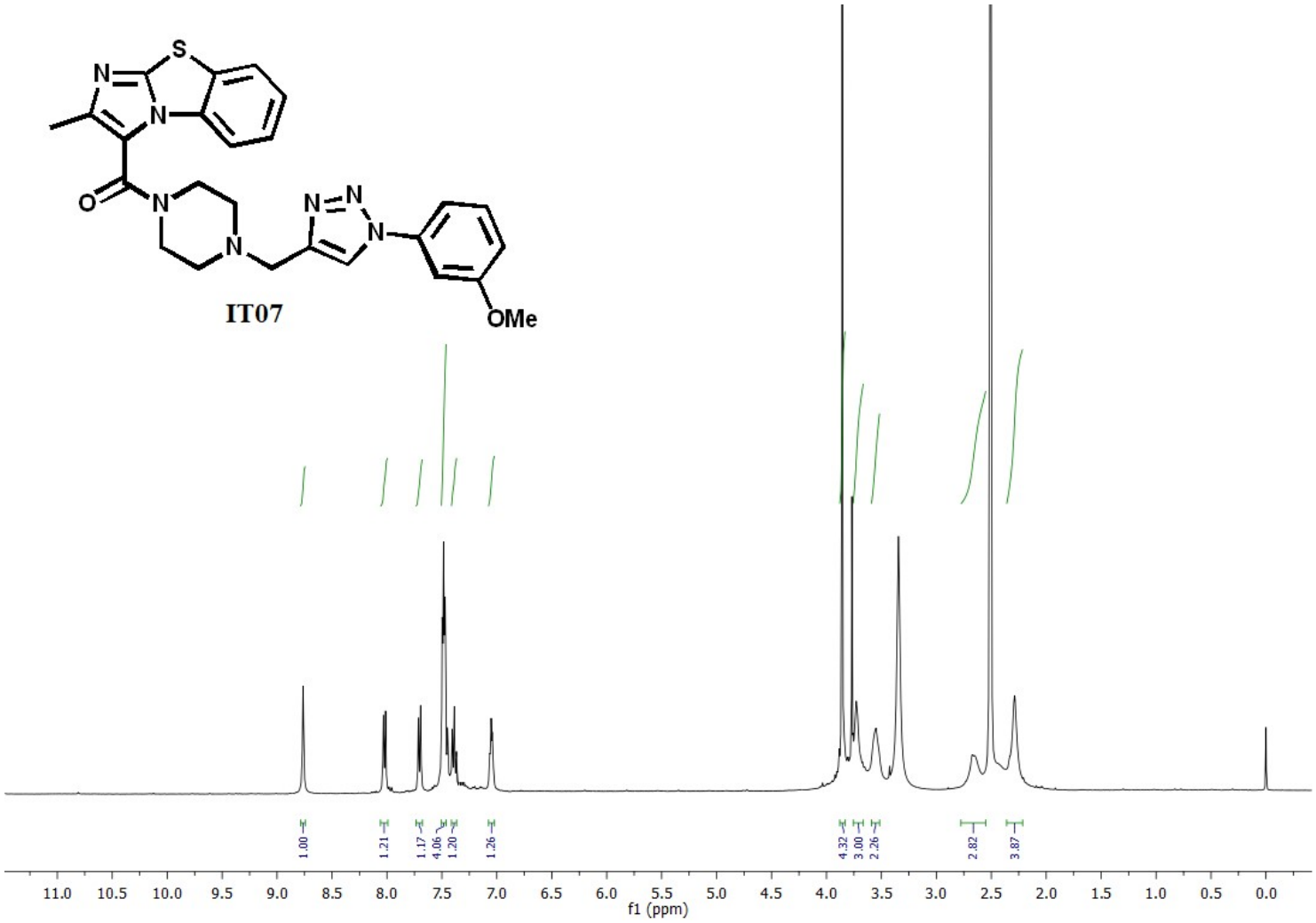

^{1}H NMR spectrum of compound **IT07 (**DMSO-d_6 400 MHz)

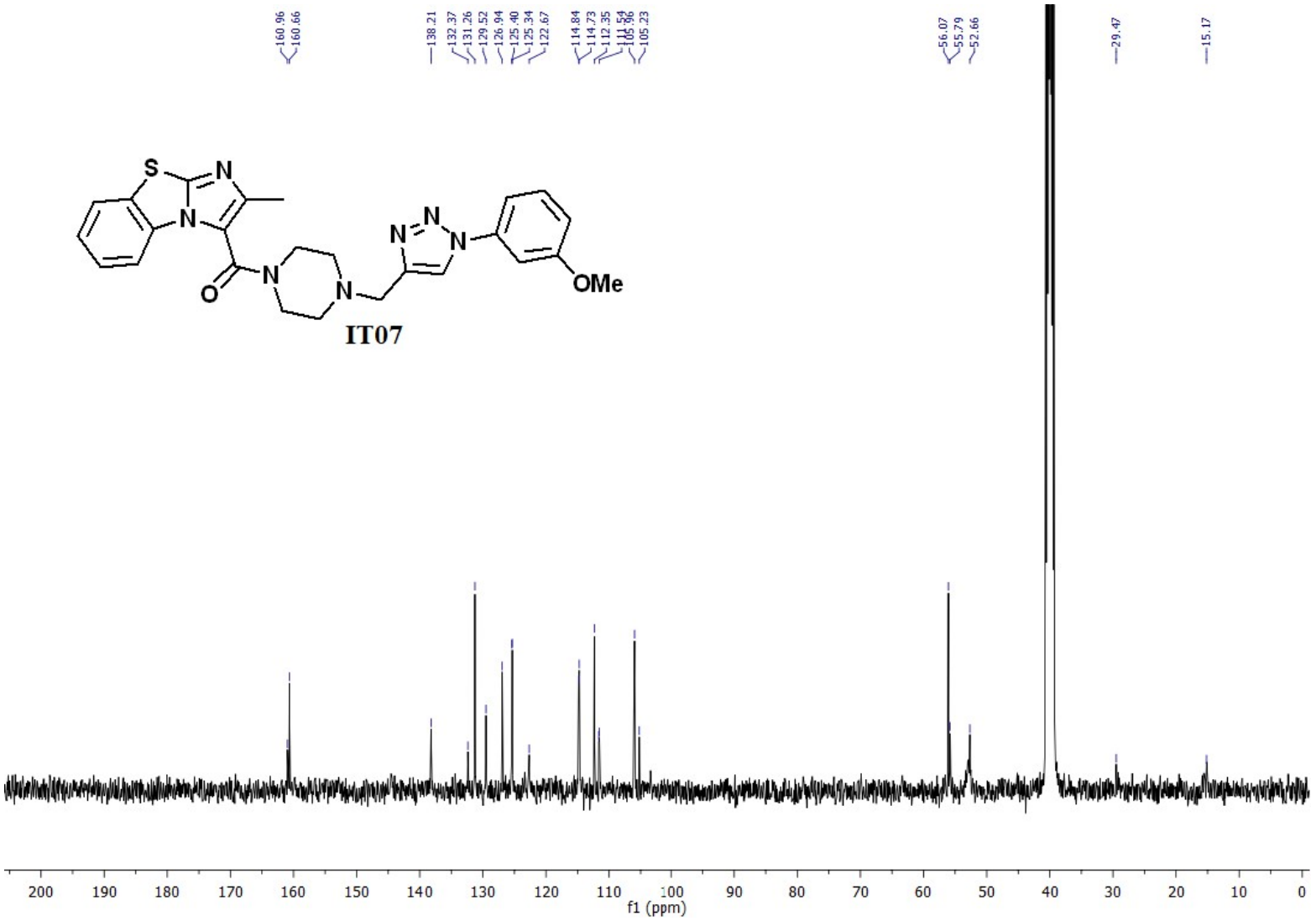

^{13}C NMR spectrum of compound **IT07** (DMSO-d_6 101 MHz)

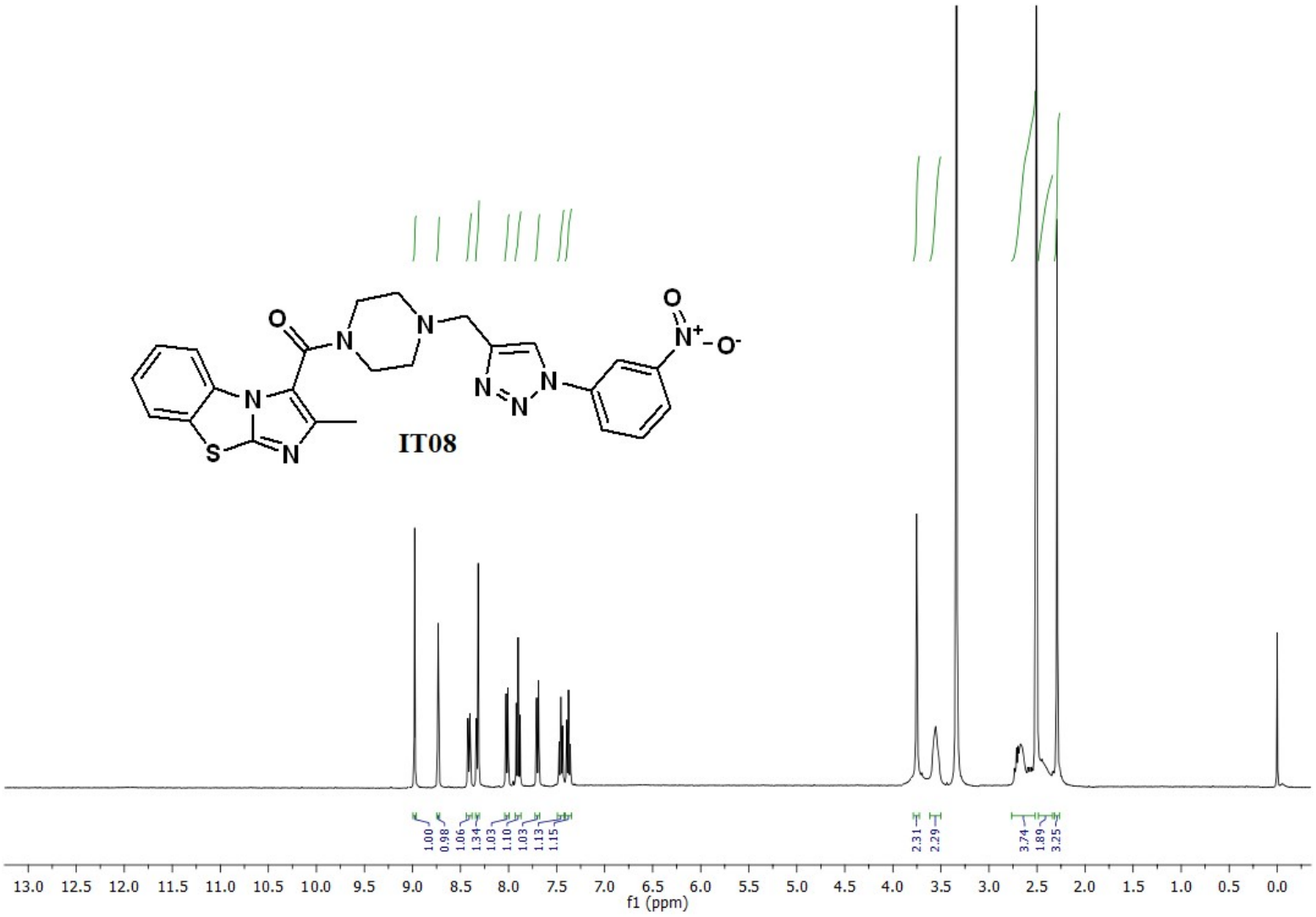

^{1}H NMR spectrum of compound **IT08 (**DMSO-d_6 400 MHz)

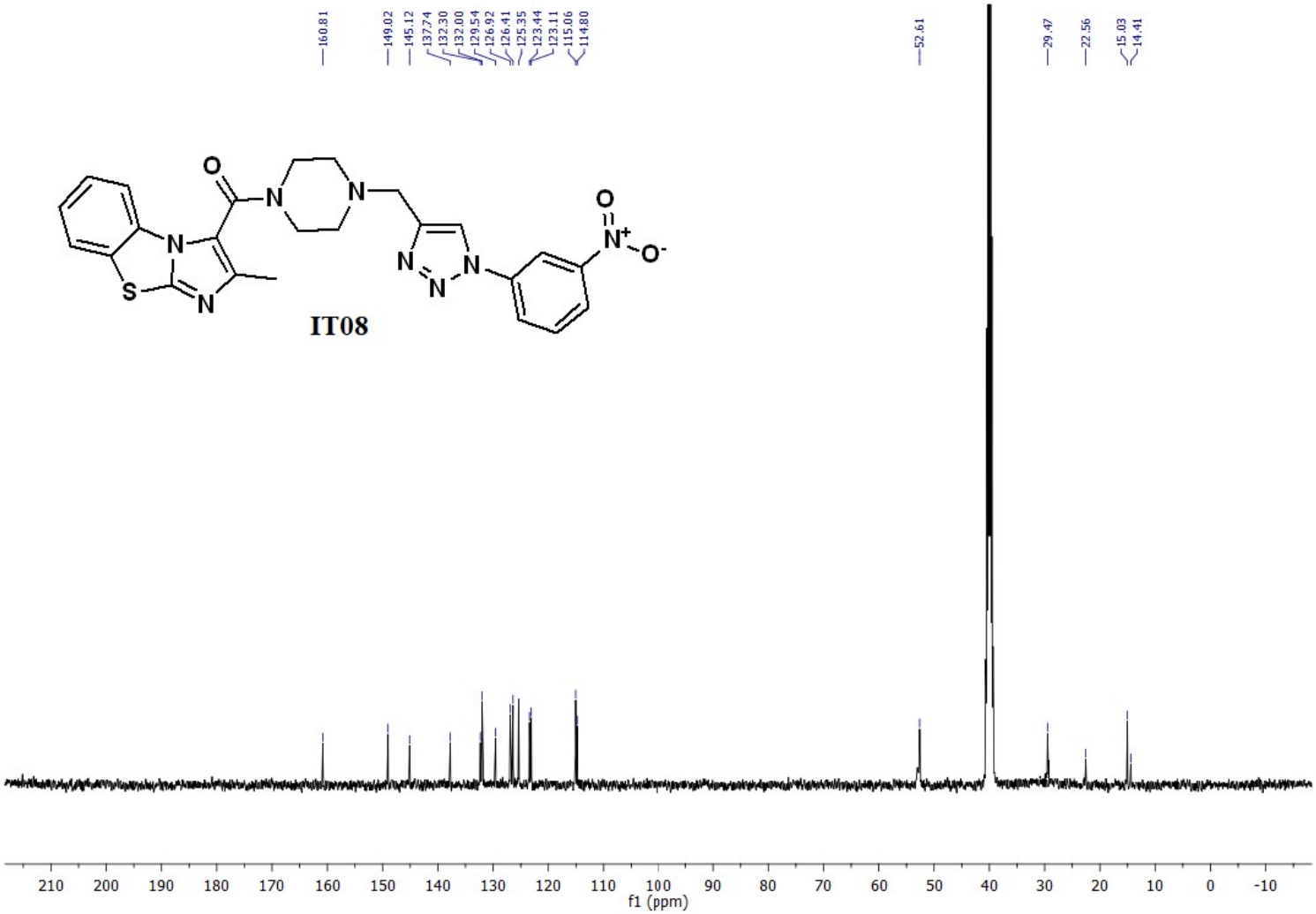

^{13}C NMR spectrum of compound **IT08** (DMSO-d_6 101 MHz)

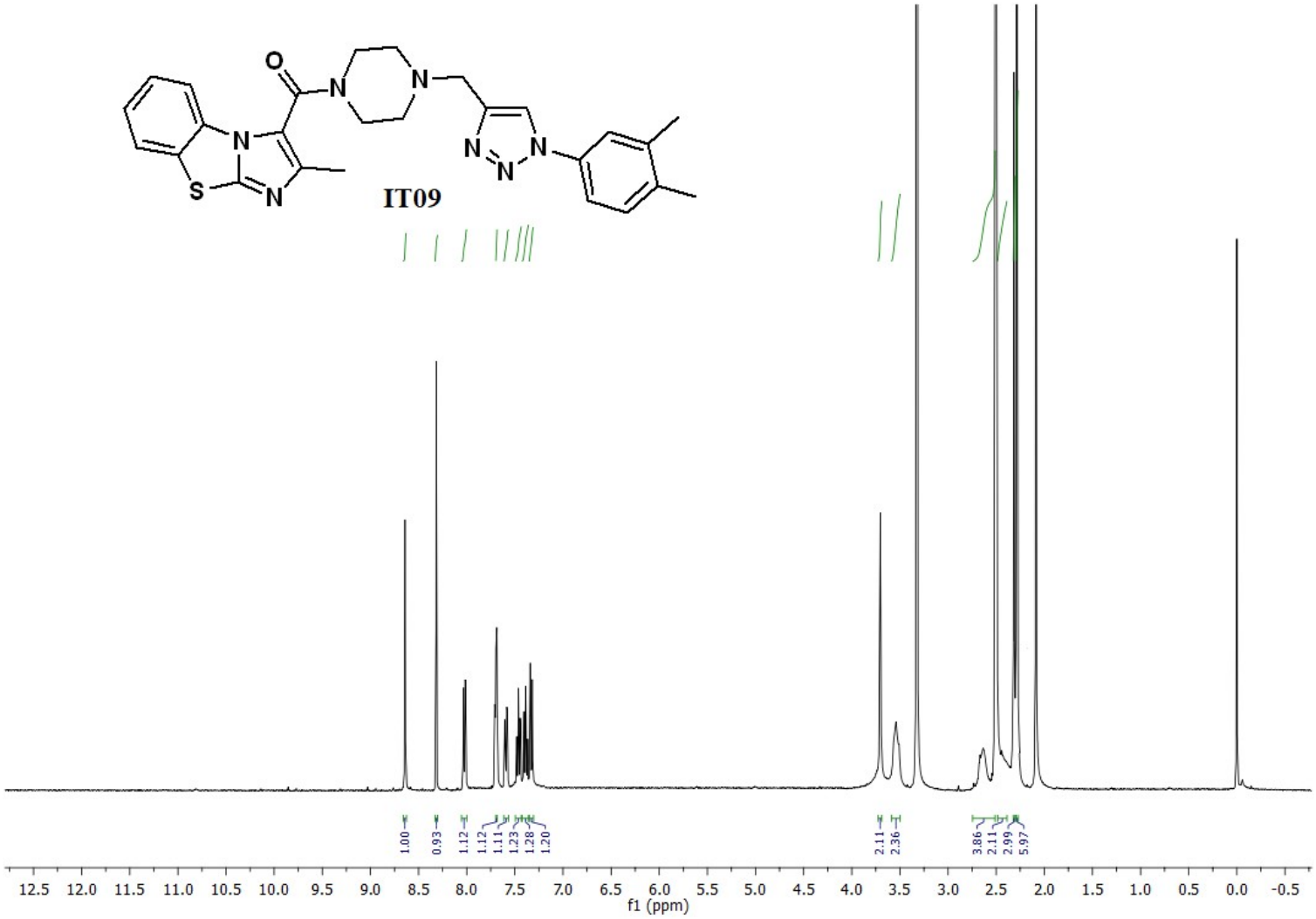

^{1}H NMR spectrum of compound **IT09 (**DMSO-d_6 400 MHz)

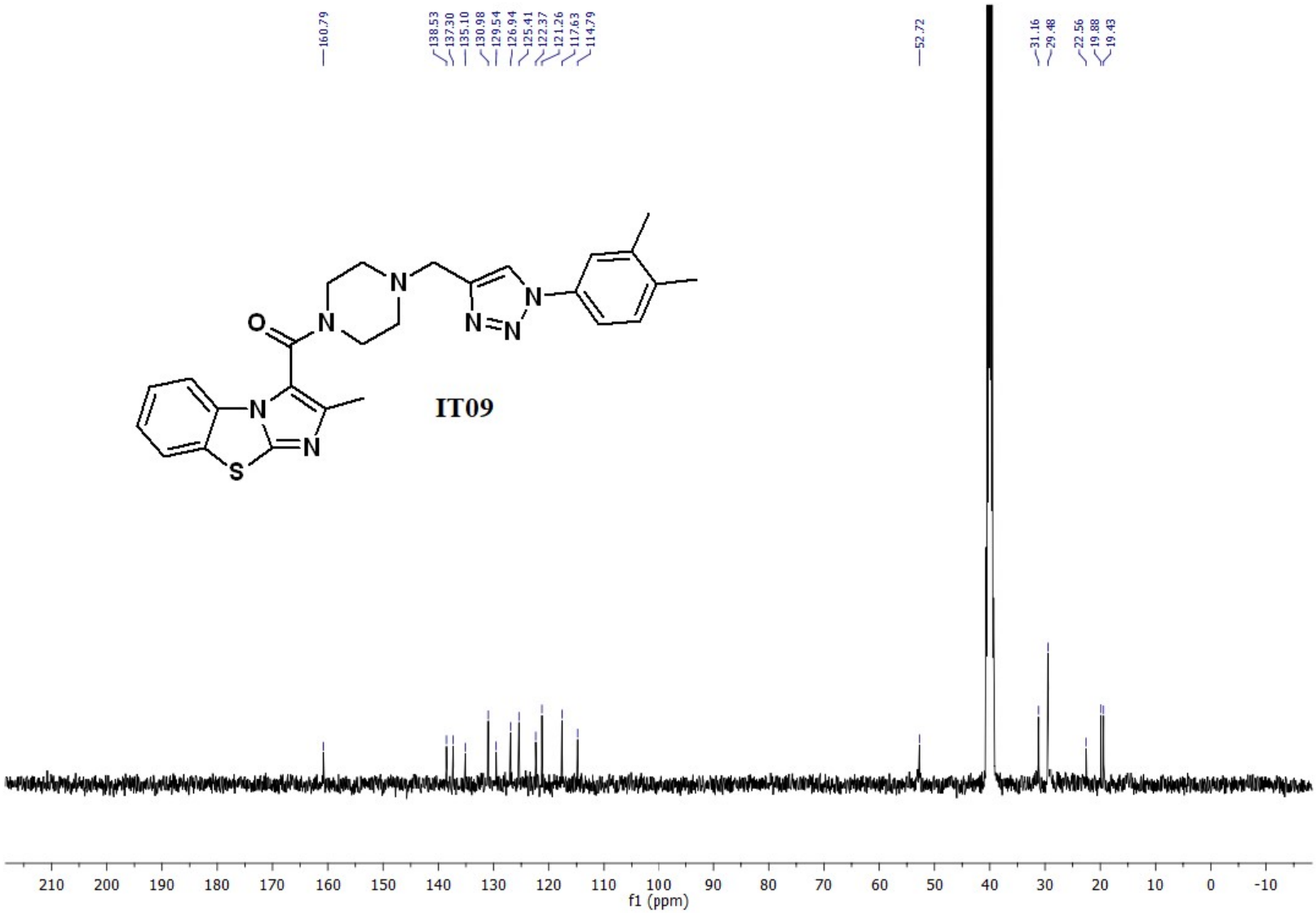

^{13}C NMR spectrum of compound **IT09** (DMSO-d_6 101 MHz)

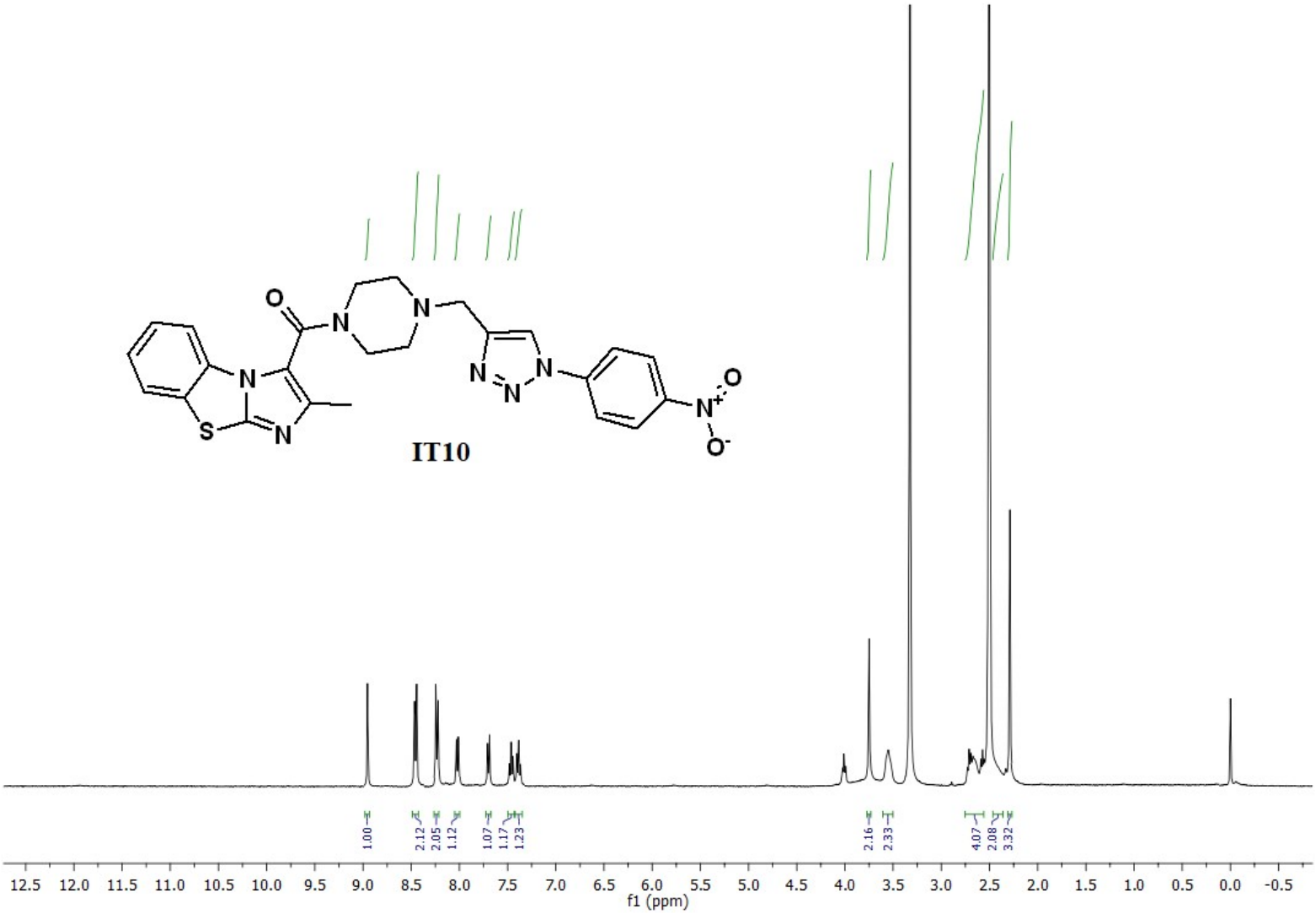

^{1}H NMR spectrum of compound **IT10 (**DMSO-d_6 400 MHz)

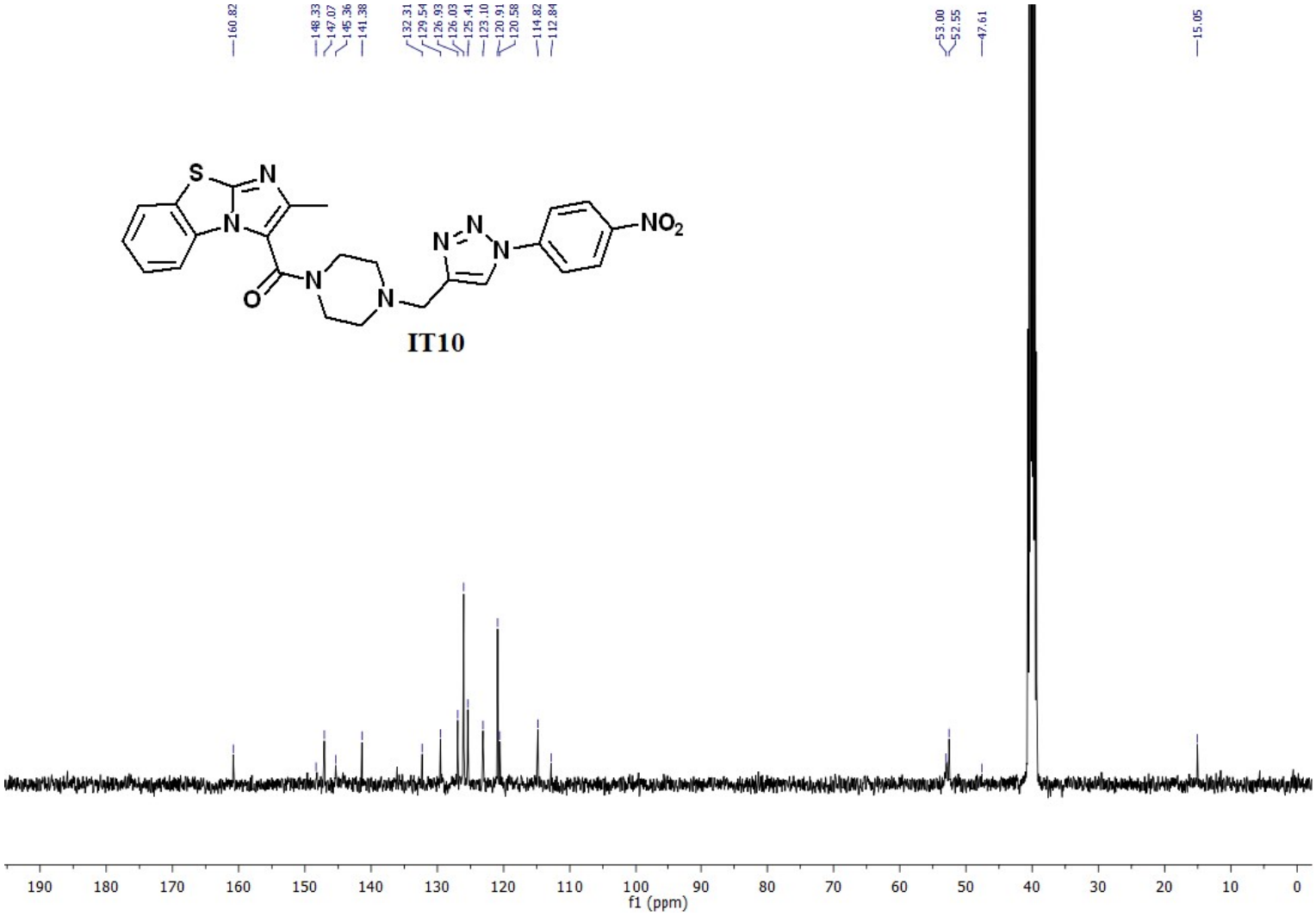

^{13}C NMR spectrum of compound **IT10** (DMSO-d_6 101 MHz)

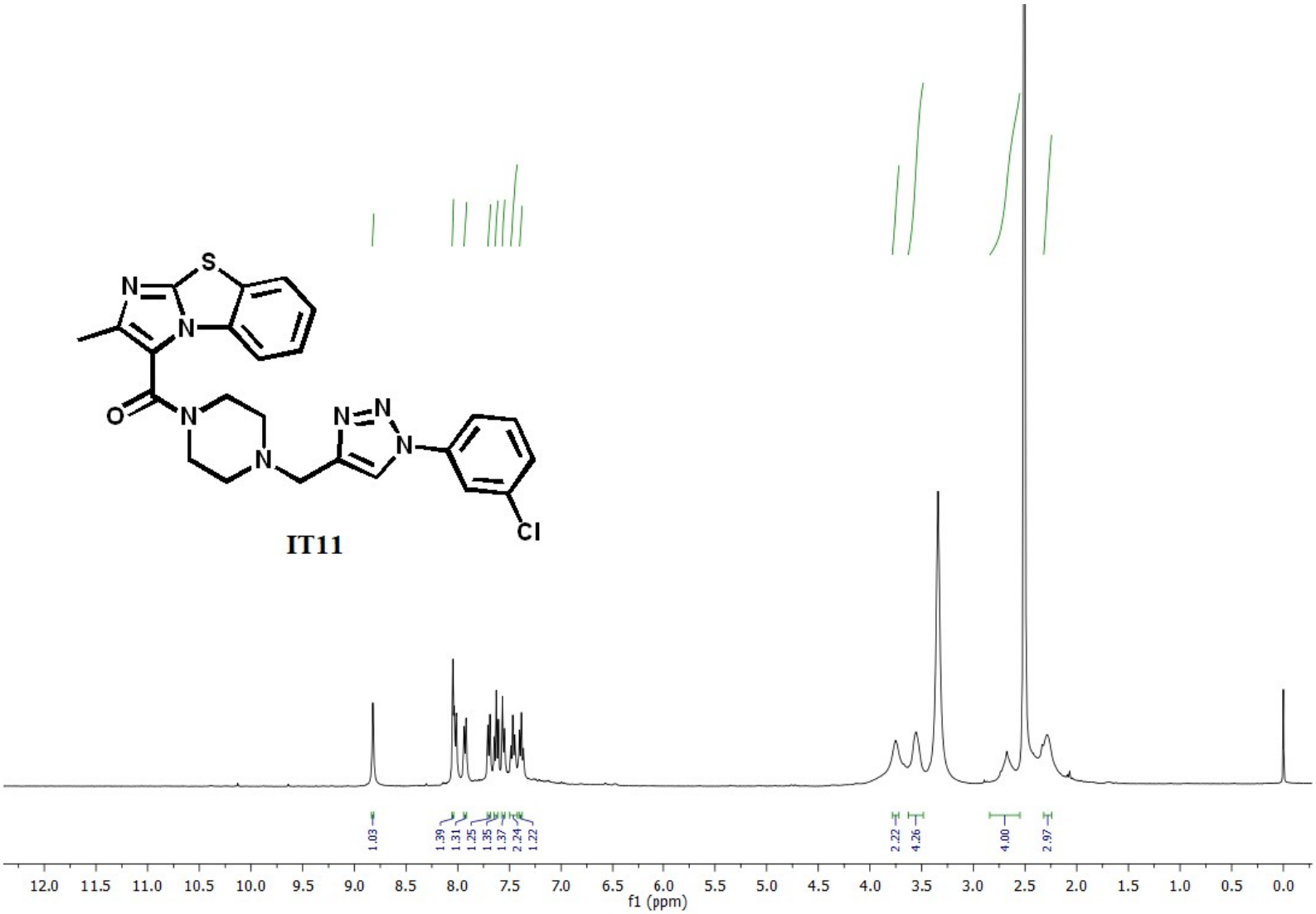

^{1}H NMR spectrum of compound **IT11 (**DMSO-d_6 400 MHz)

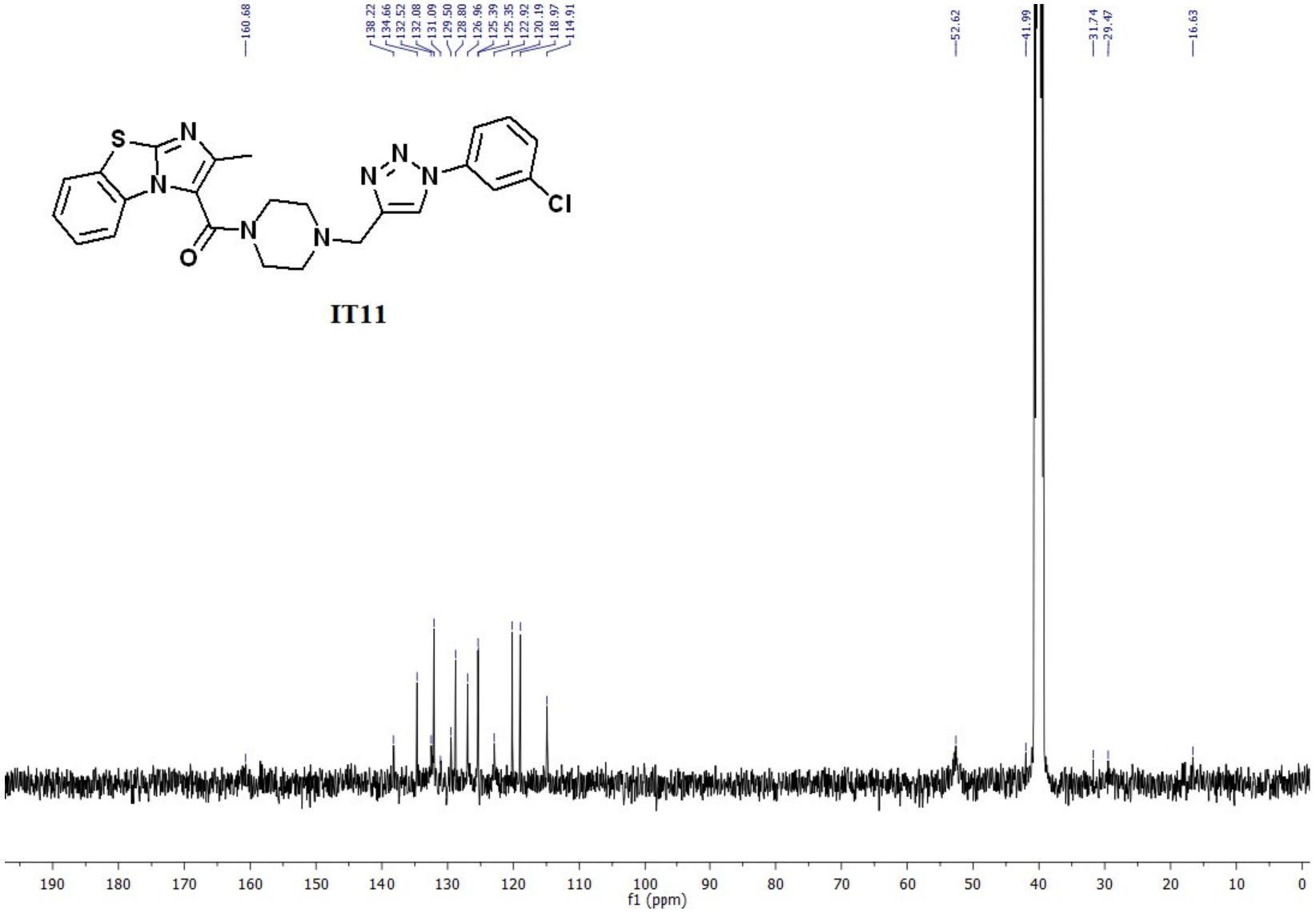

^{13}C NMR spectrum of compound **IT11** (DMSO-d_6 101 MHz)

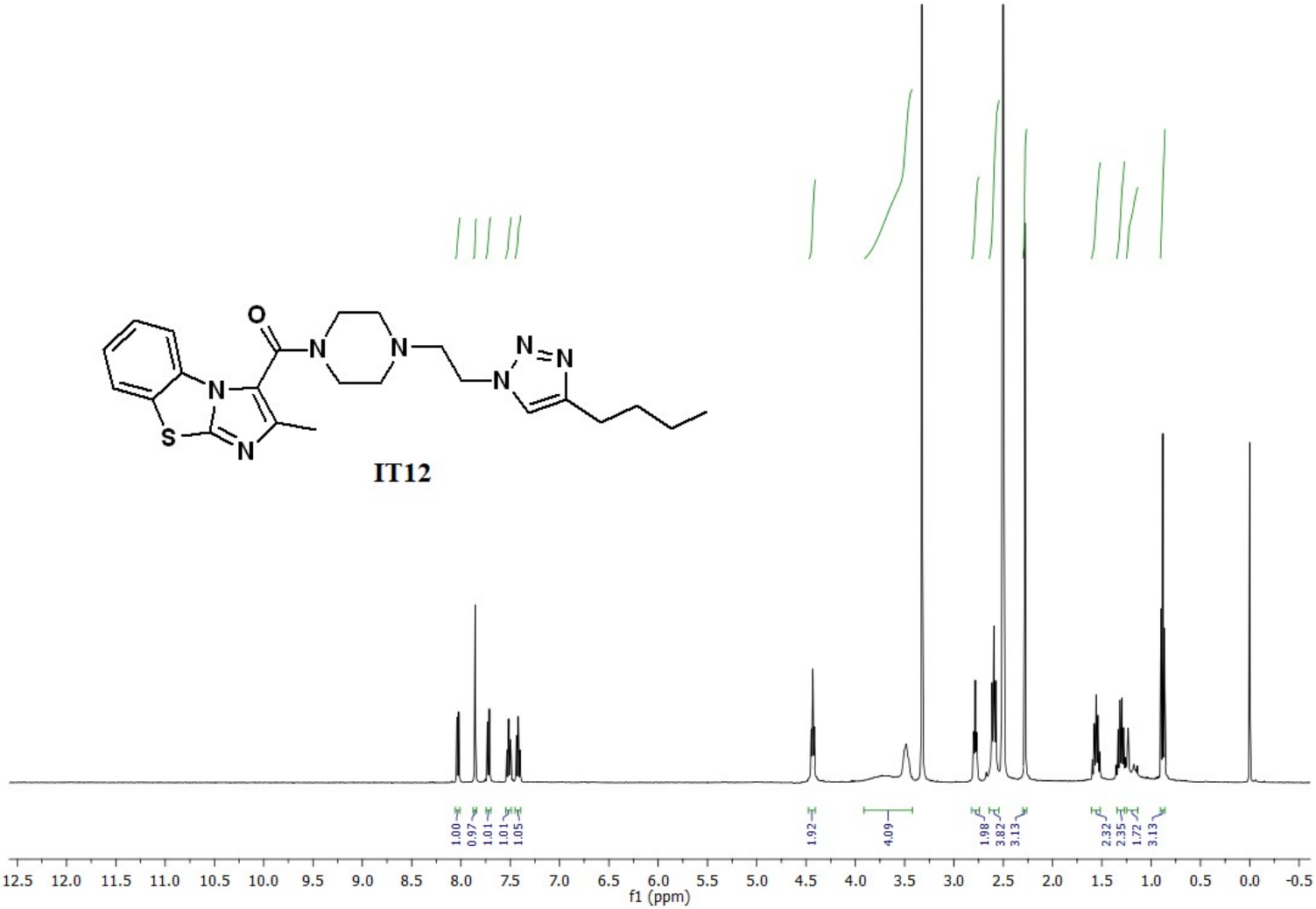

^{1}H NMR spectrum of compound **IT12 (**DMSO-d_6 400 MHz)

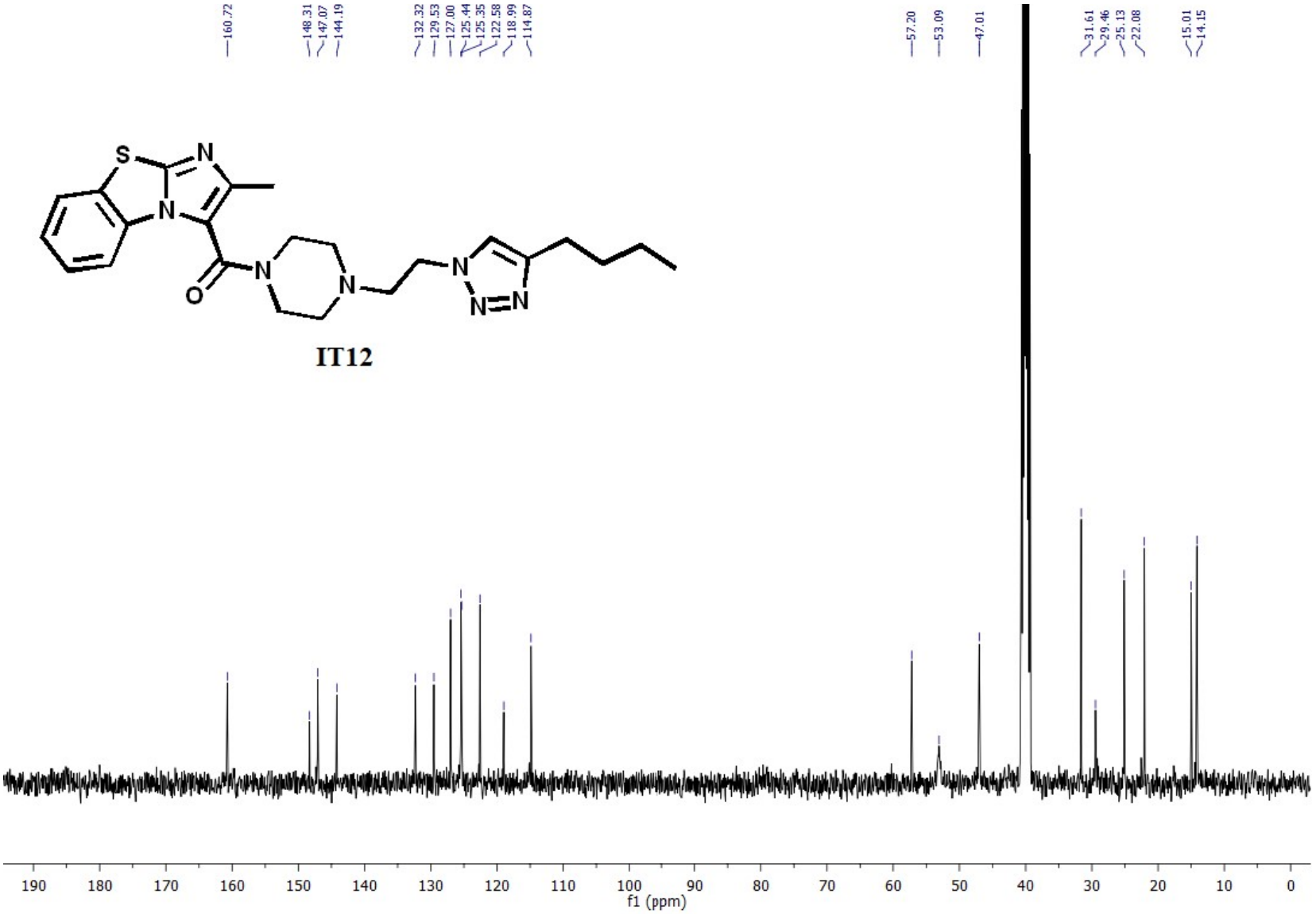

^{13}C NMR spectrum of compound **IT12** (DMSO-d_6 101 MHz)

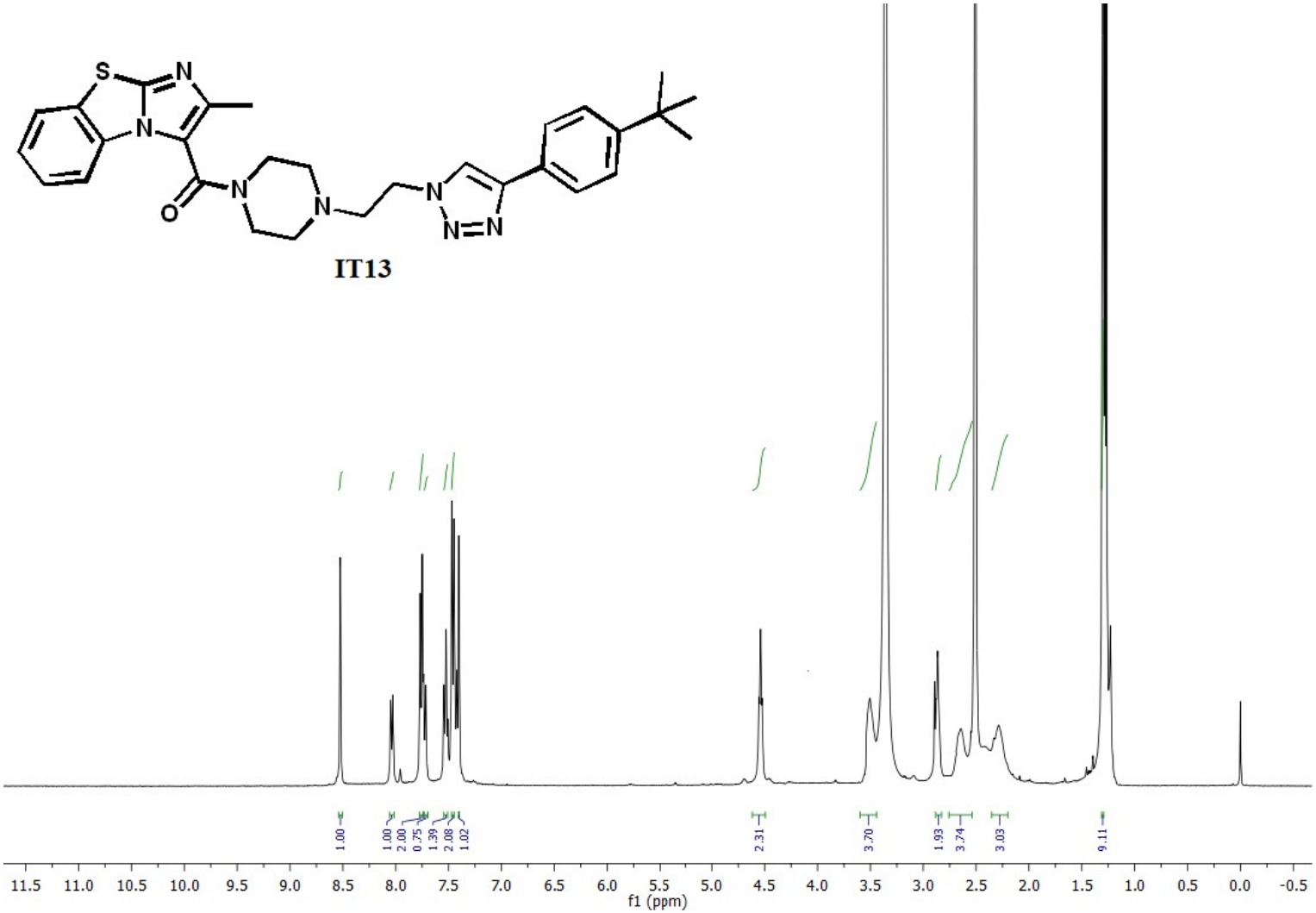

^{1}H NMR spectrum of compound **IT13 (**DMSO-d_6 400 MHz)

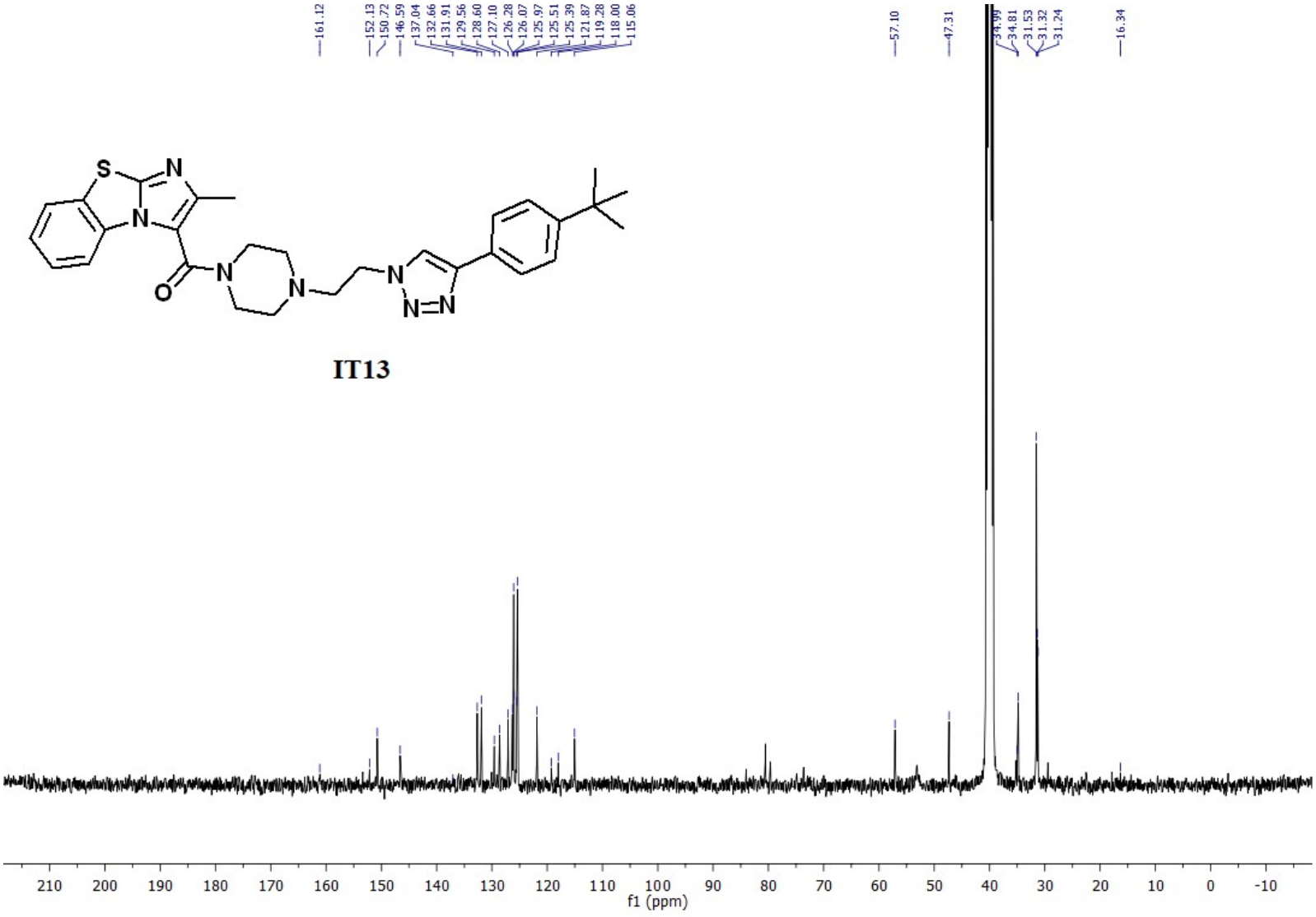

^{13}C NMR spectrum of compound **IT13** (DMSO-d_6 101 MHz)

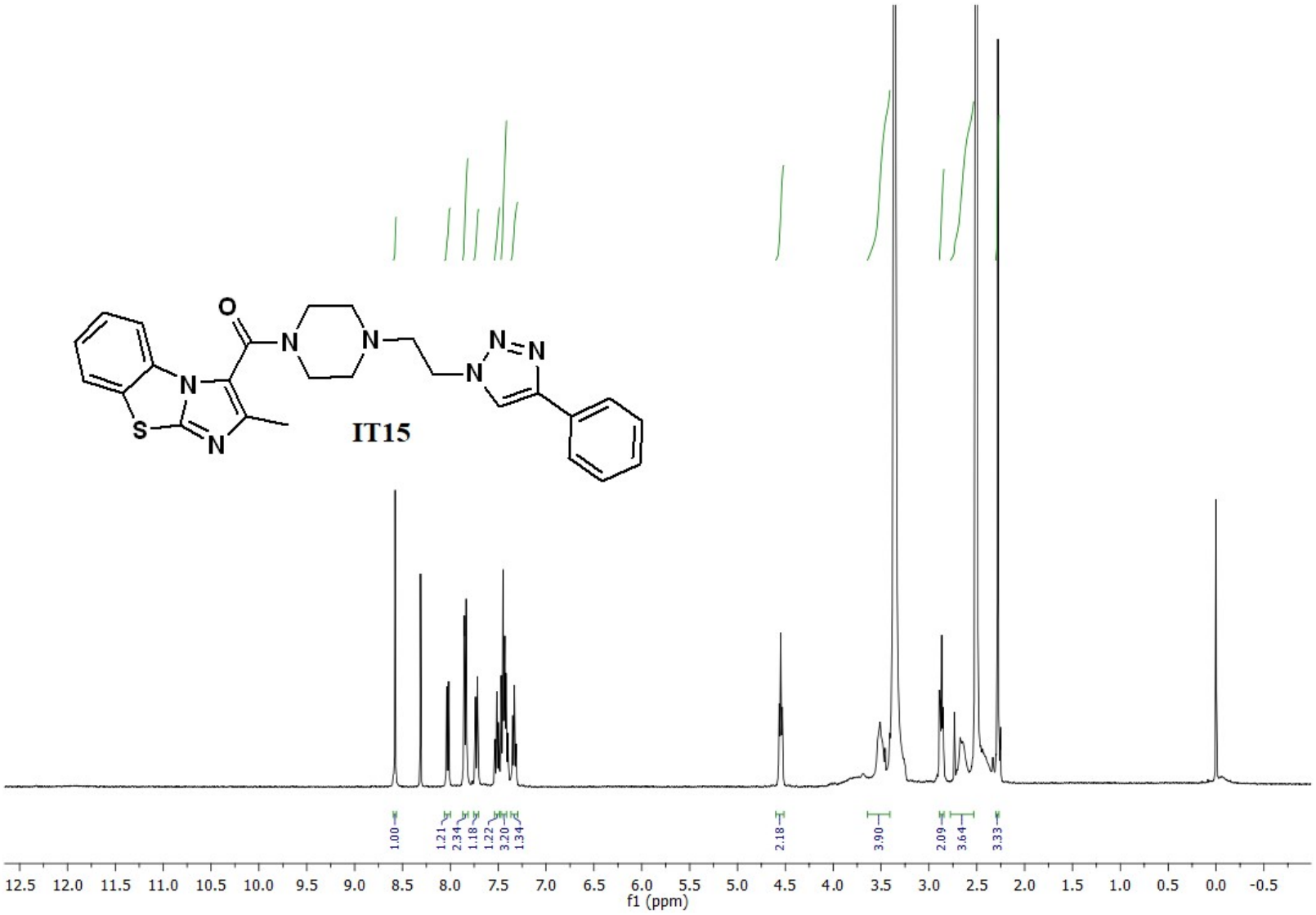

^{1}H NMR spectrum of compound **IT15 (**DMSO-d_6 400 MHz)

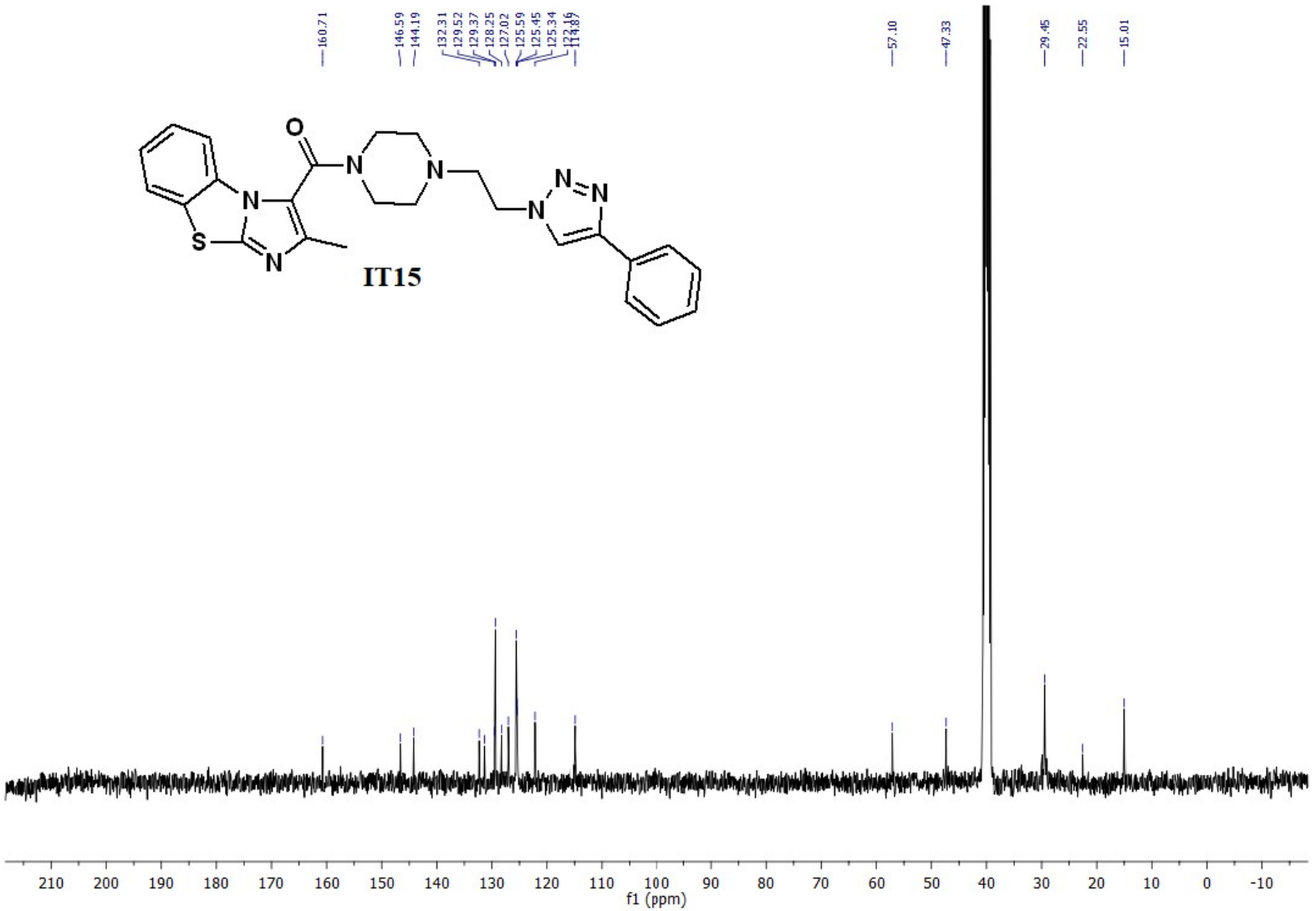

^{13}C NMR spectrum of compound **IT15** (DMSO-d_6 101 MHz)

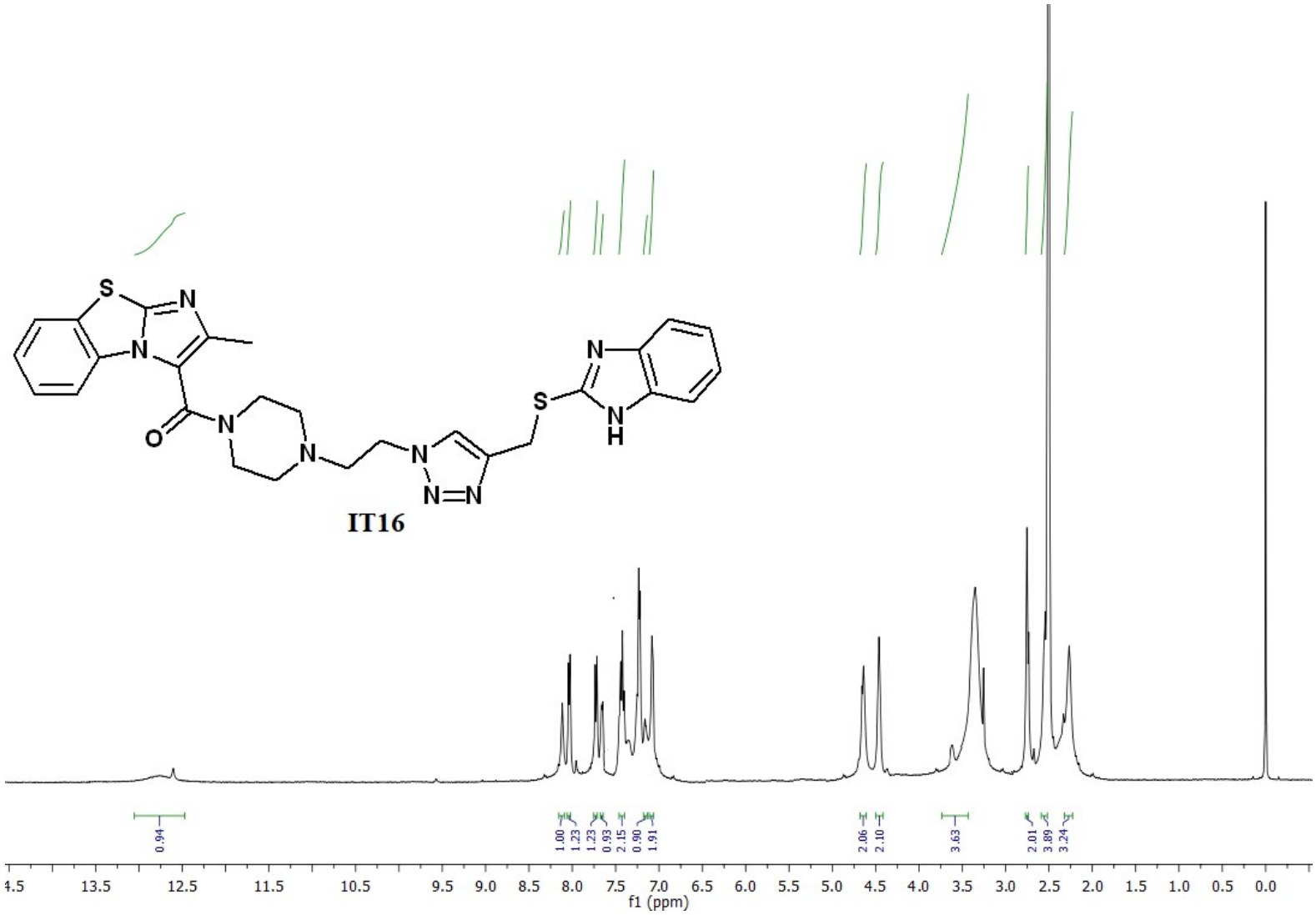

^{1}H NMR spectrum of compound **IT16 (**DMSO-d_6 400 MHz)

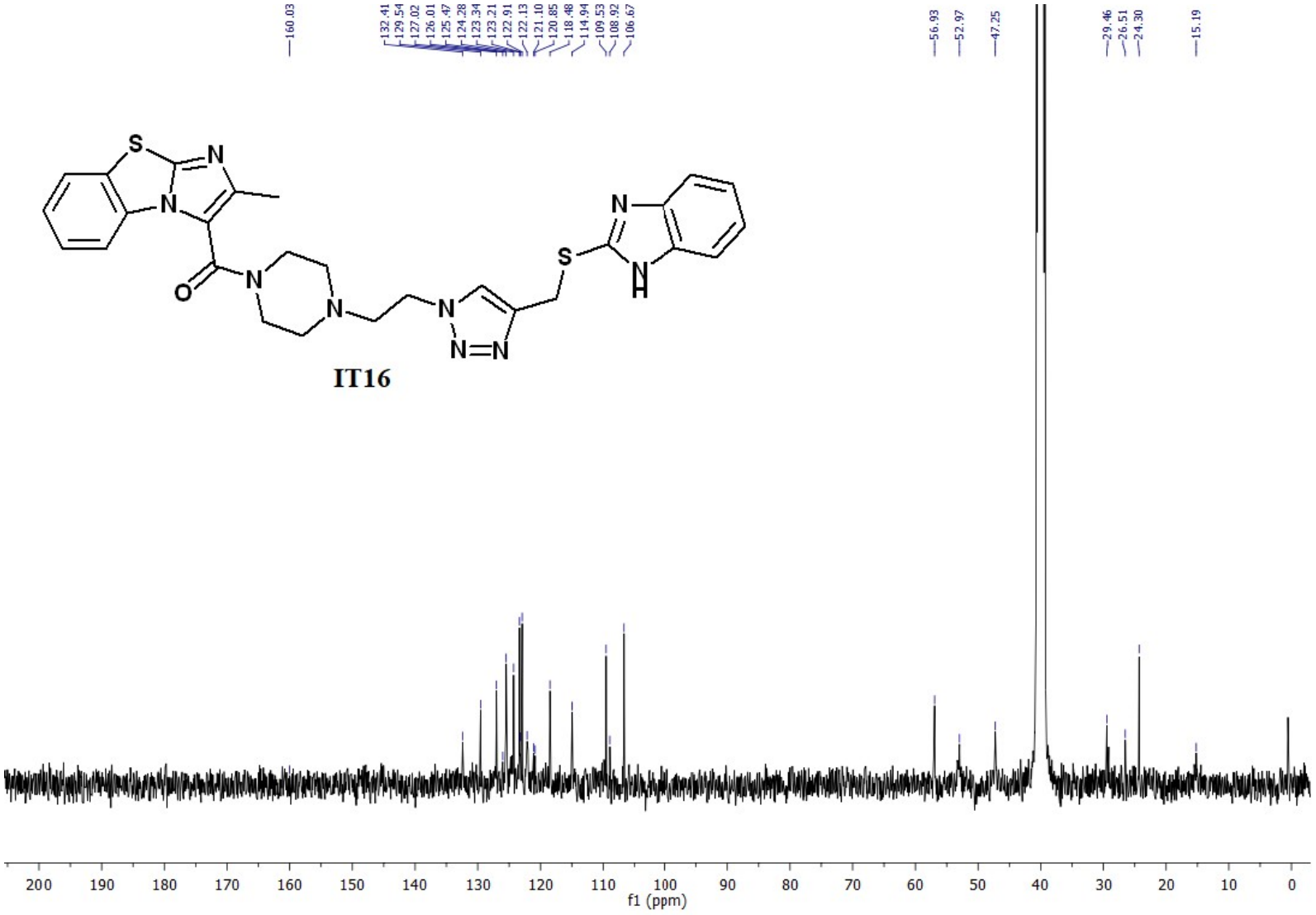

^{13}C NMR spectrum of compound **IT16** (DMSO-d_6 101 MHz)

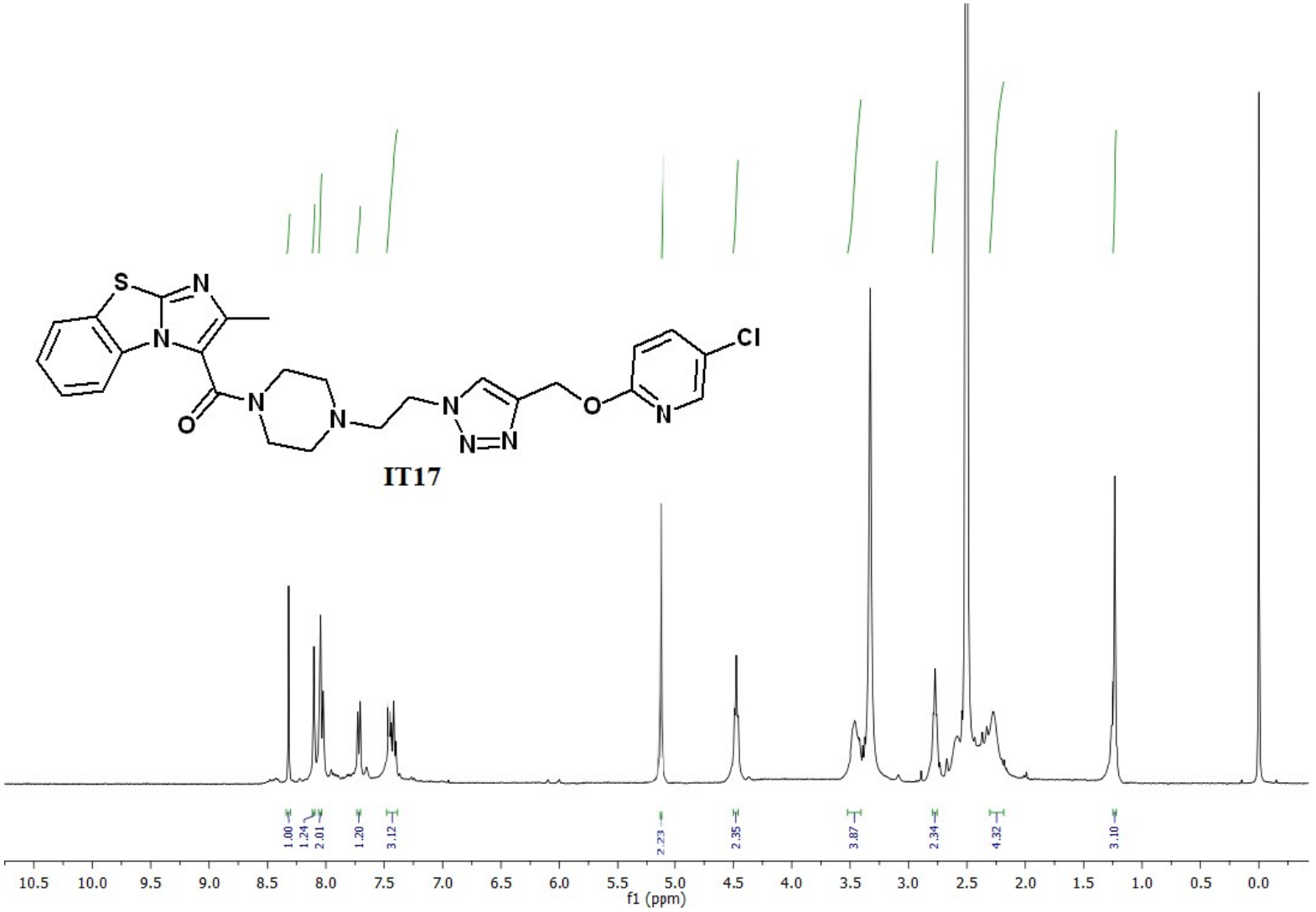

^{1}H NMR spectrum of compound **IT17 (**DMSO-d_6 400 MHz)

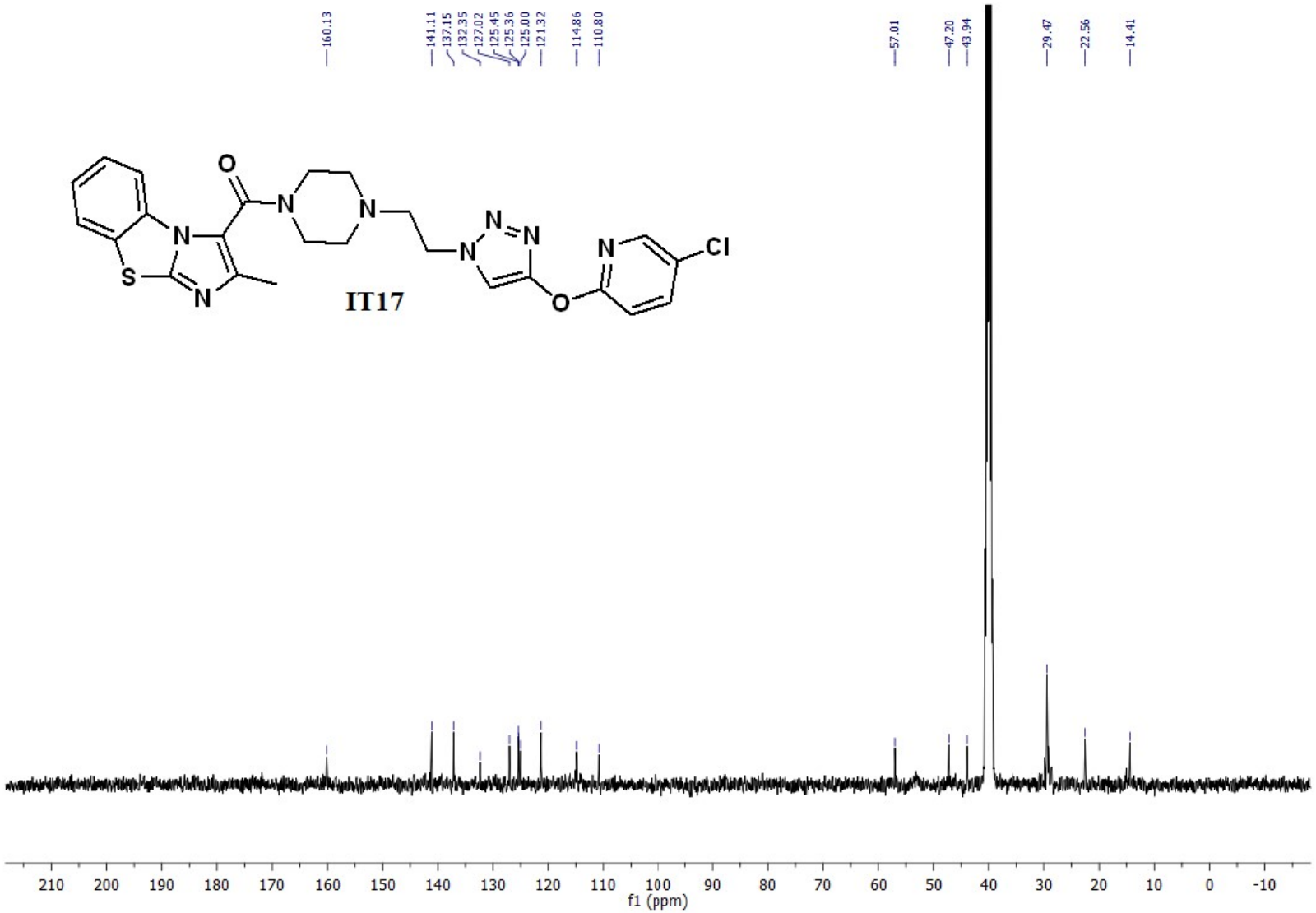

^{13}C NMR spectrum of compound **IT17** (DMSO-d_6 101 MHz)

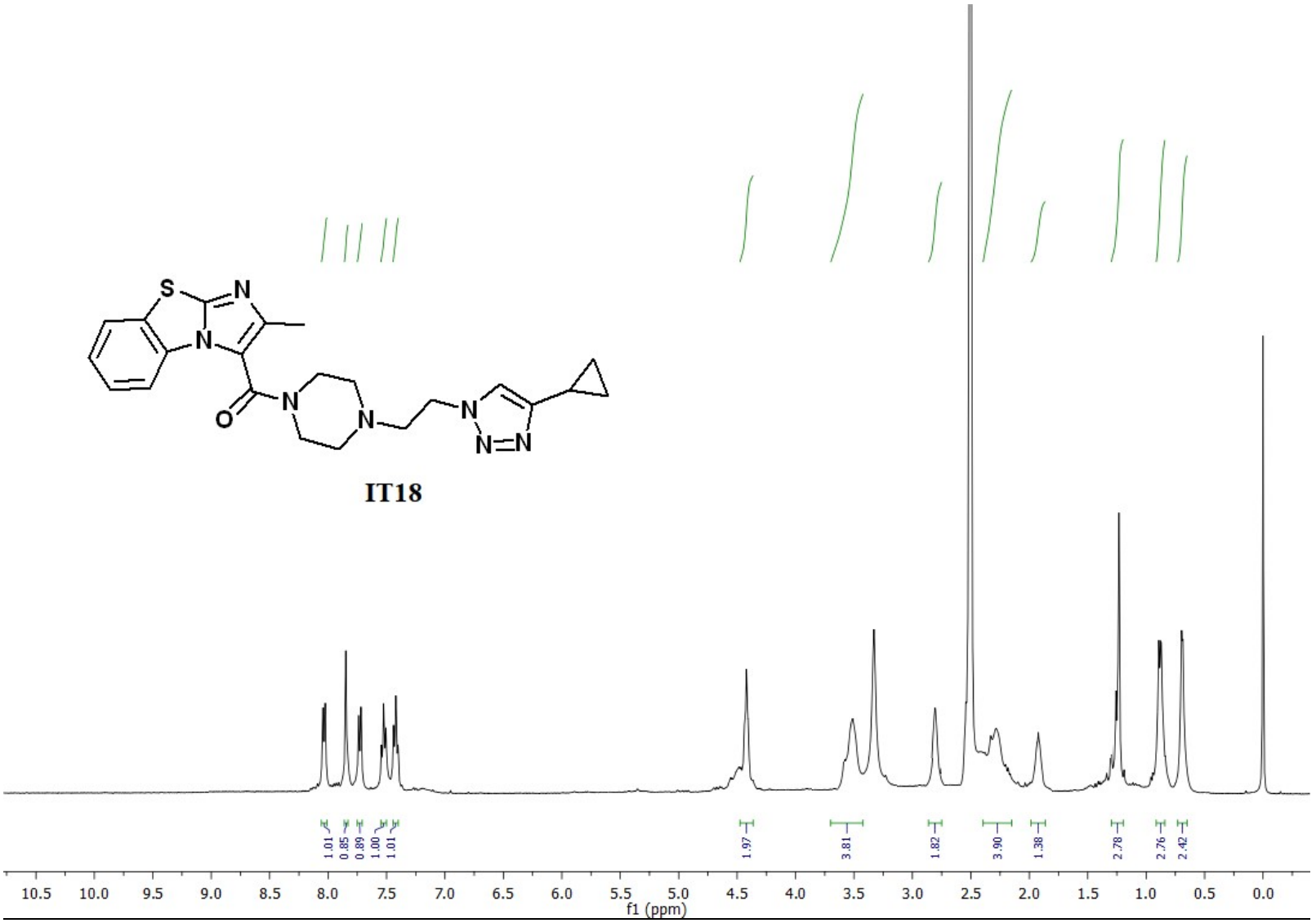

^{1}H NMR spectrum of compound **IT18 (**DMSO-d_6 400 MHz)

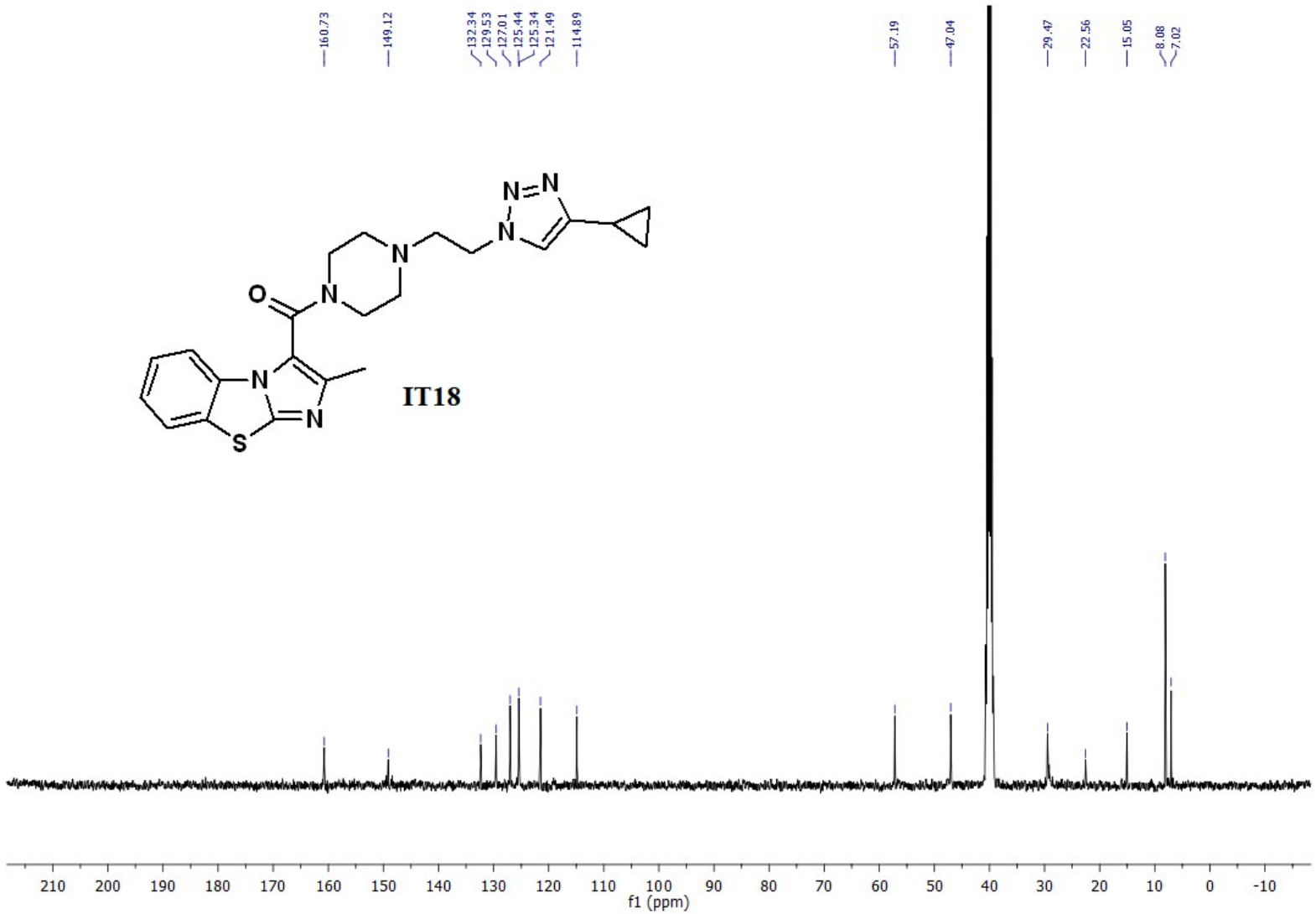

^{13}C NMR spectrum of compound **IT18** (DMSO-d_6 101 MHz)

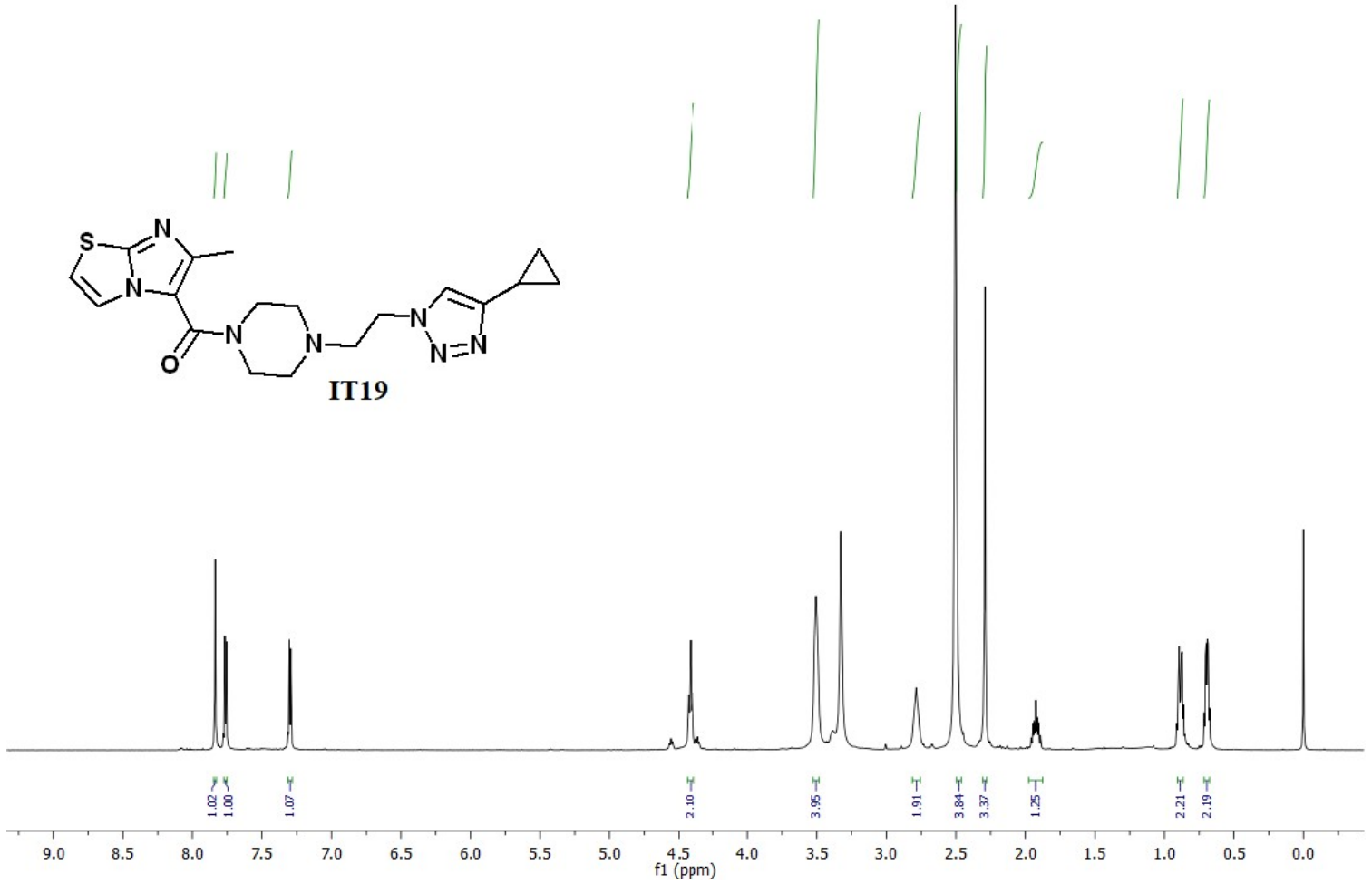

^{1}H NMR spectrum of compound **IT19 (**DMSO-d_6 400 MHz)

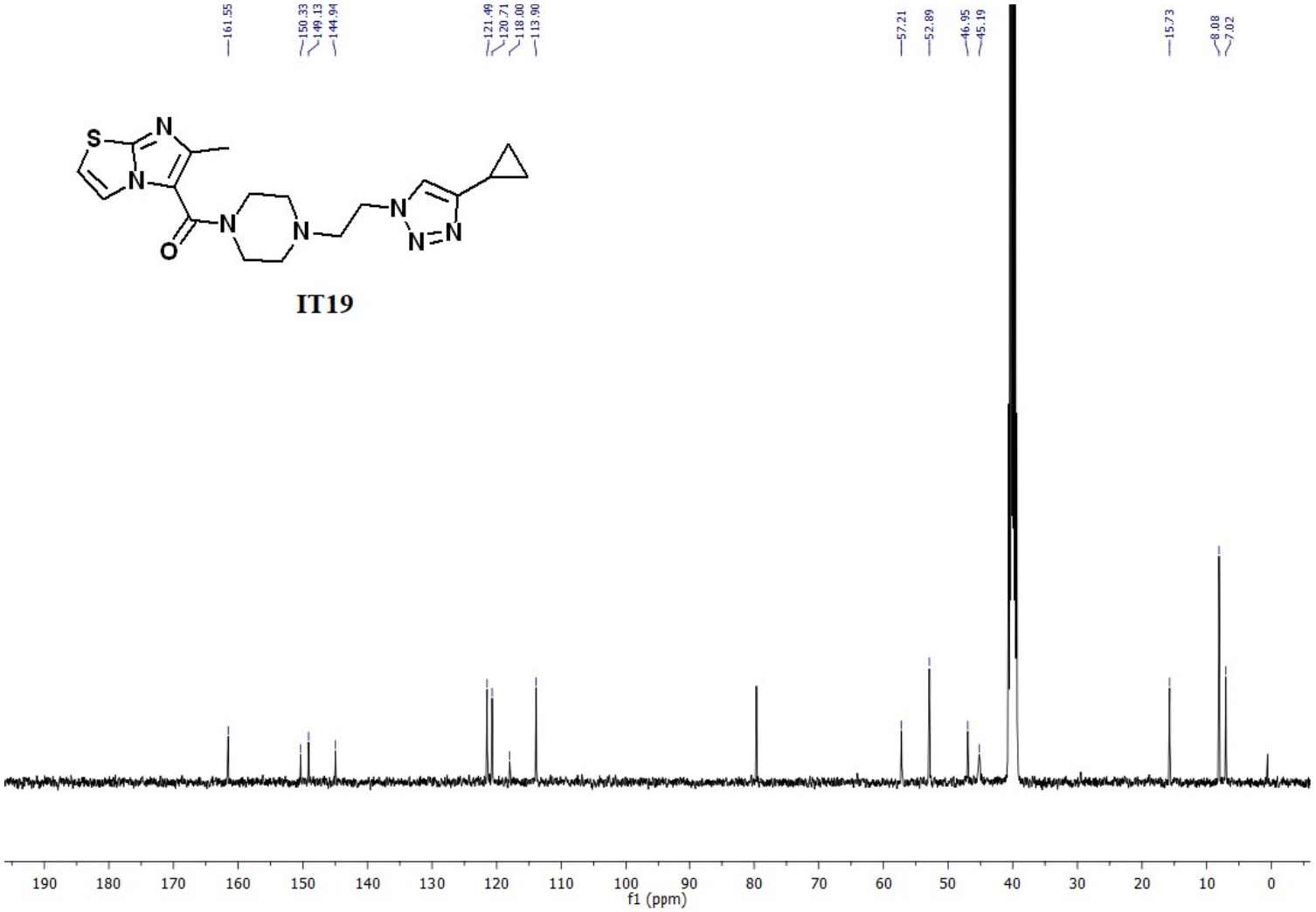

^{13}C NMR spectrum of compound **IT19** (DMSO-d_6 101 MHz)

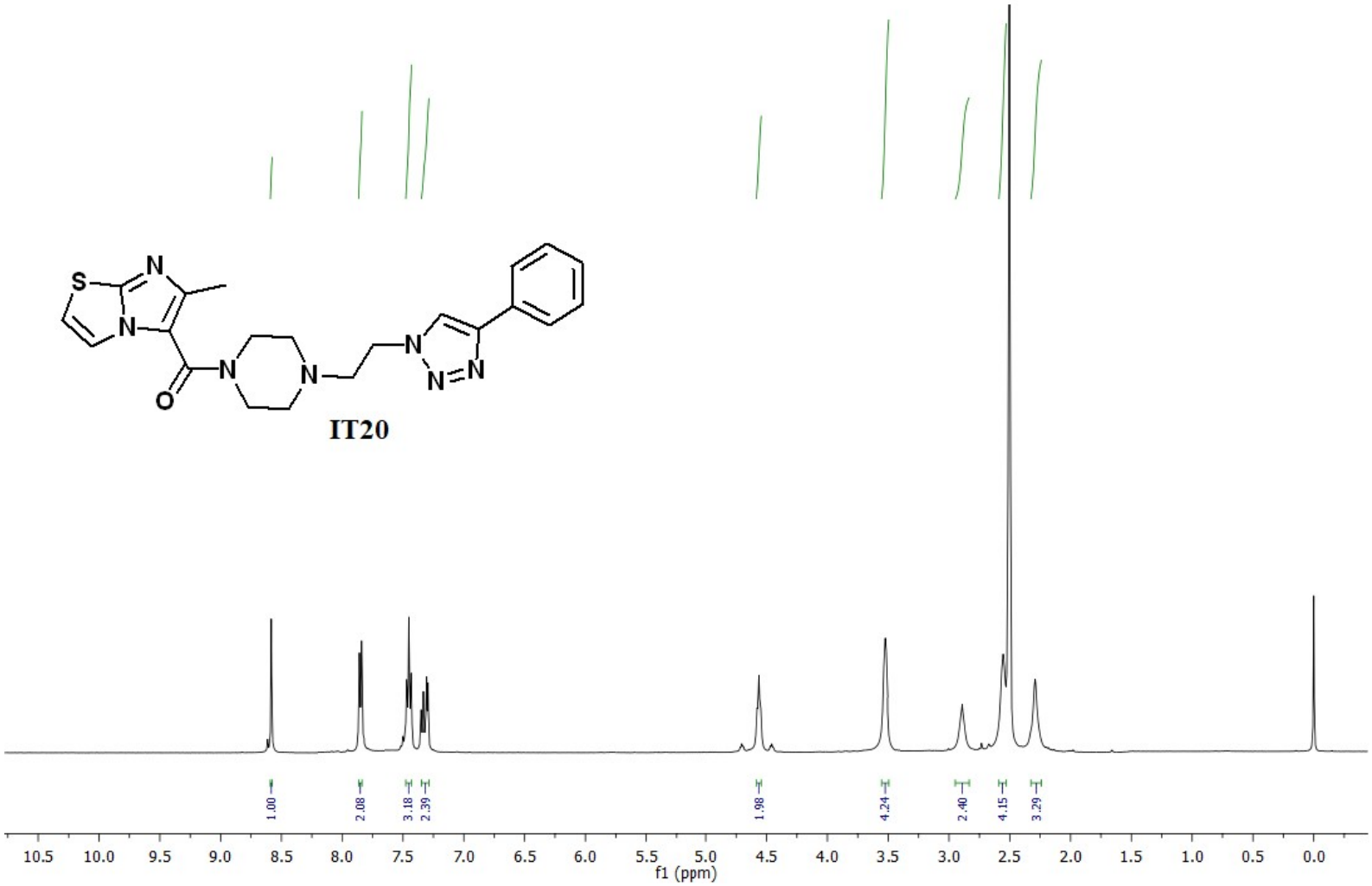

^{1}H NMR spectrum of compound **IT20 (**DMSO-d_6 400 MHz)

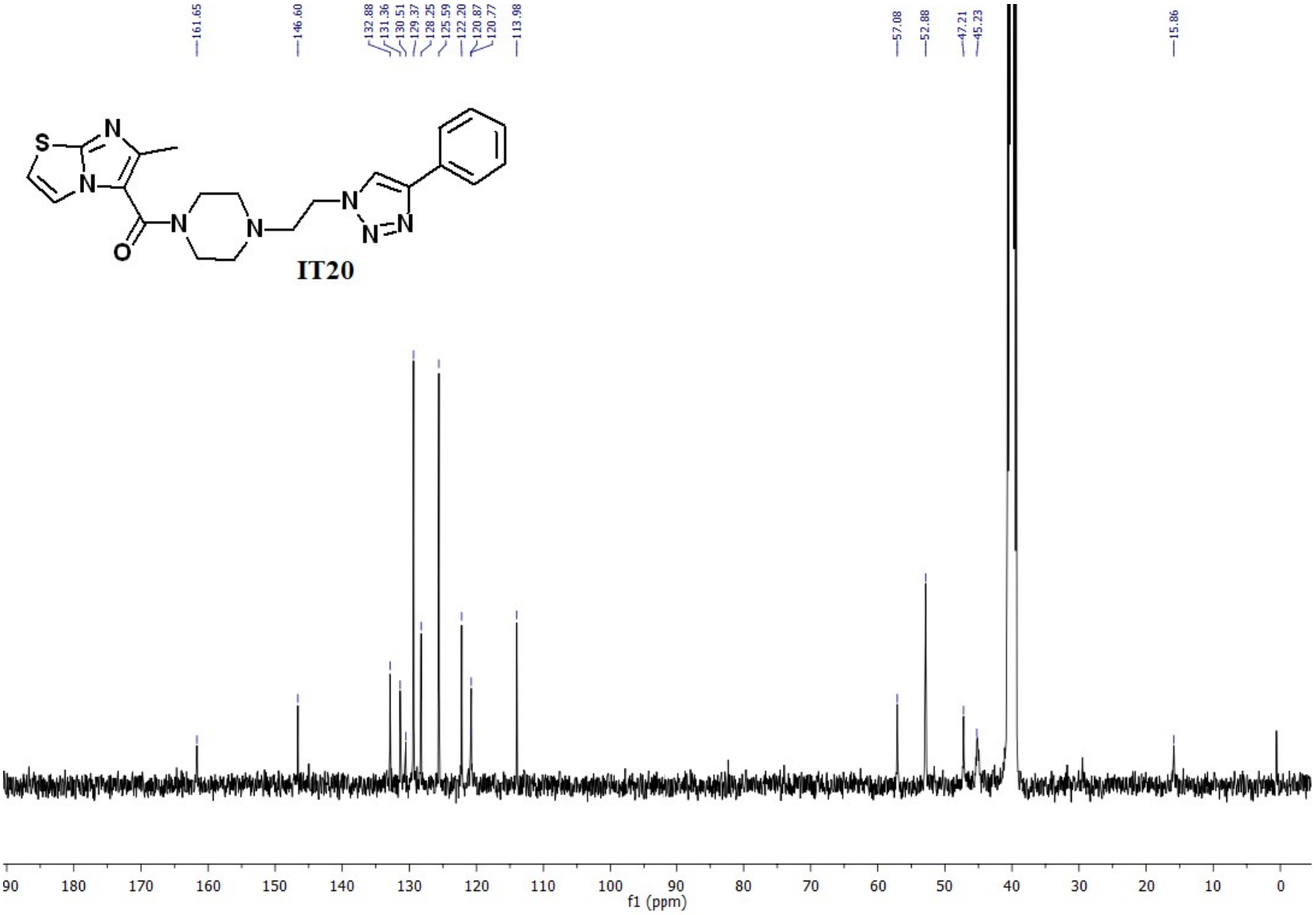

^{13}C NMR spectrum of compound **IT20** (DMSO-d_6 101 MHz)

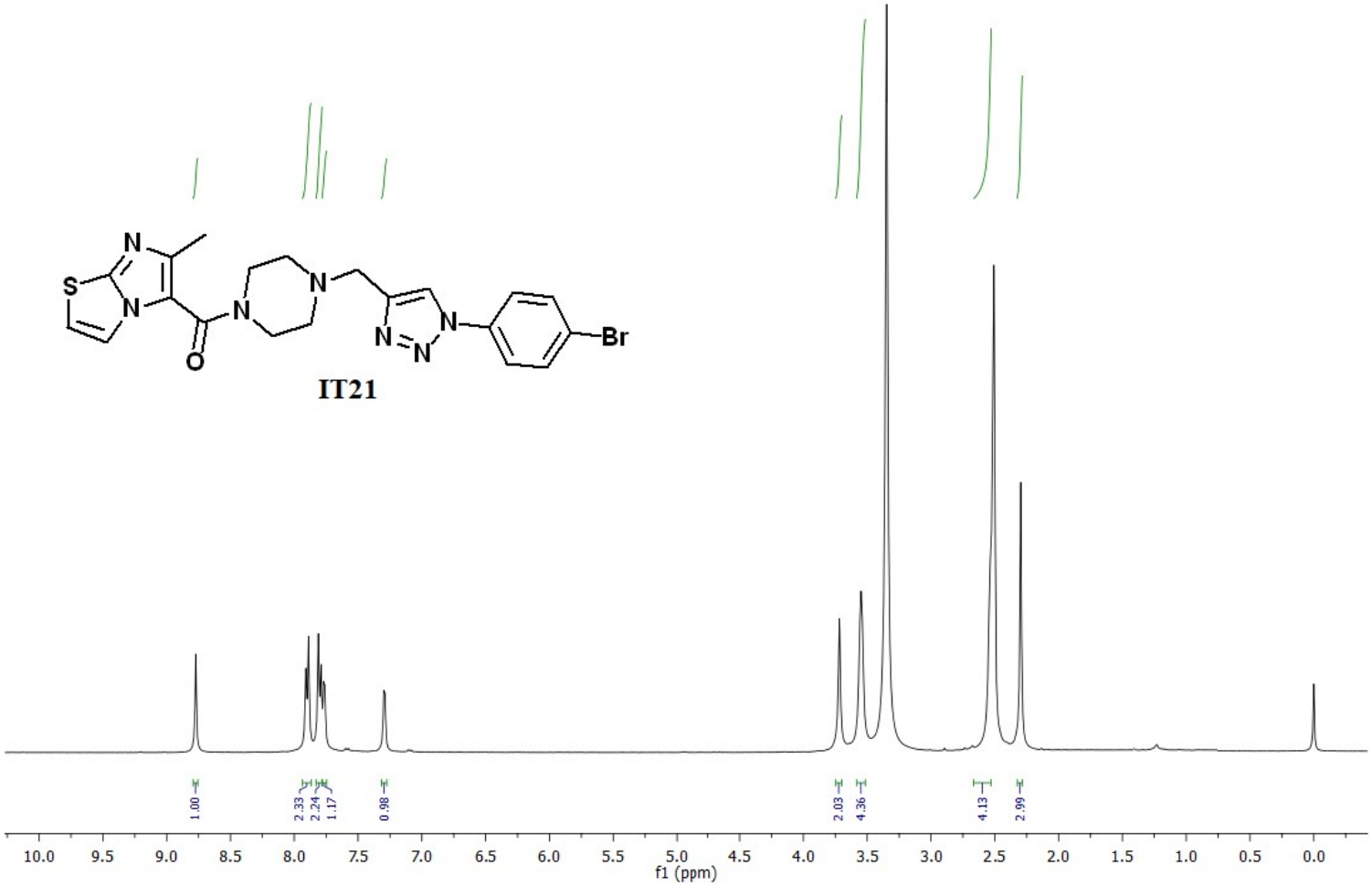

^{1}H NMR spectrum of compound **IT21 (**DMSO-d_6 400 MHz)

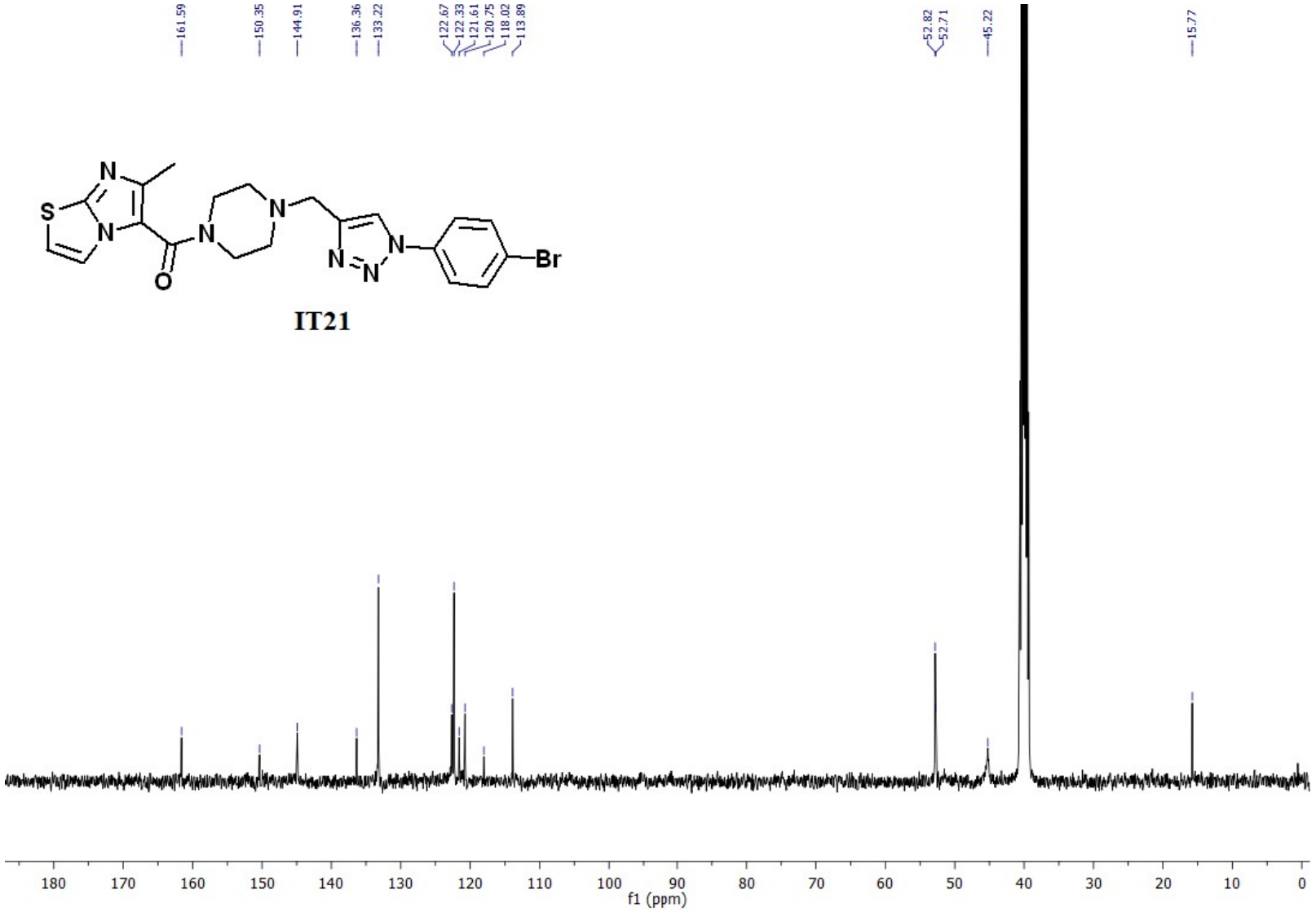

^{13}C NMR spectrum of compound **IT21** (DMSO-d_6 101 MHz)

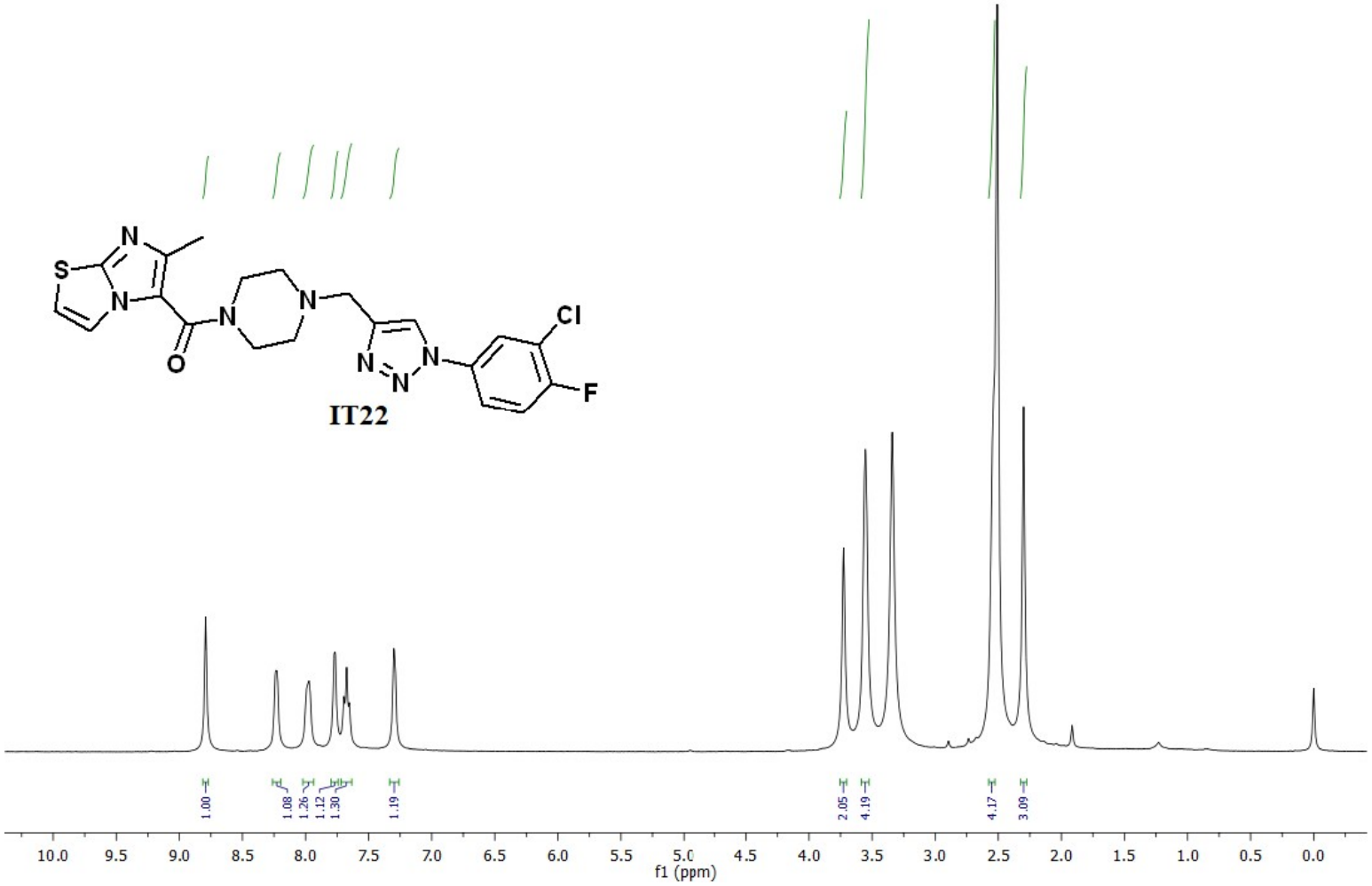

^{1}H NMR spectrum of compound **IT22 (**DMSO-d_6 400 MHz)

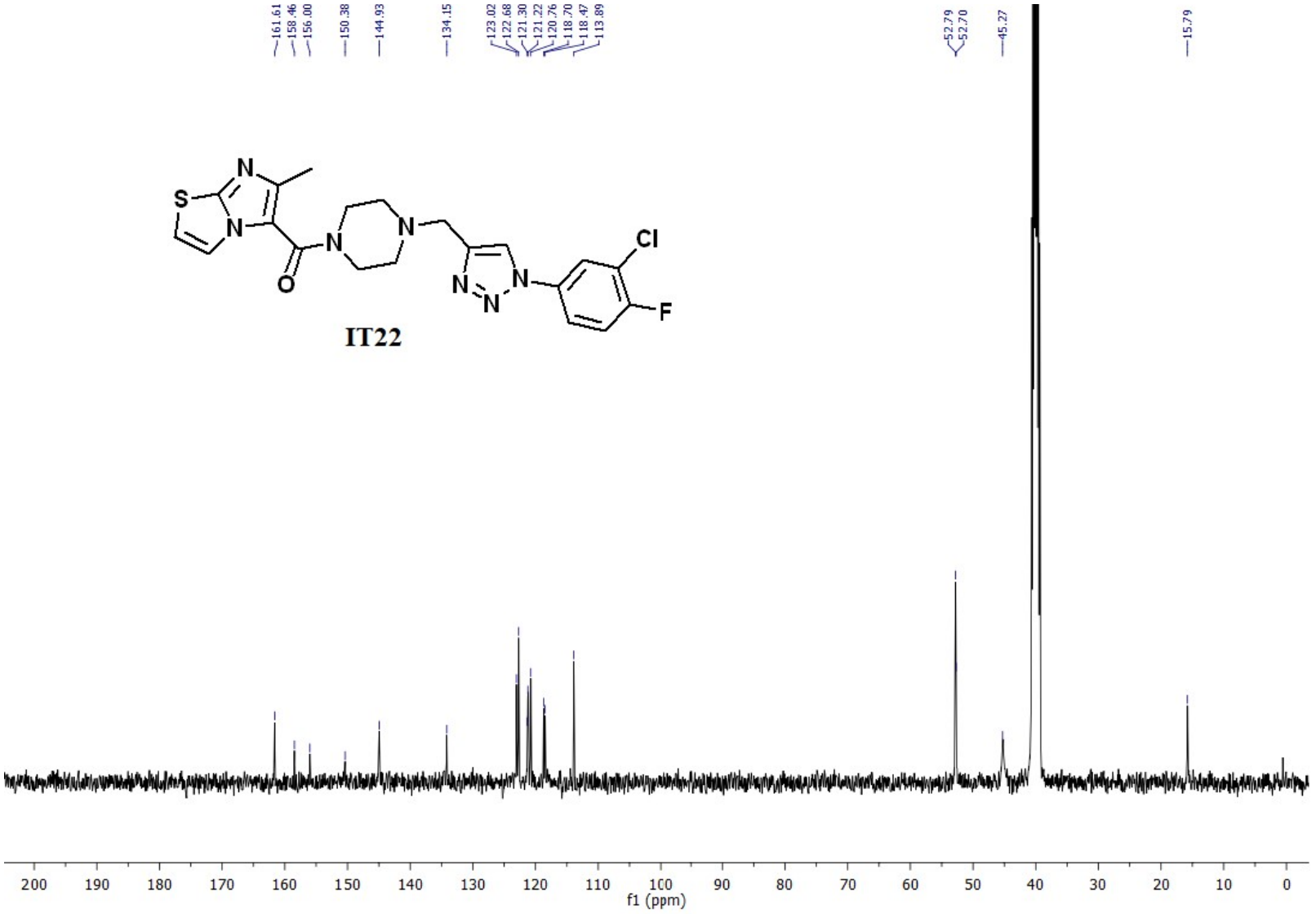

^{13}C NMR spectrum of compound **IT22** (DMSO-d_6 101 MHz)

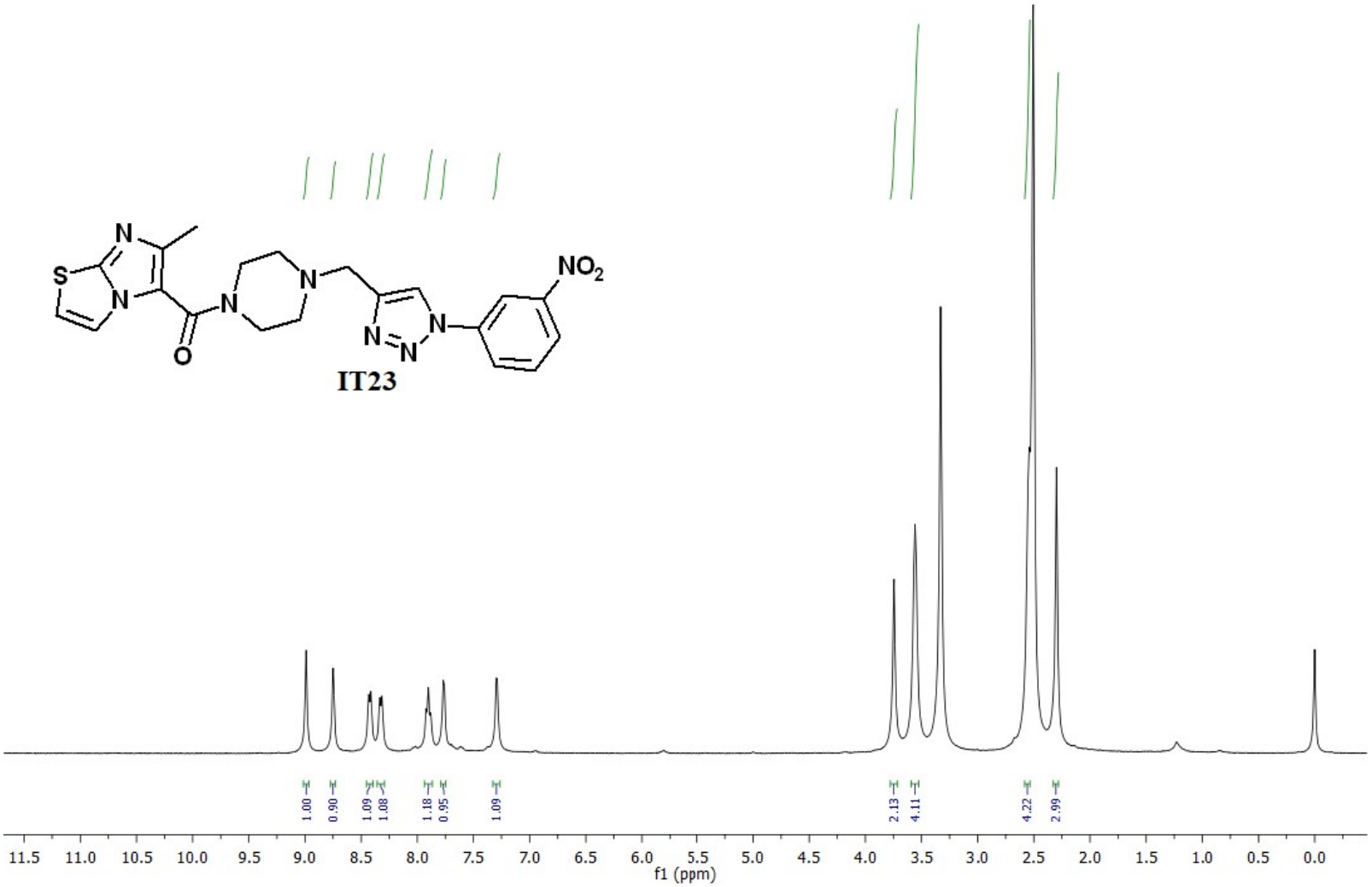

^{1}H NMR spectrum of compound **IT23 (**DMSO-d_6 400 MHz)

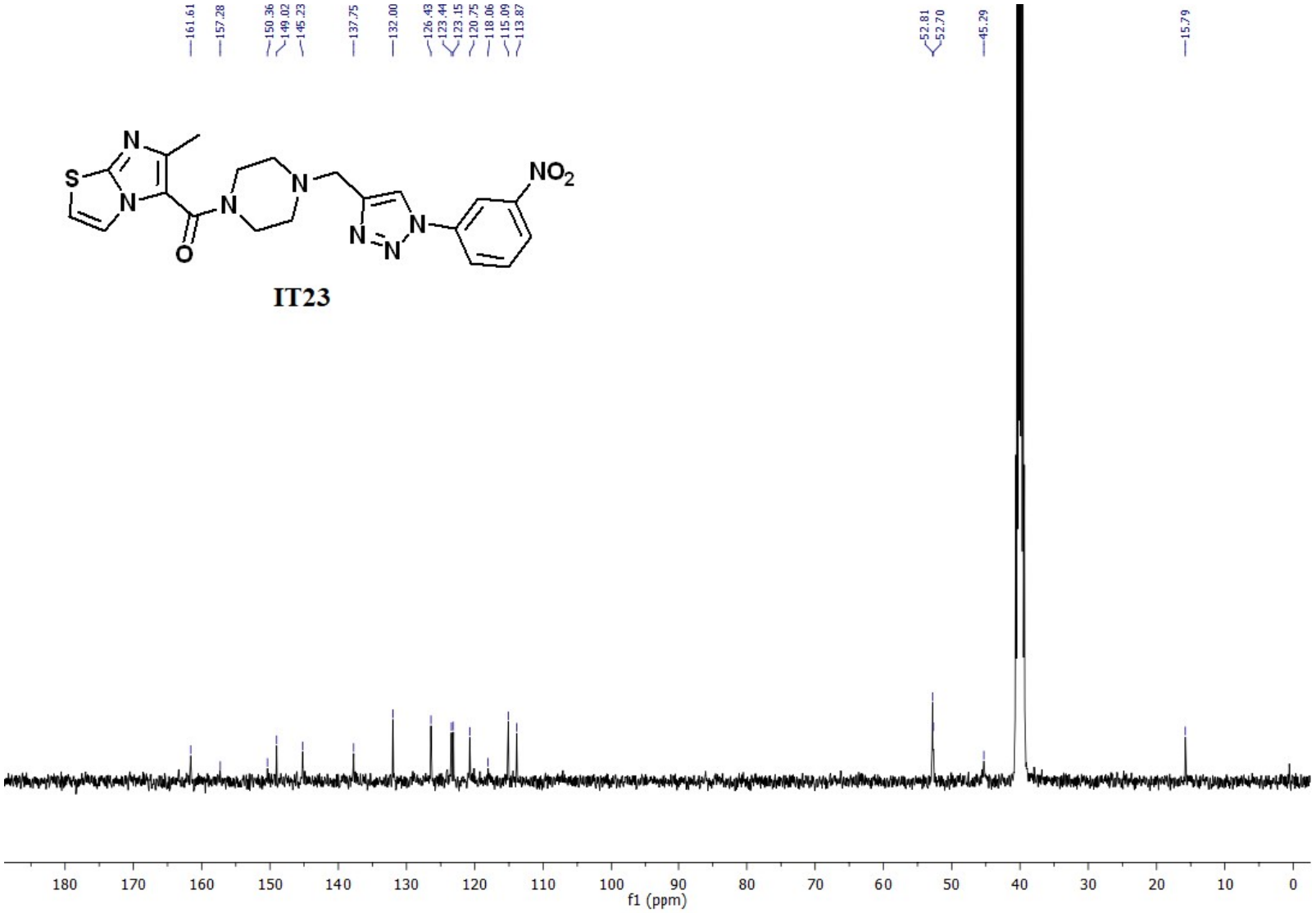

^{13}C NMR spectrum of compound **IT23** (DMSO-d_6 101 MHz)

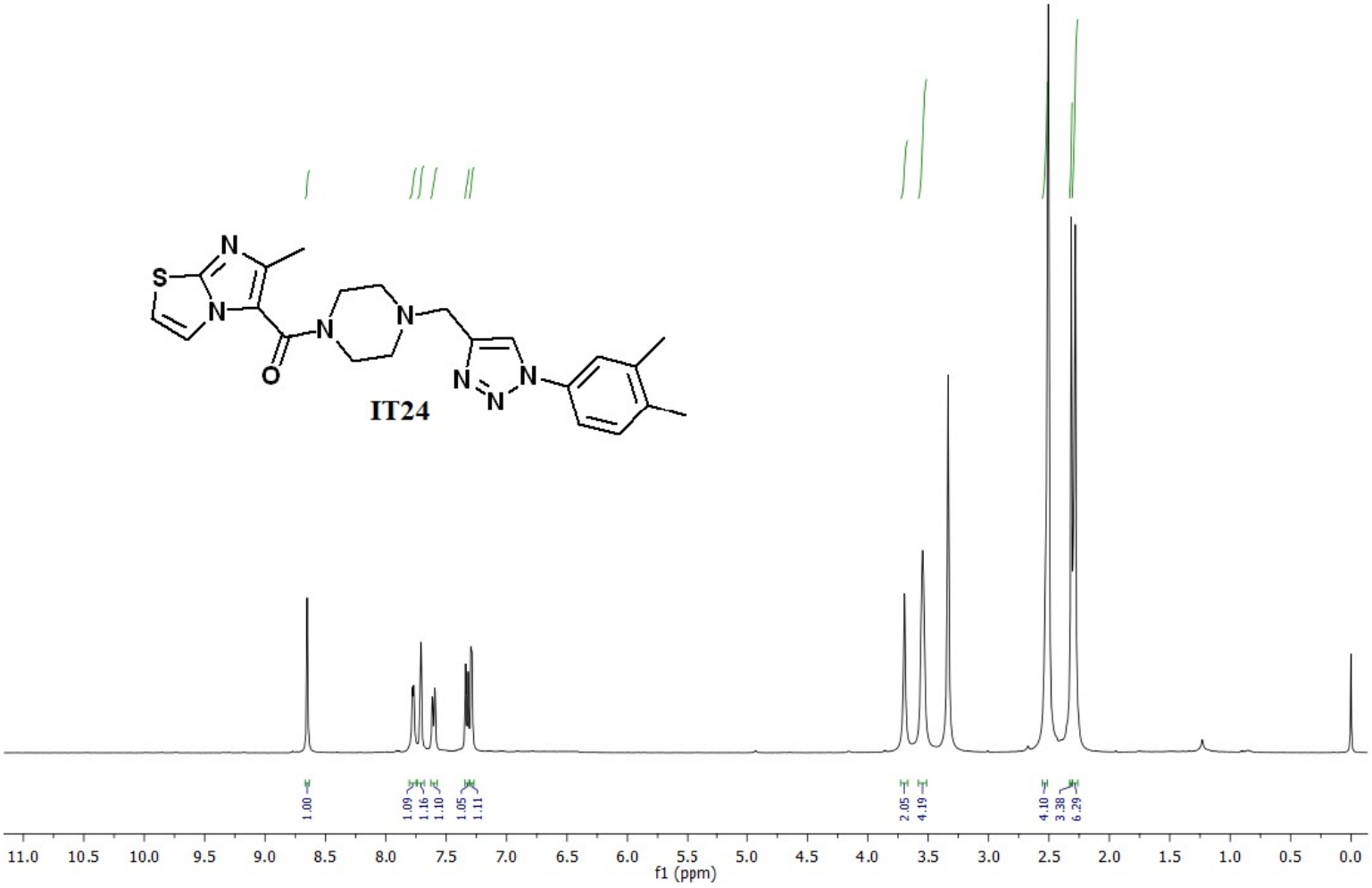

^{1}H NMR spectrum of compound **IT24 (**DMSO-d_6 400 MHz)

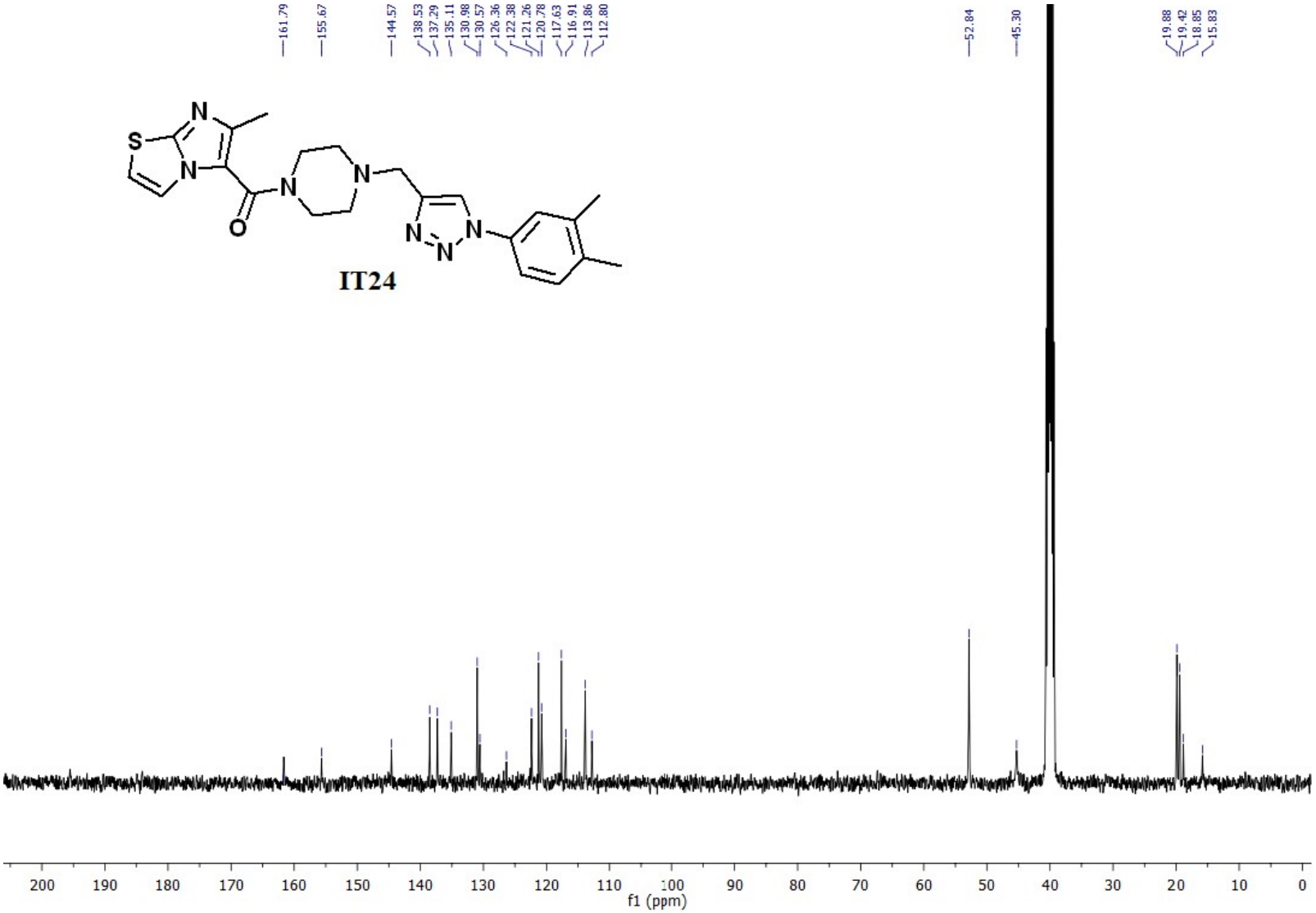

^{13}C NMR spectrum of compound **IT24** (DMSO-d_6 101 MHz)

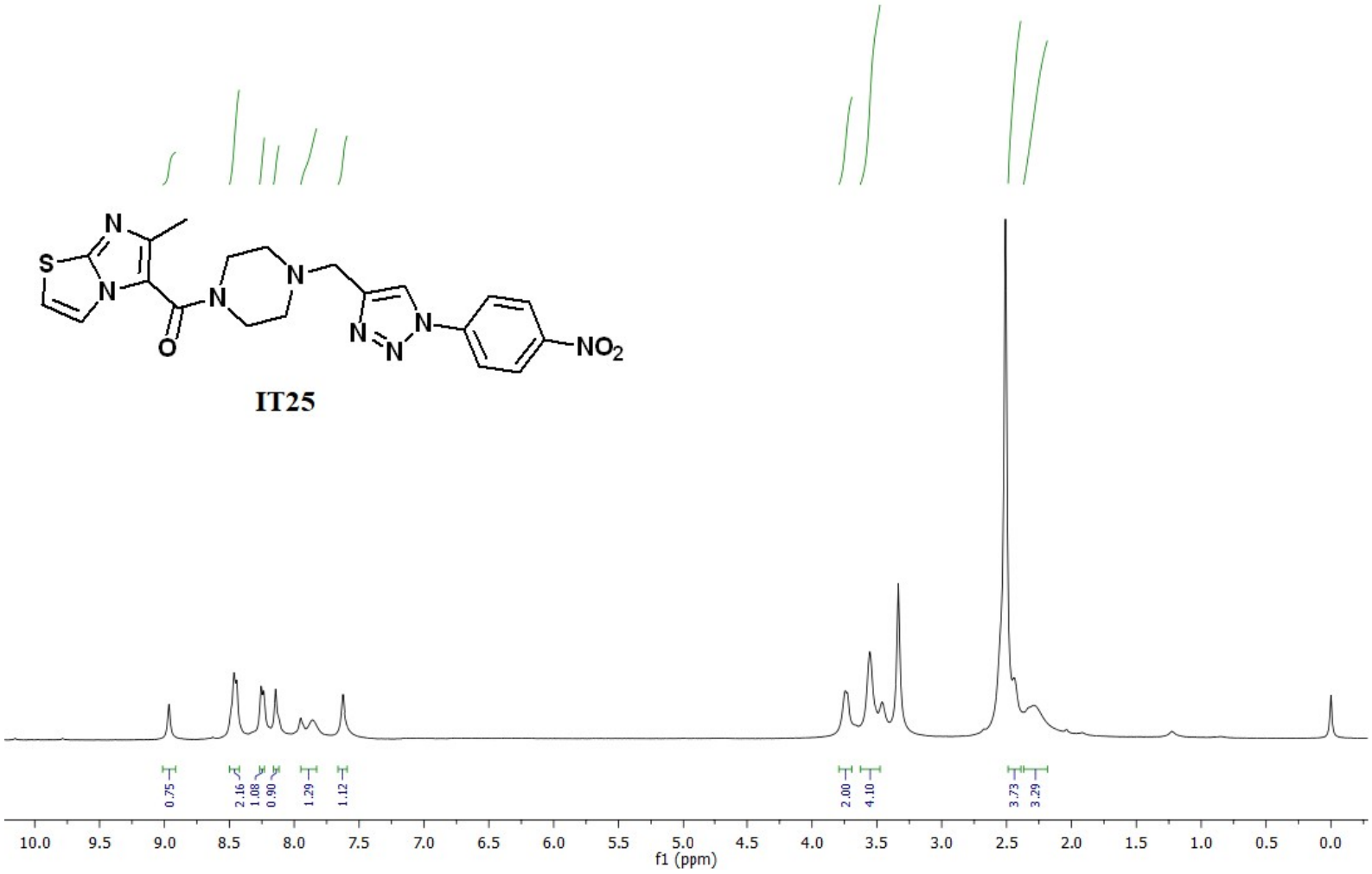

^{1}H NMR spectrum of compound **IT25 (**DMSO-d_6 400 MHz)

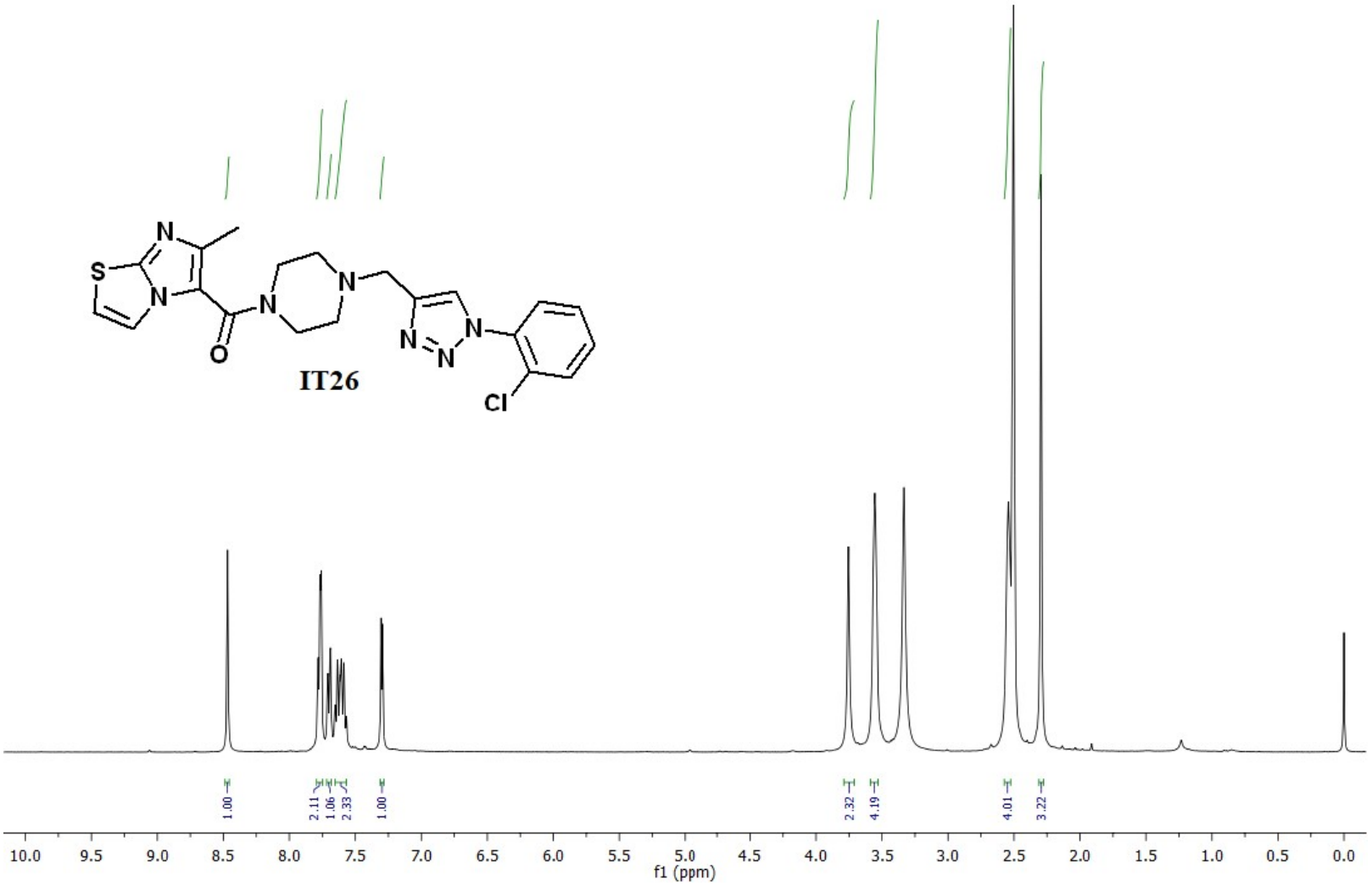

^{1}H NMR spectrum of compound **IT26 (**DMSO-d_6 400 MHz)

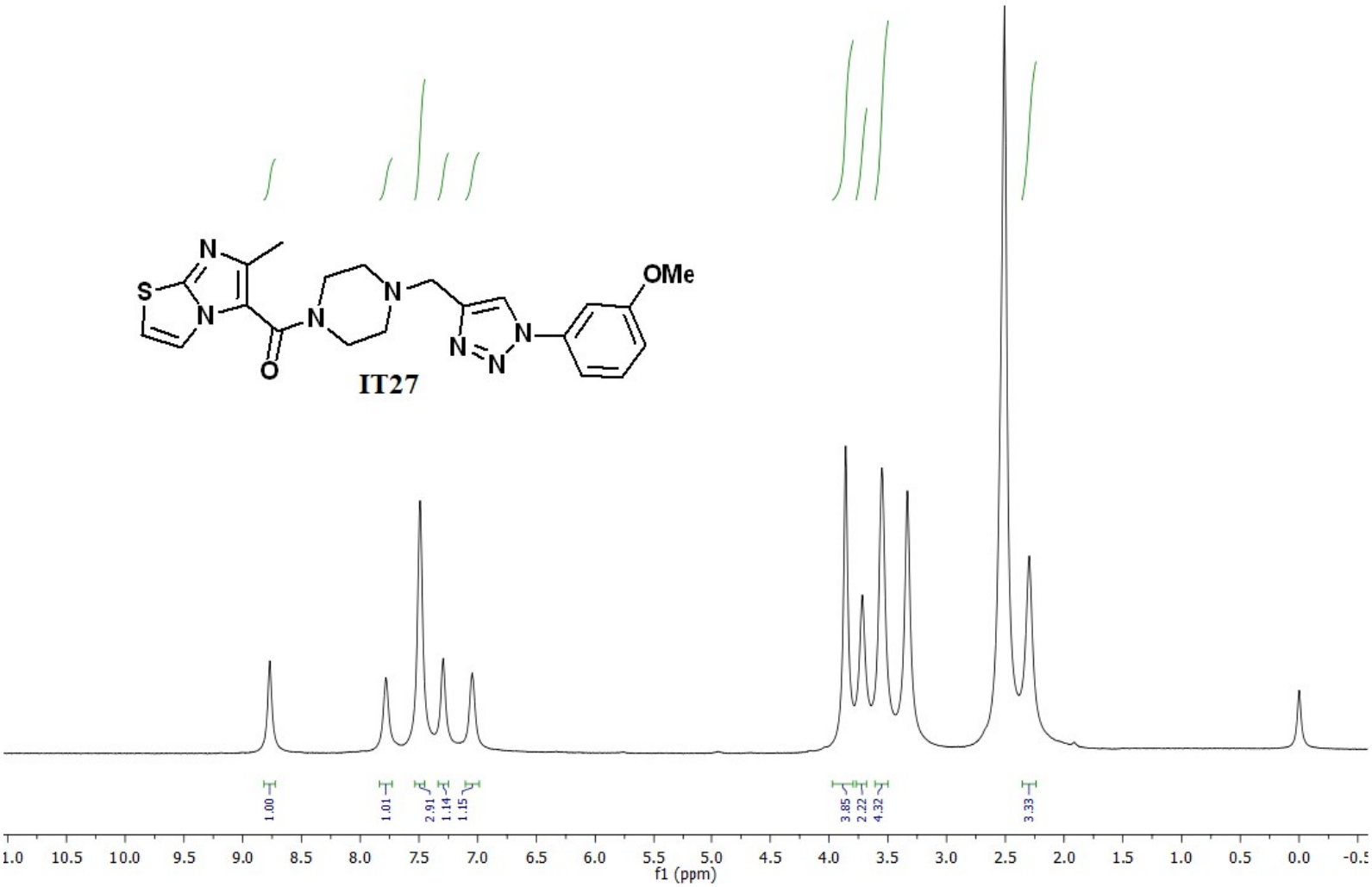

^{1}H NMR spectrum of compound **IT27 (**DMSO-d_6 400 MHz)

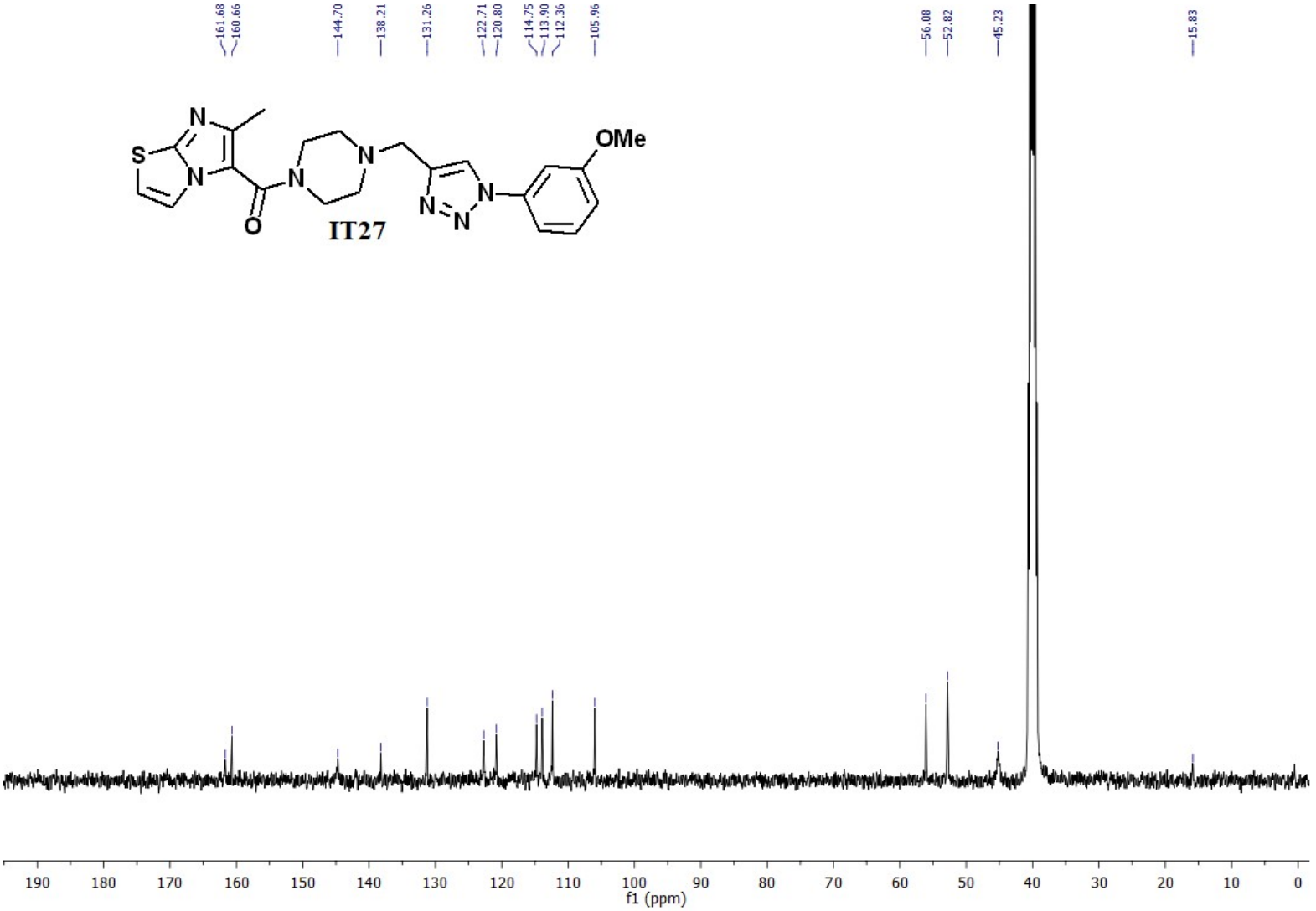

^{13}C NMR spectrum of compound **IT27** (DMSO-d_6 101 MHz)

4.0. ESI MS spectra of IT series compounds

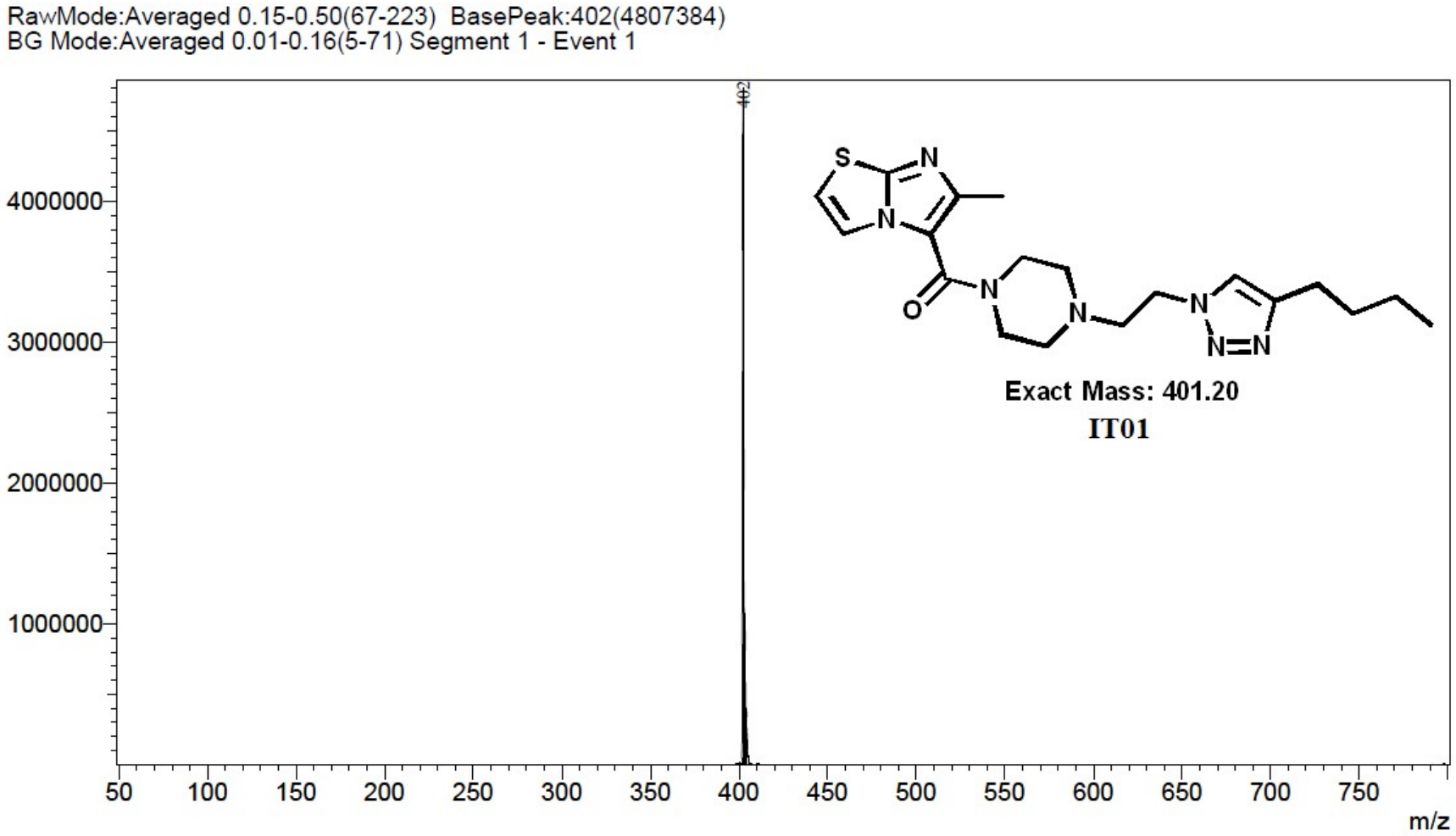

ESI MS spectrum of compound **IT01**

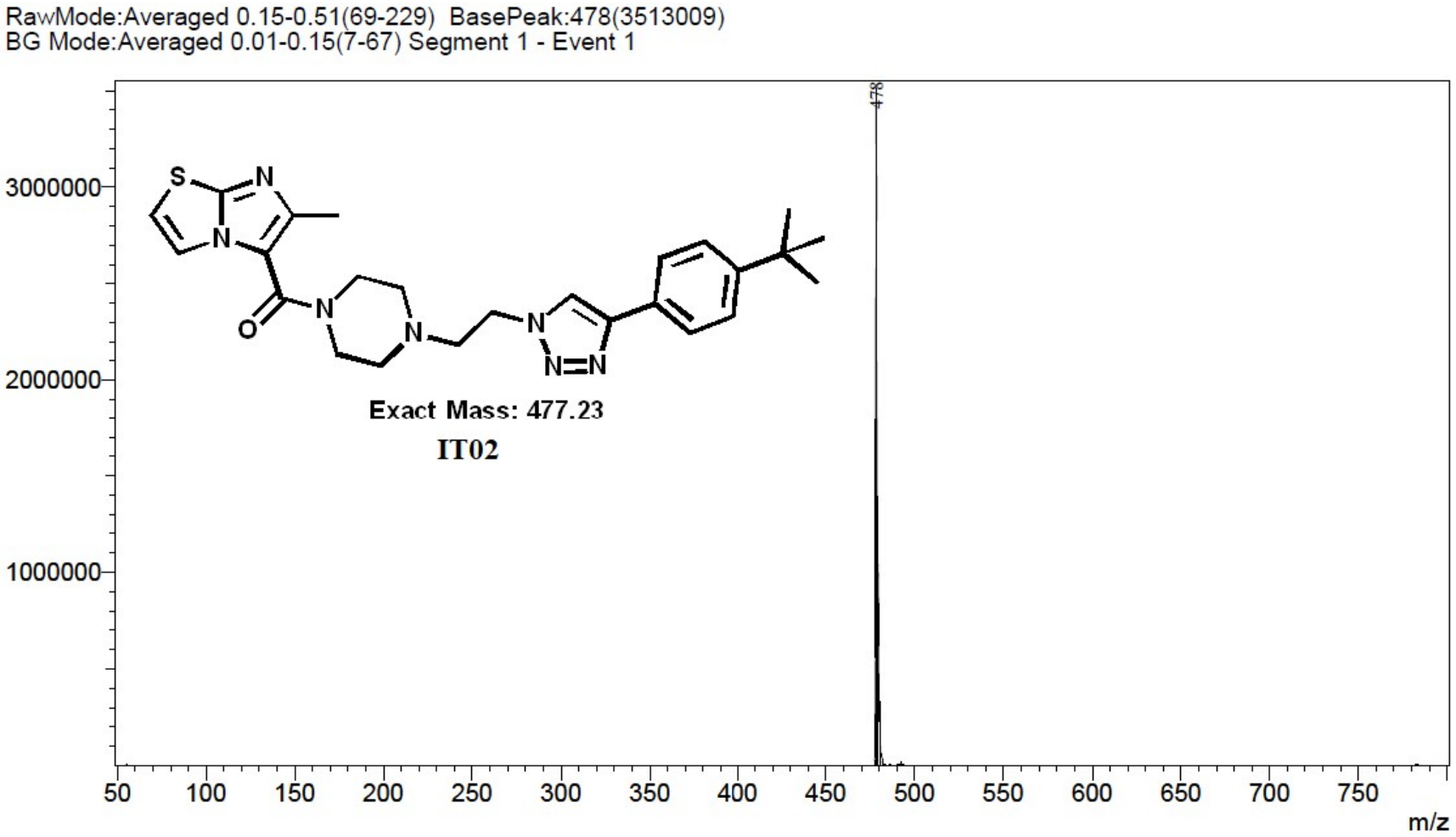

ESI MS spectrum of compound **IT02**

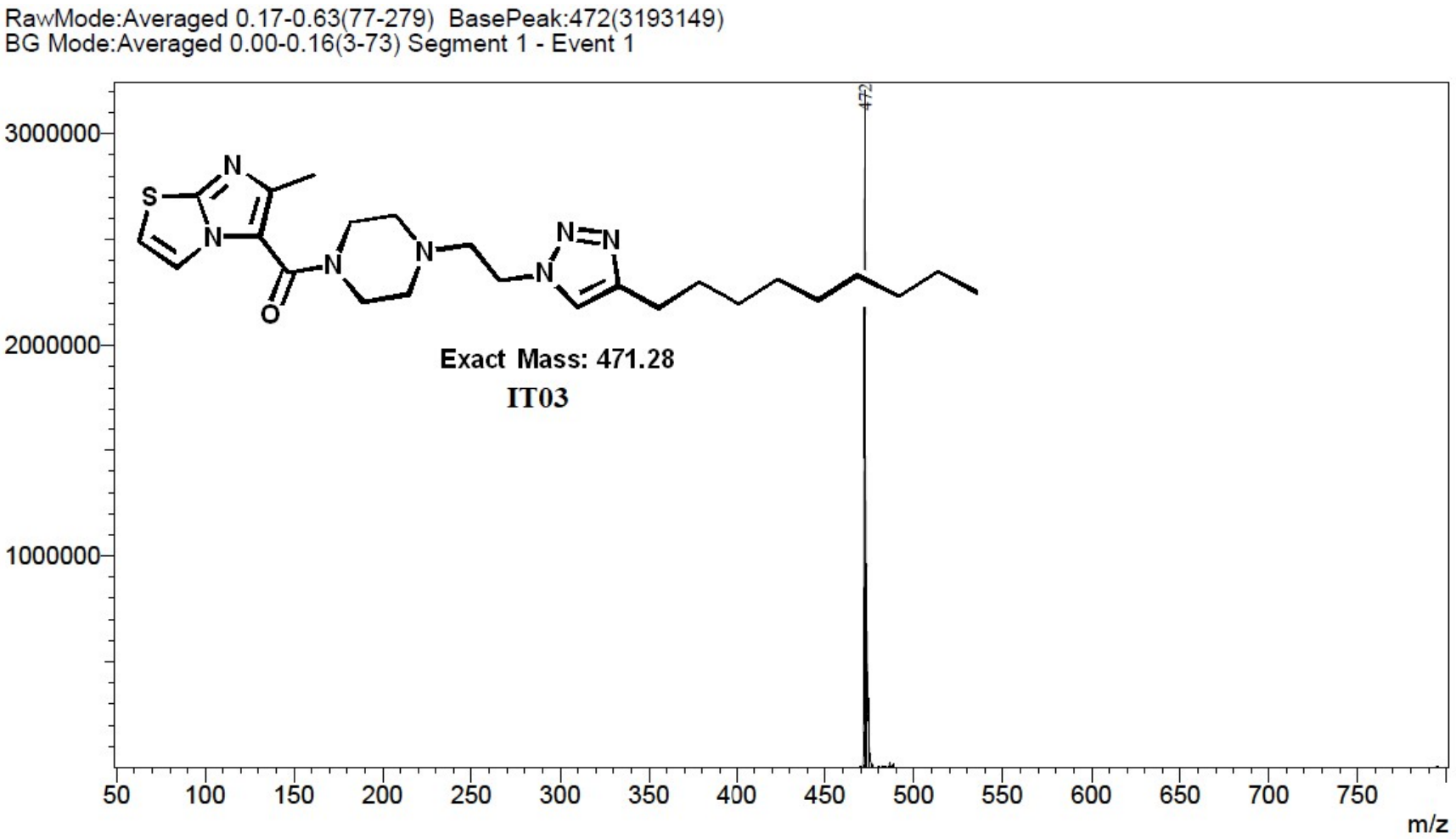

ESI MS spectrum of compound **IT03**

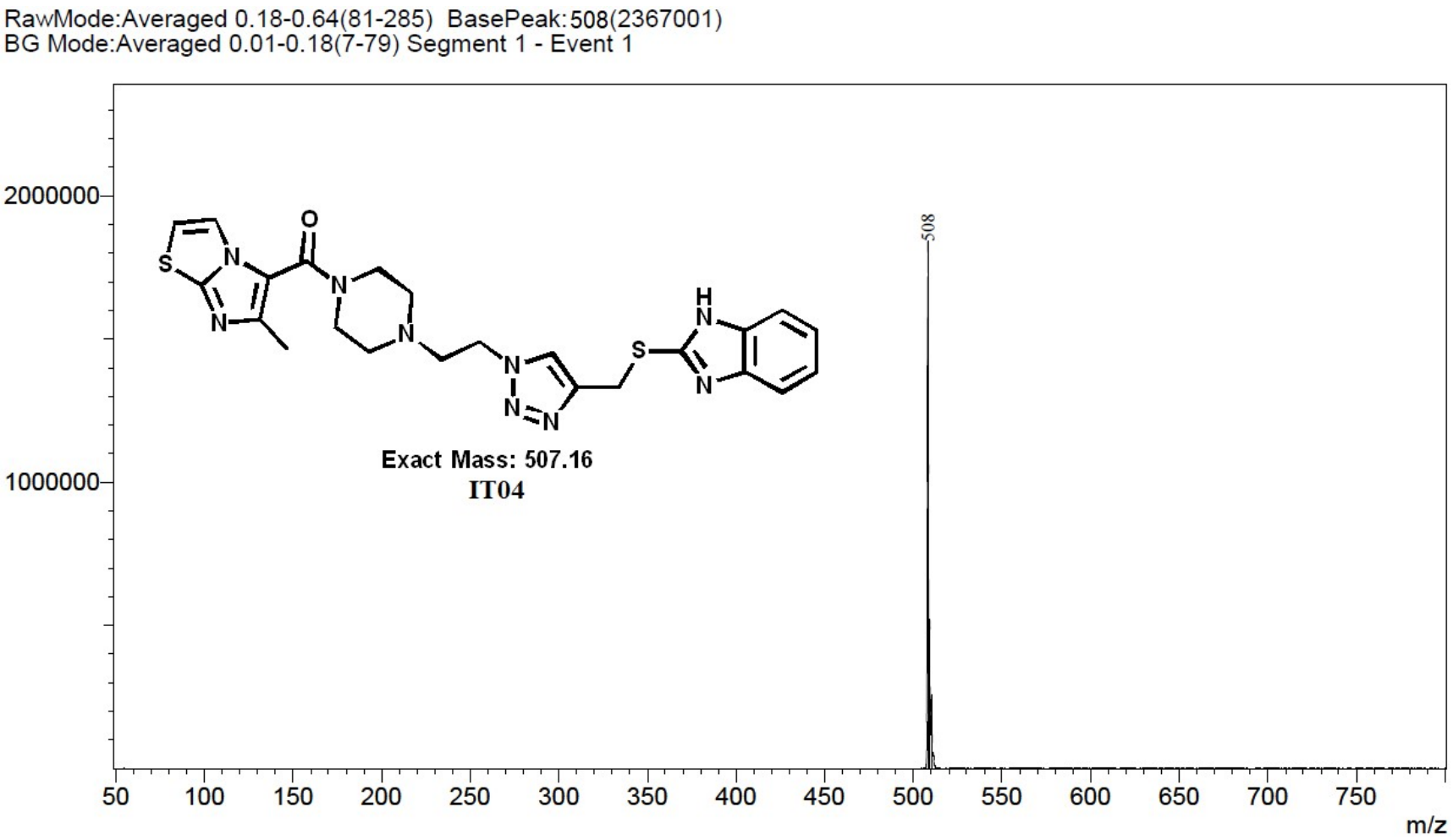

ESI MS spectrum of compound **IT04**

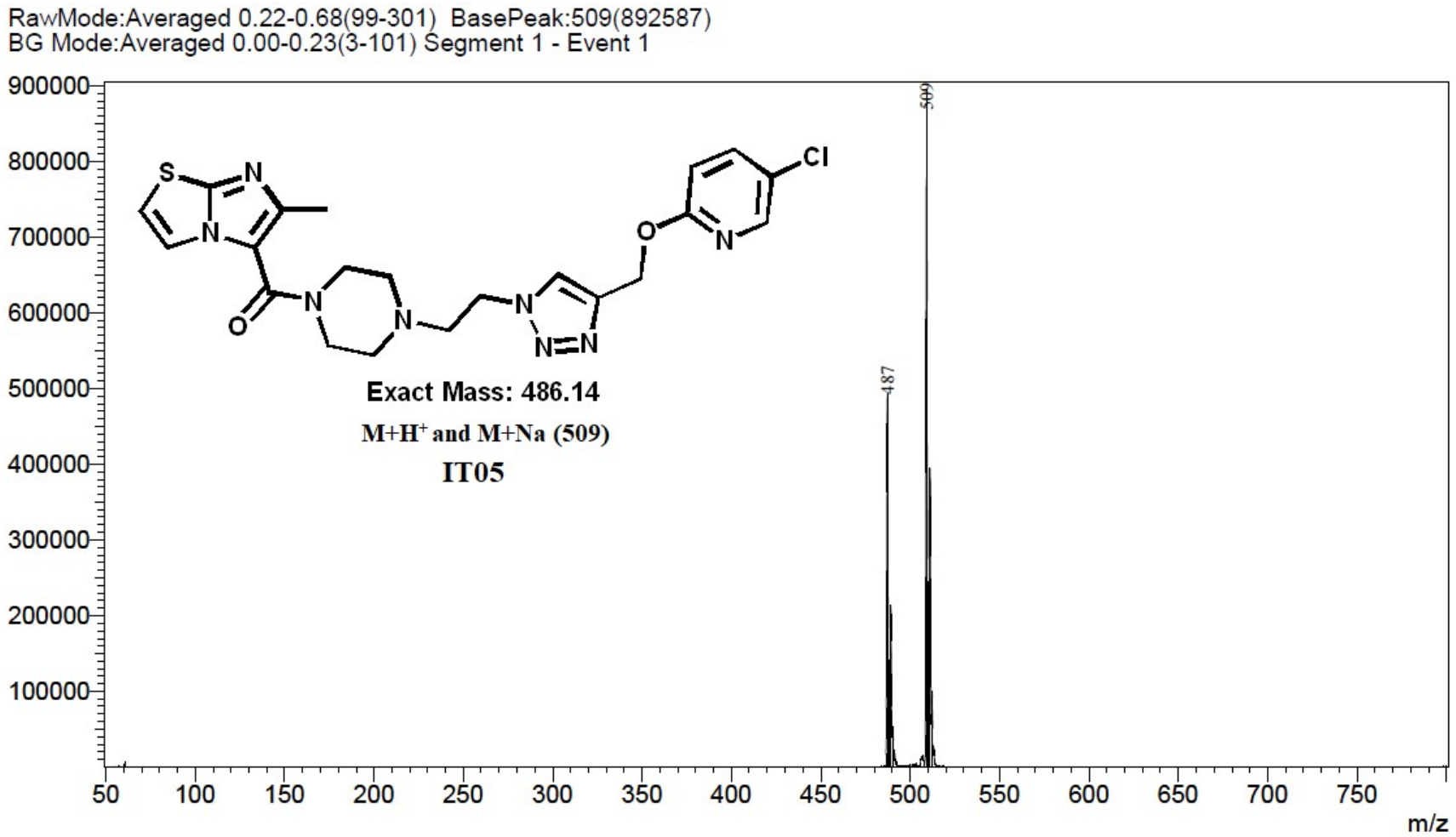

ESI MS spectrum of compound **IT05**

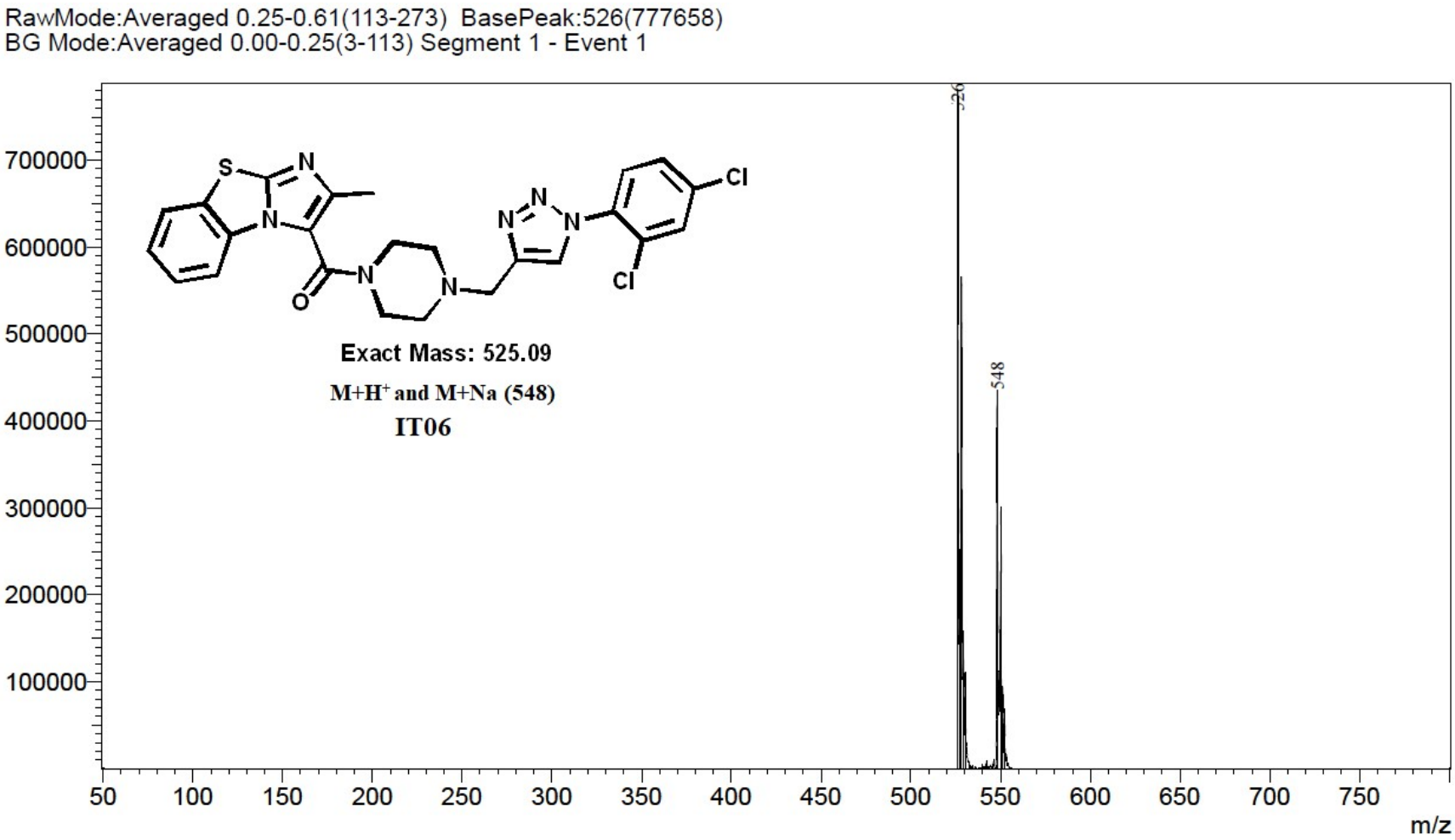

ESI MS spectrum of compound **IT06**

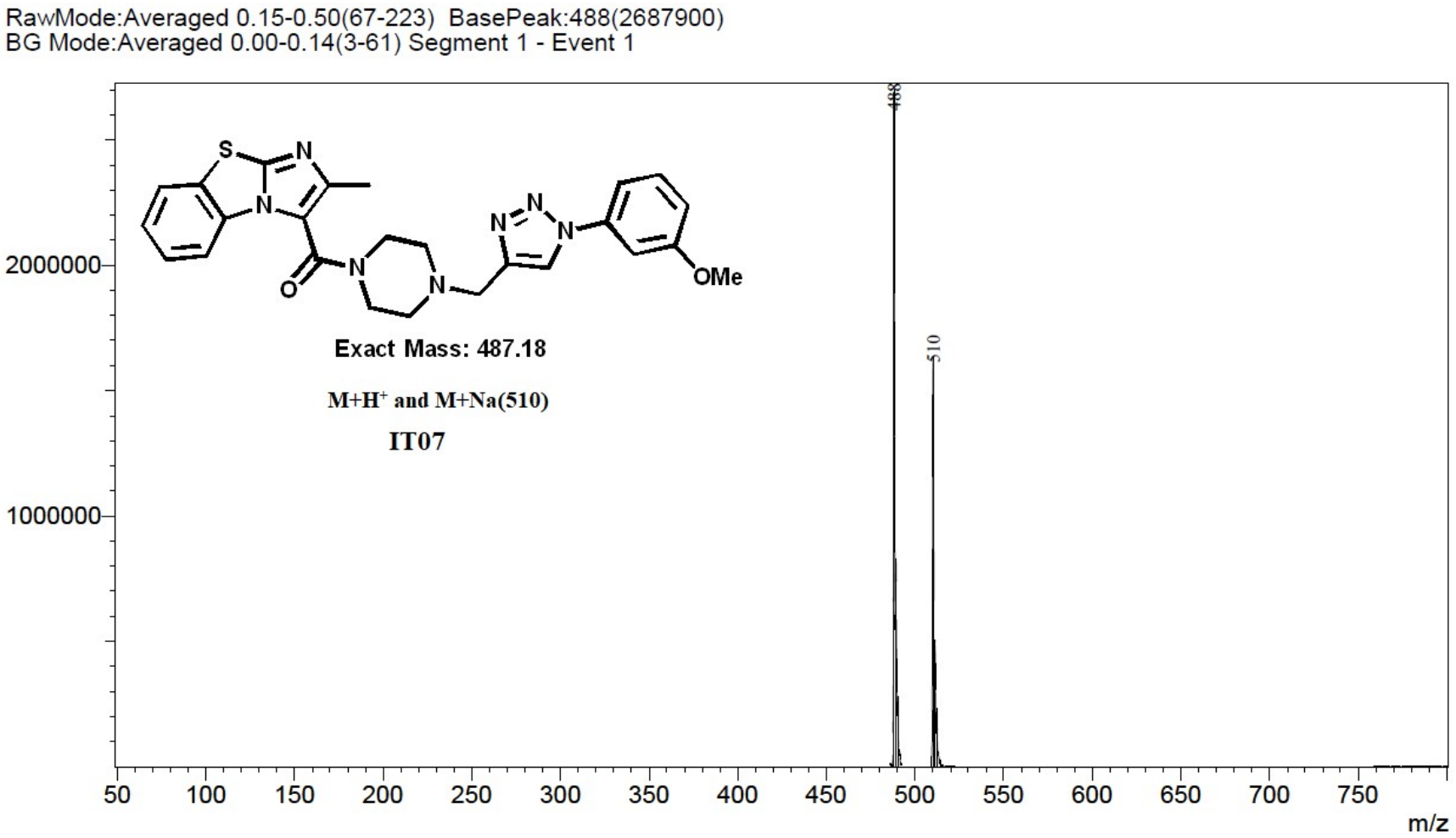

ESI MS spectrum of compound **IT07**

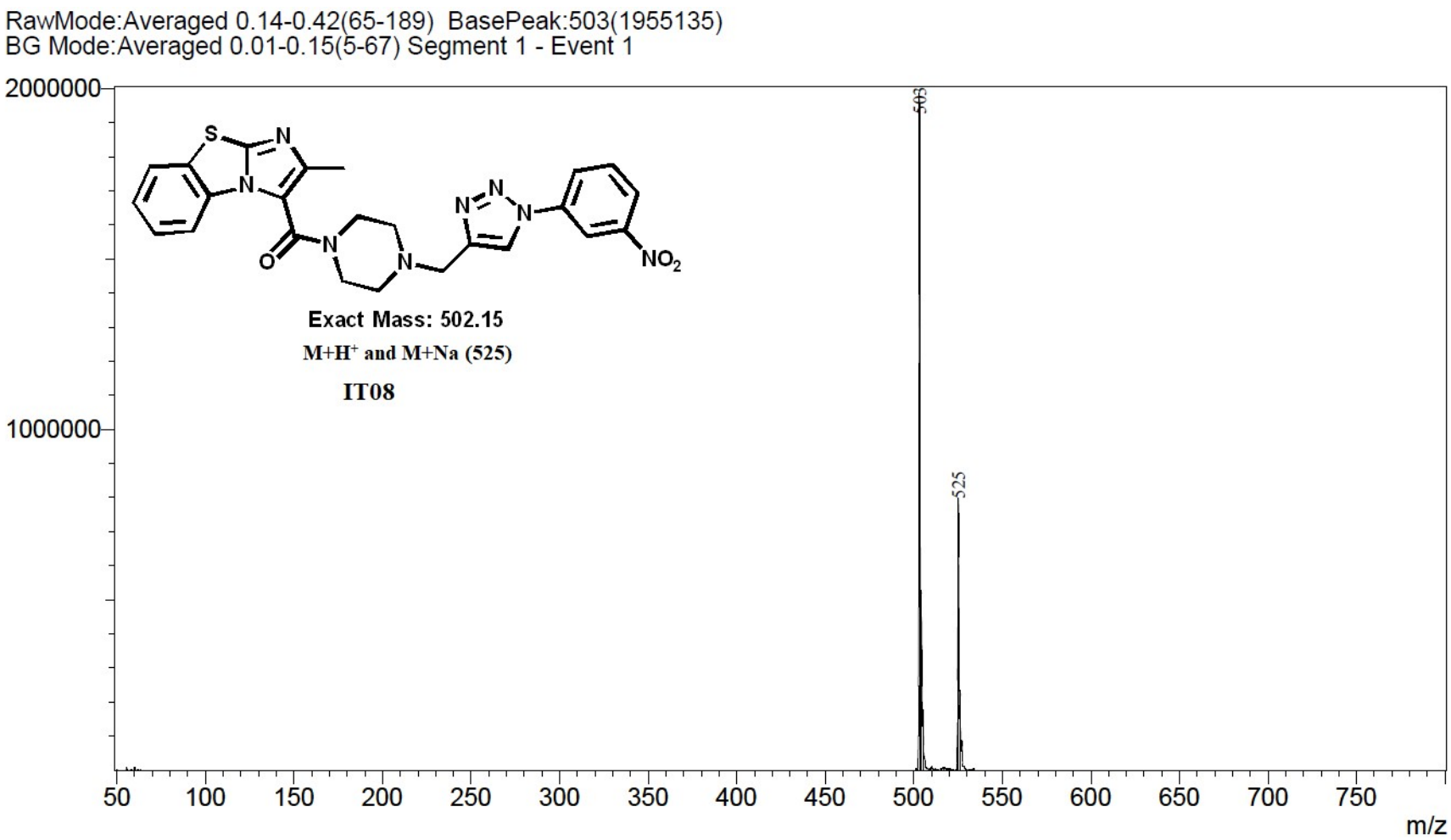

ESI MS spectrum of compound **IT08**

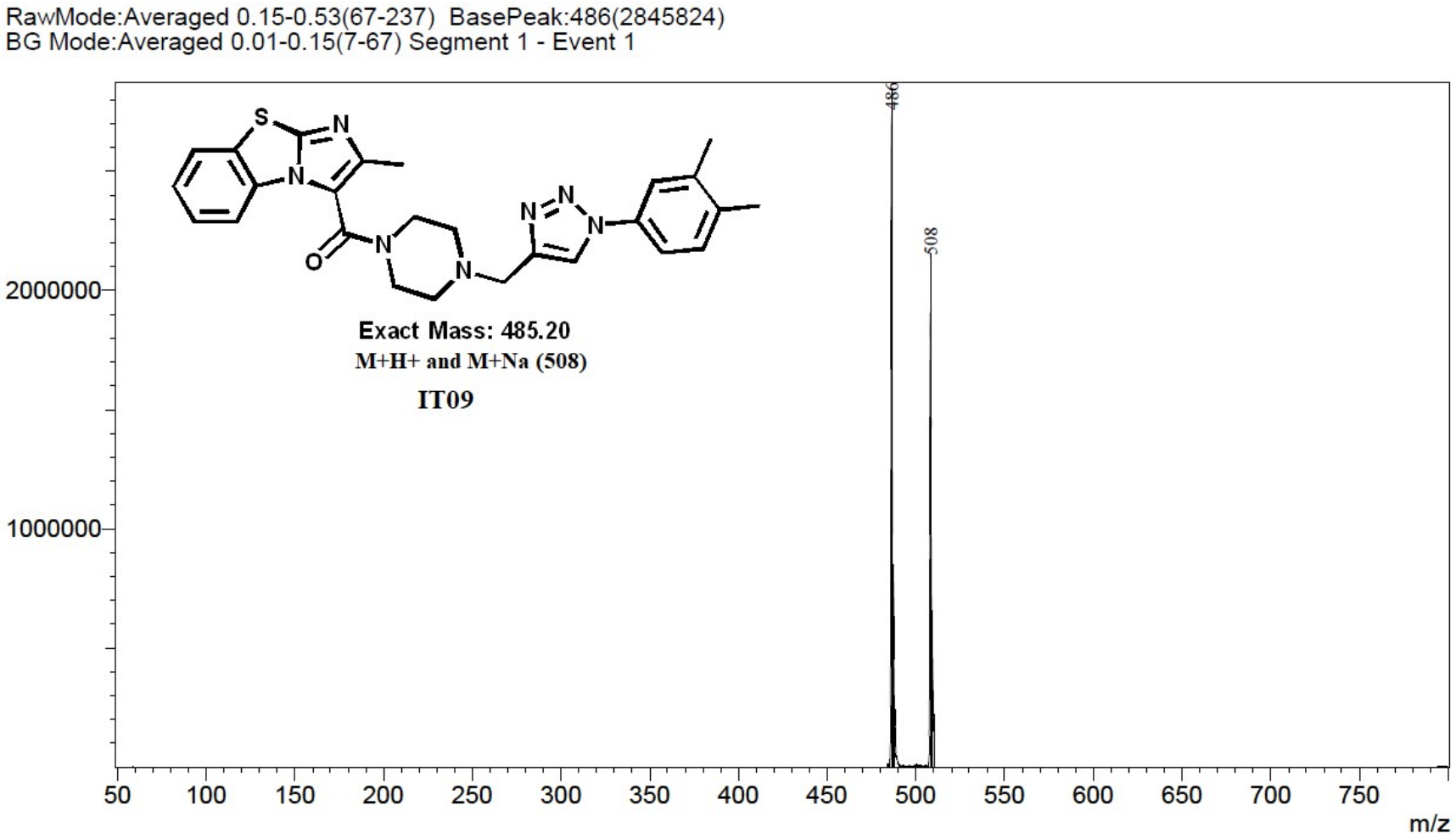

ESI MS spectrum of compound **IT09**

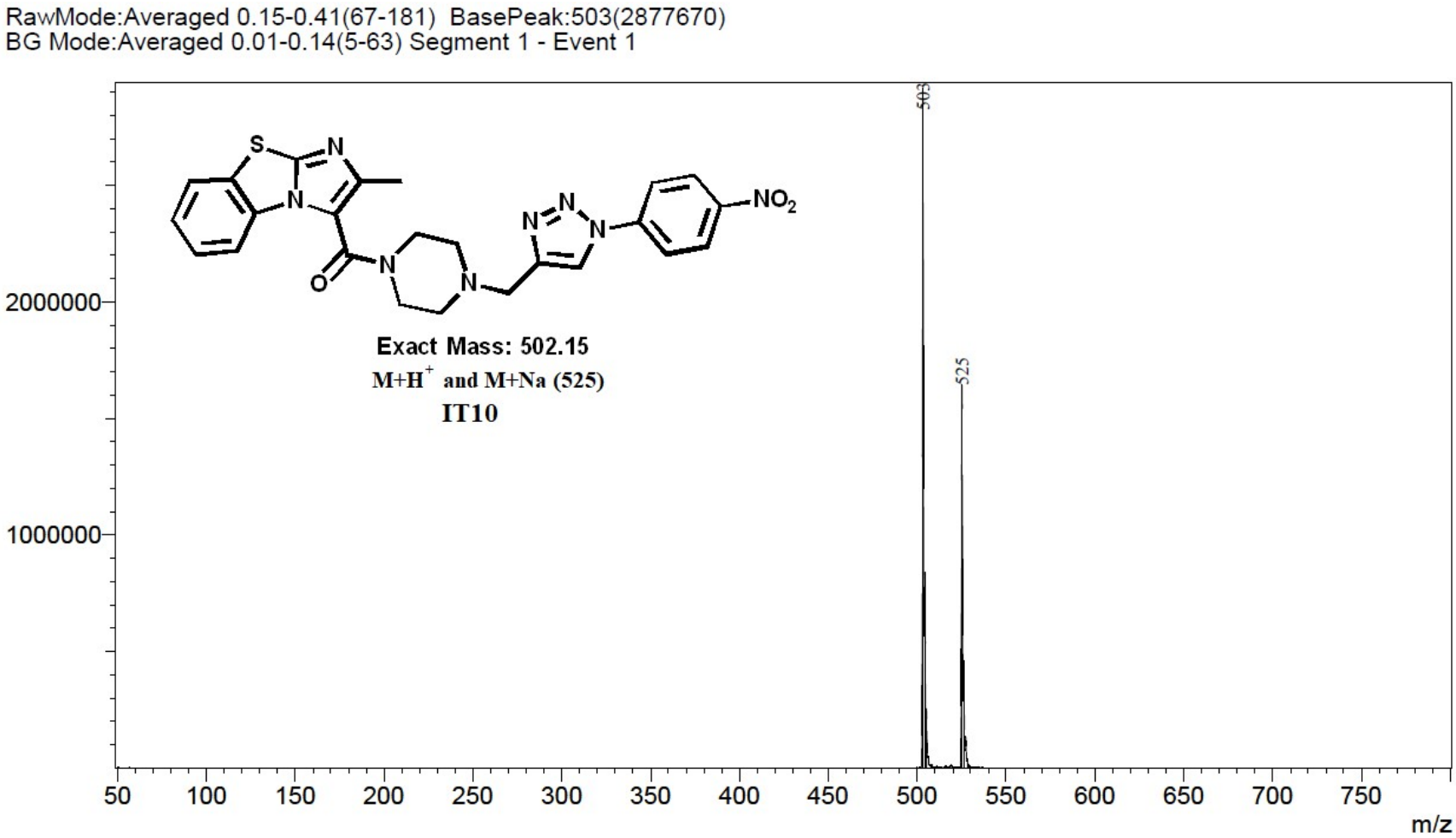

ESI MS spectrum of compound **IT10**

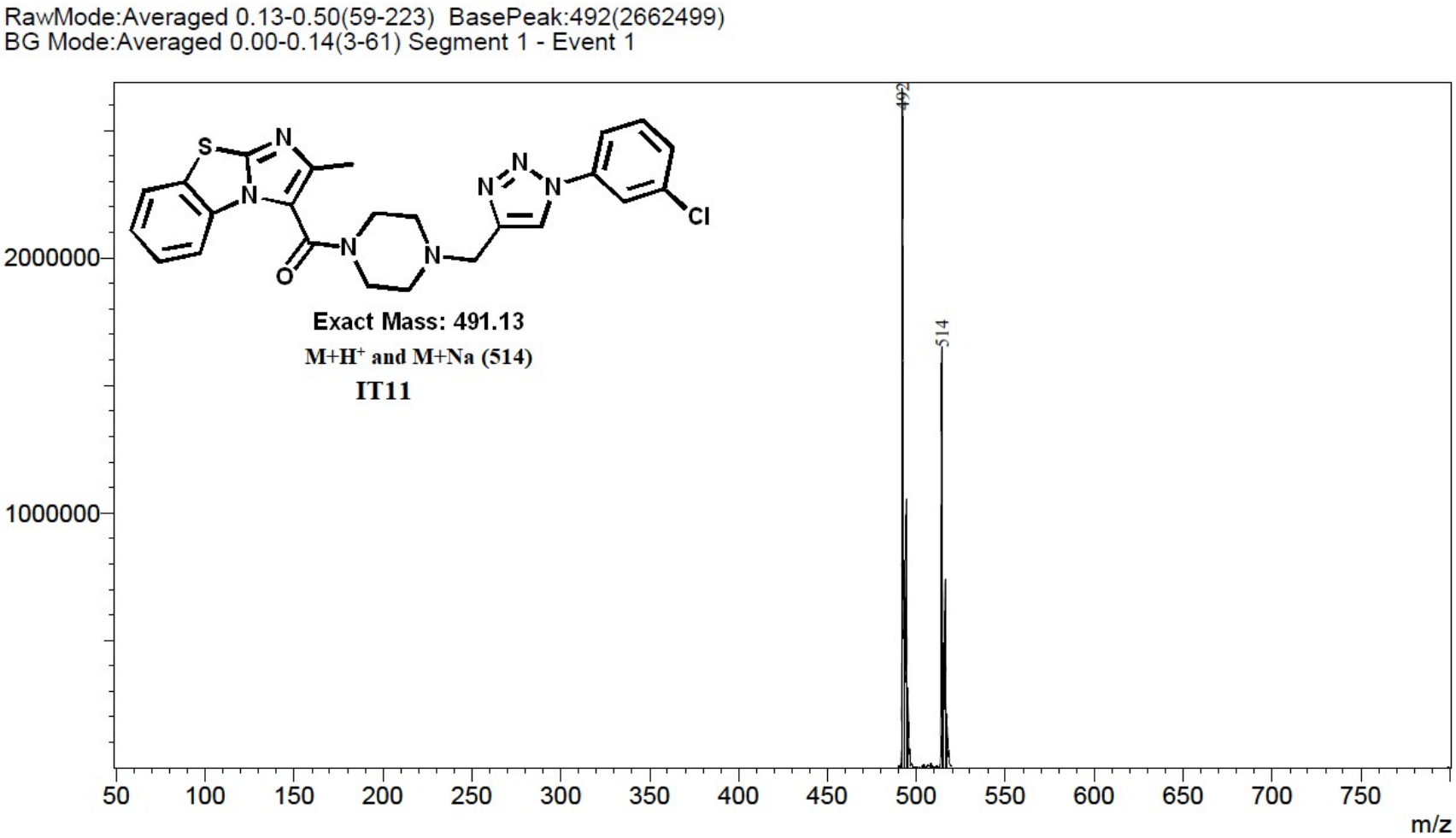

ESI MS spectrum of compound **IT11**

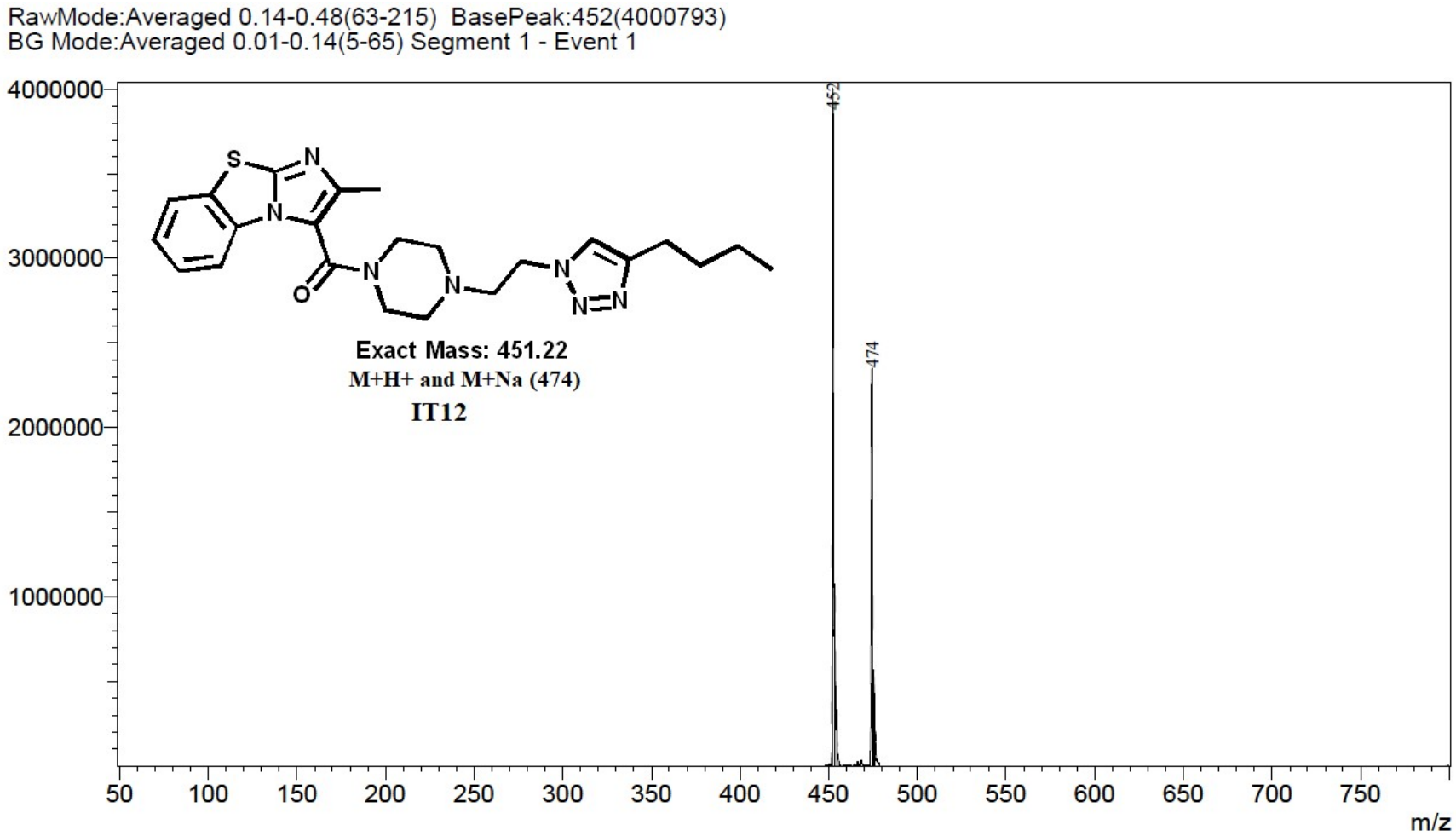

ESI MS spectrum of compound **IT12**

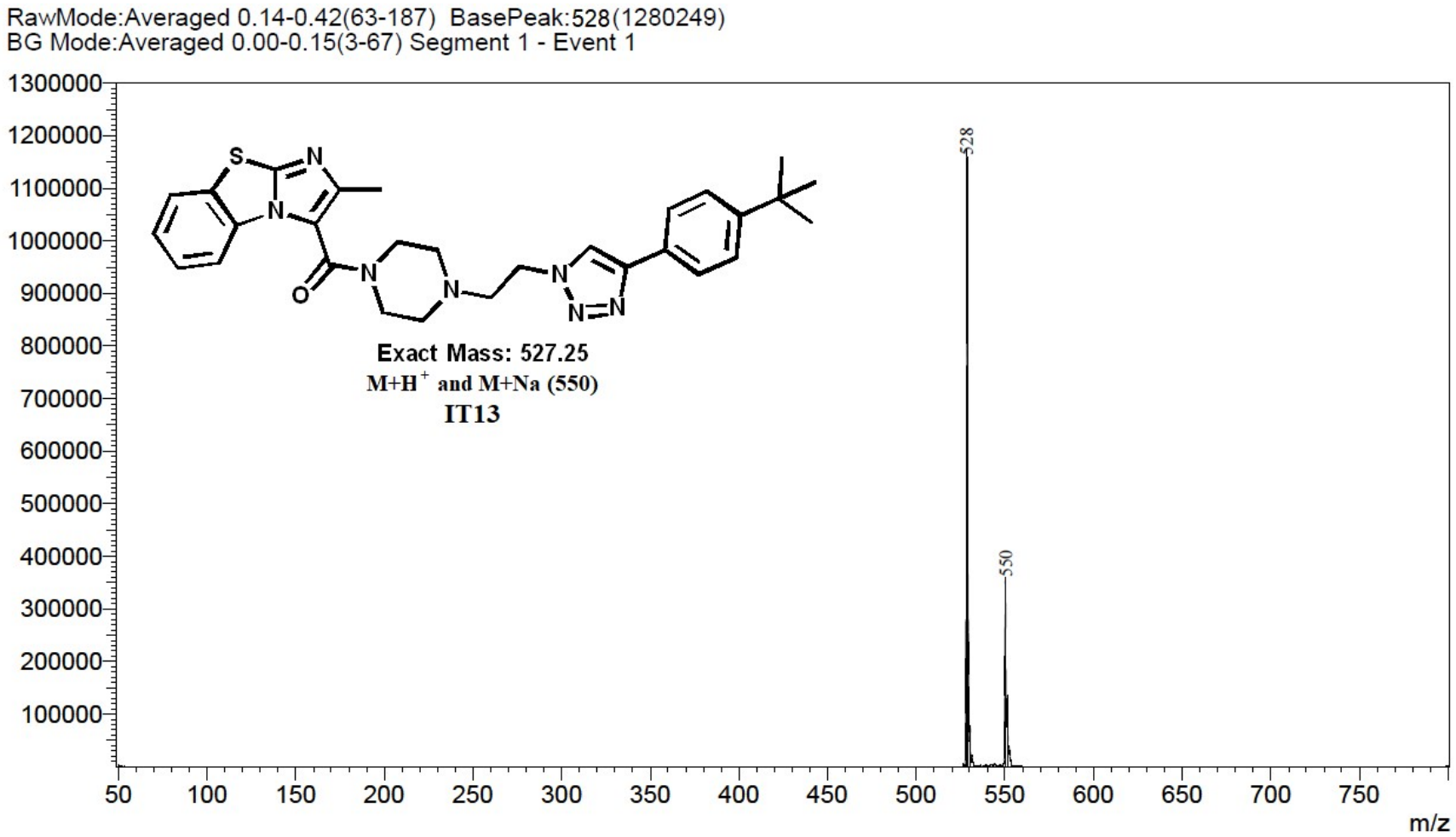

ESI MS spectrum of compound **IT13**

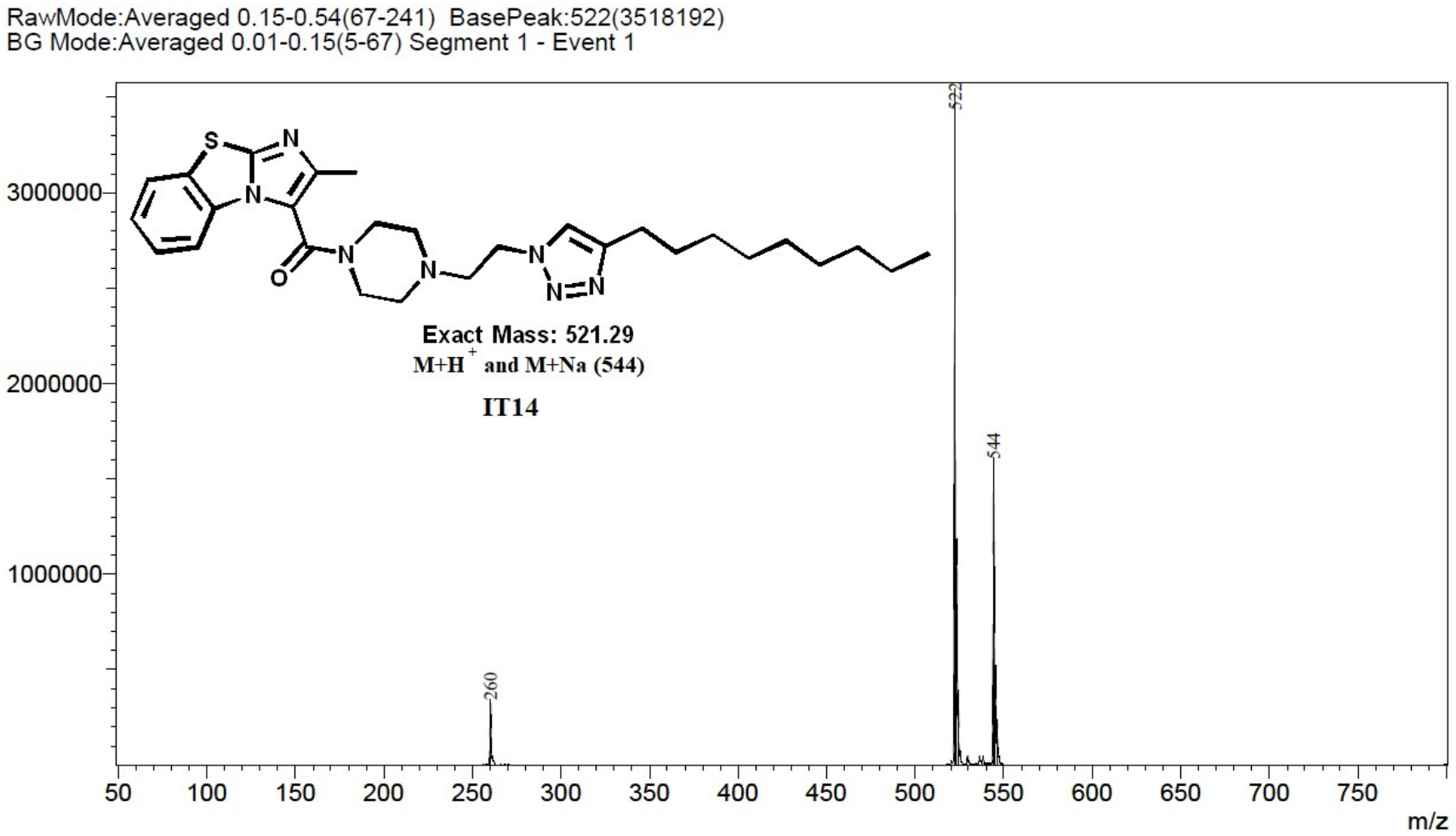

ESI MS spectrum of compound **IT14**

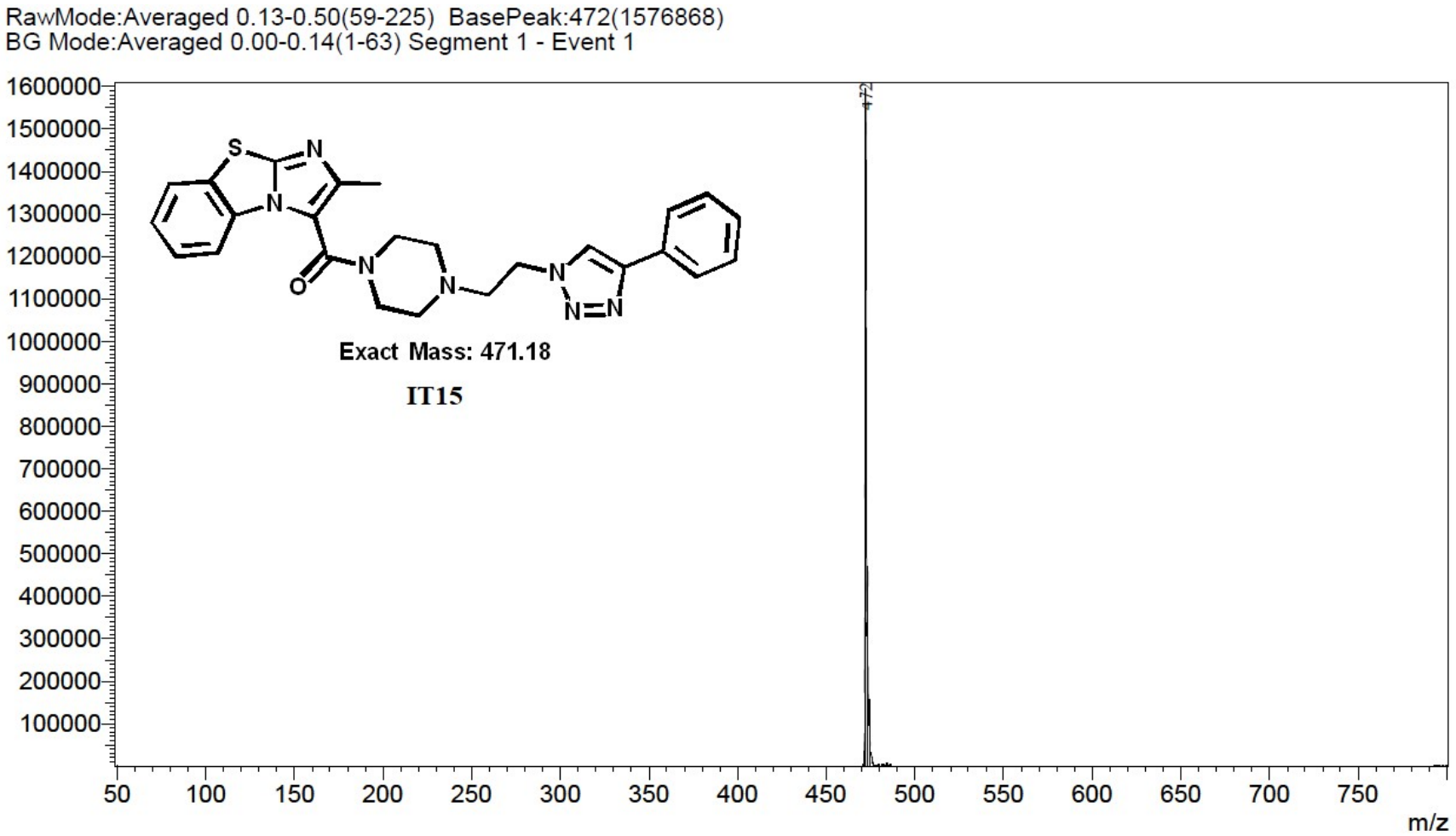

ESI MS spectrum of compound **IT15**

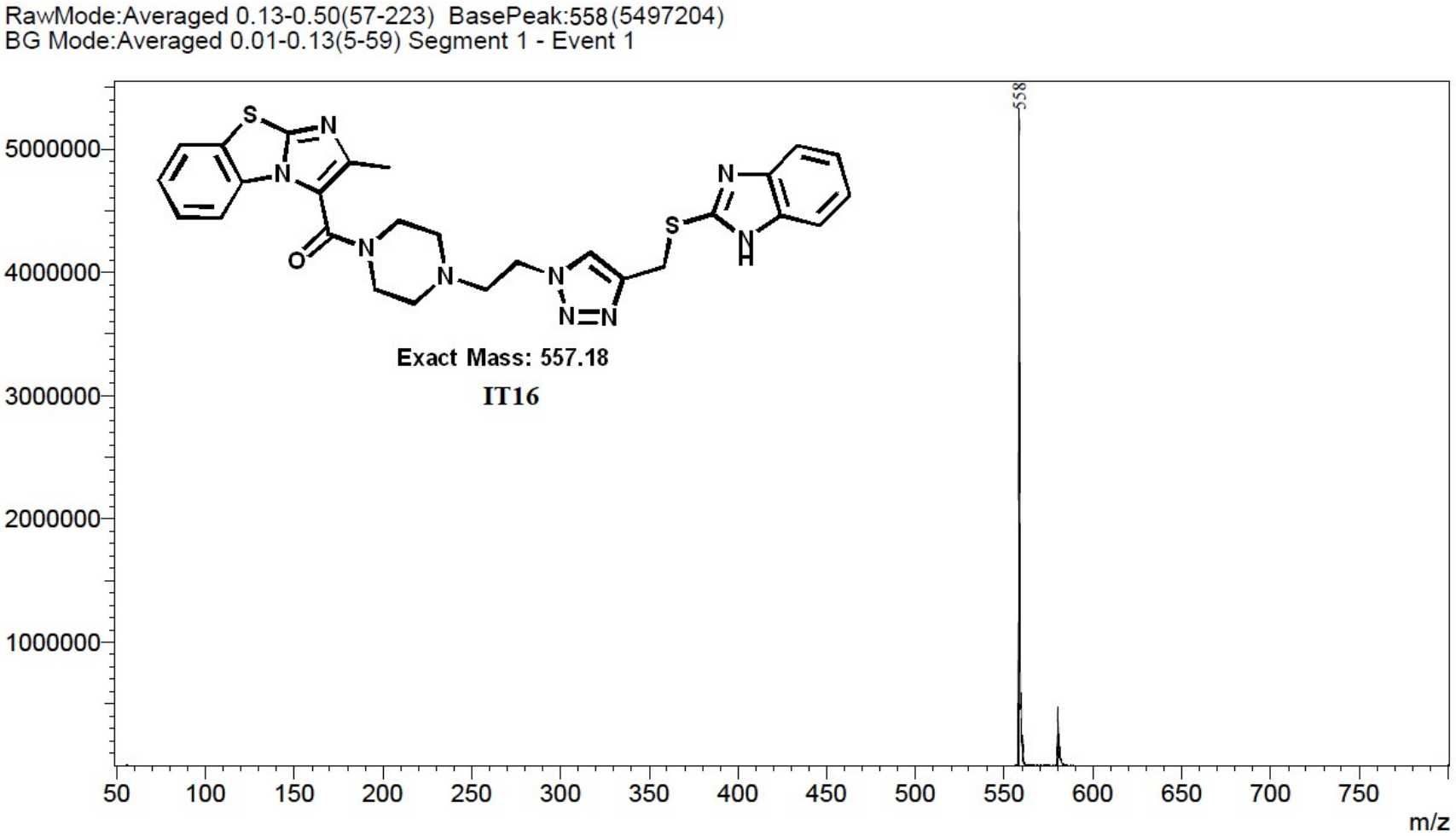

ESI MS spectrum of compound **IT16**

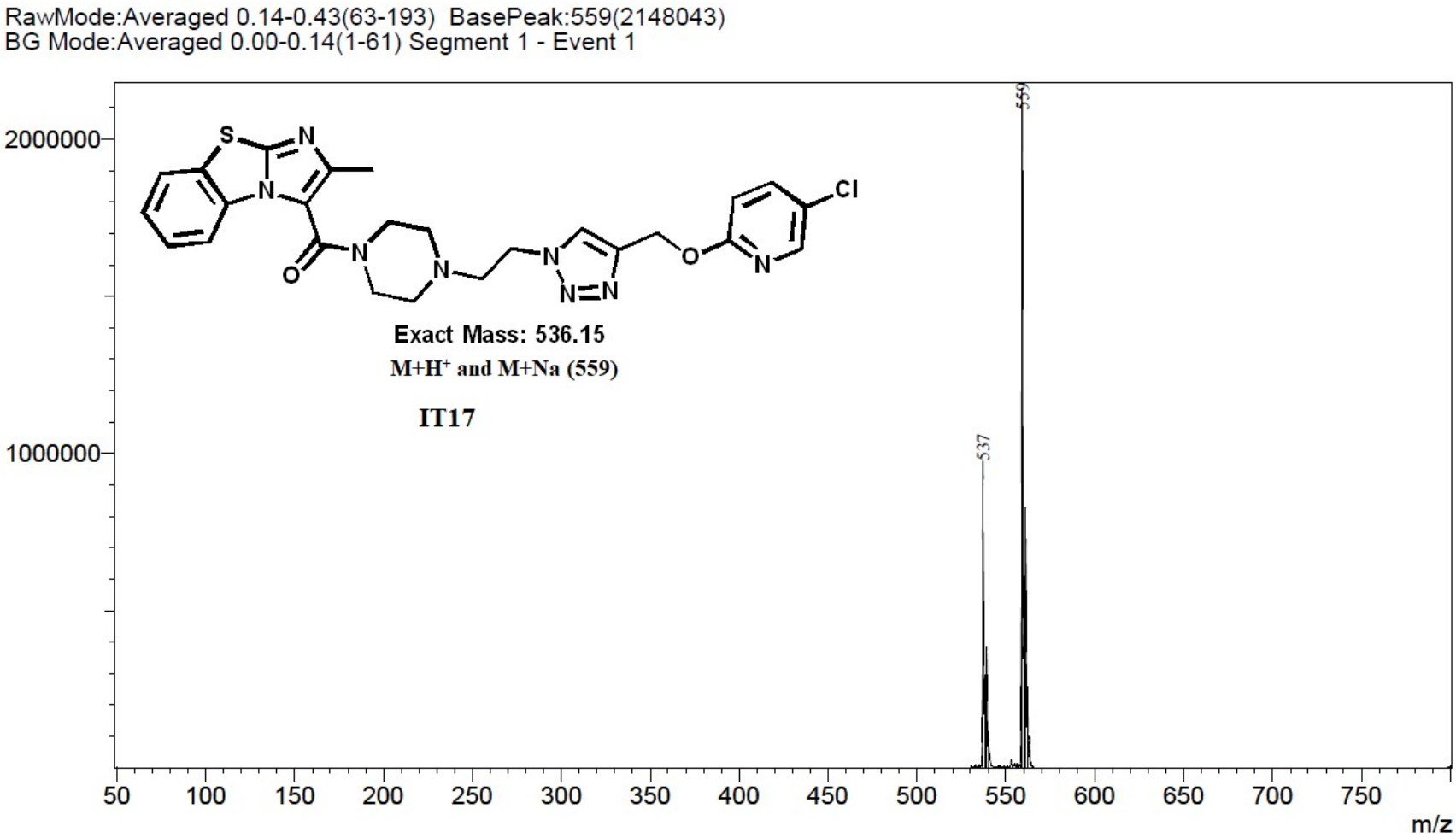

ESI MS spectrum of compound **IT17**

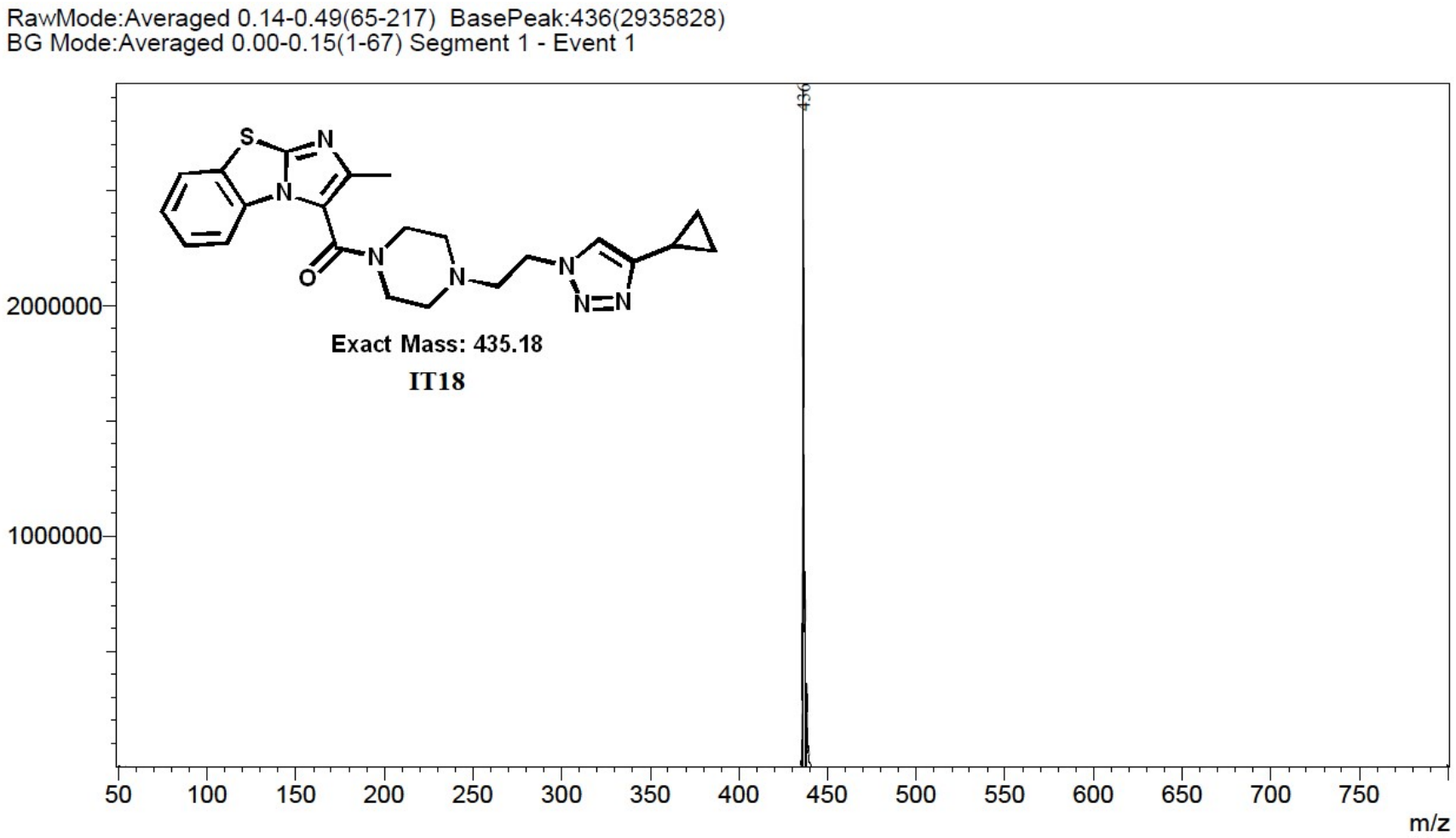

ESI MS spectrum of compound **IT18**

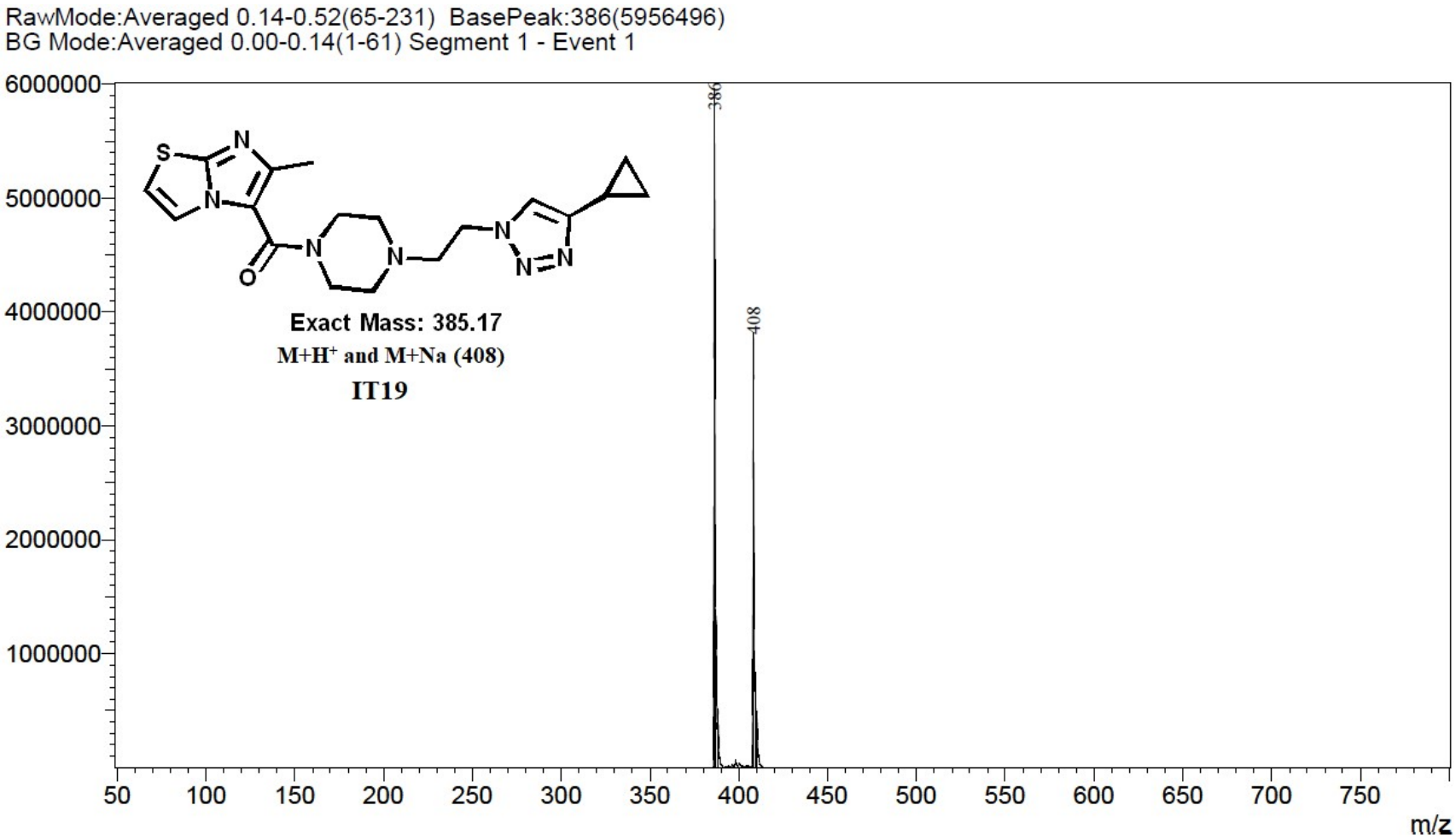

ESI MS spectrum of compound **IT19**

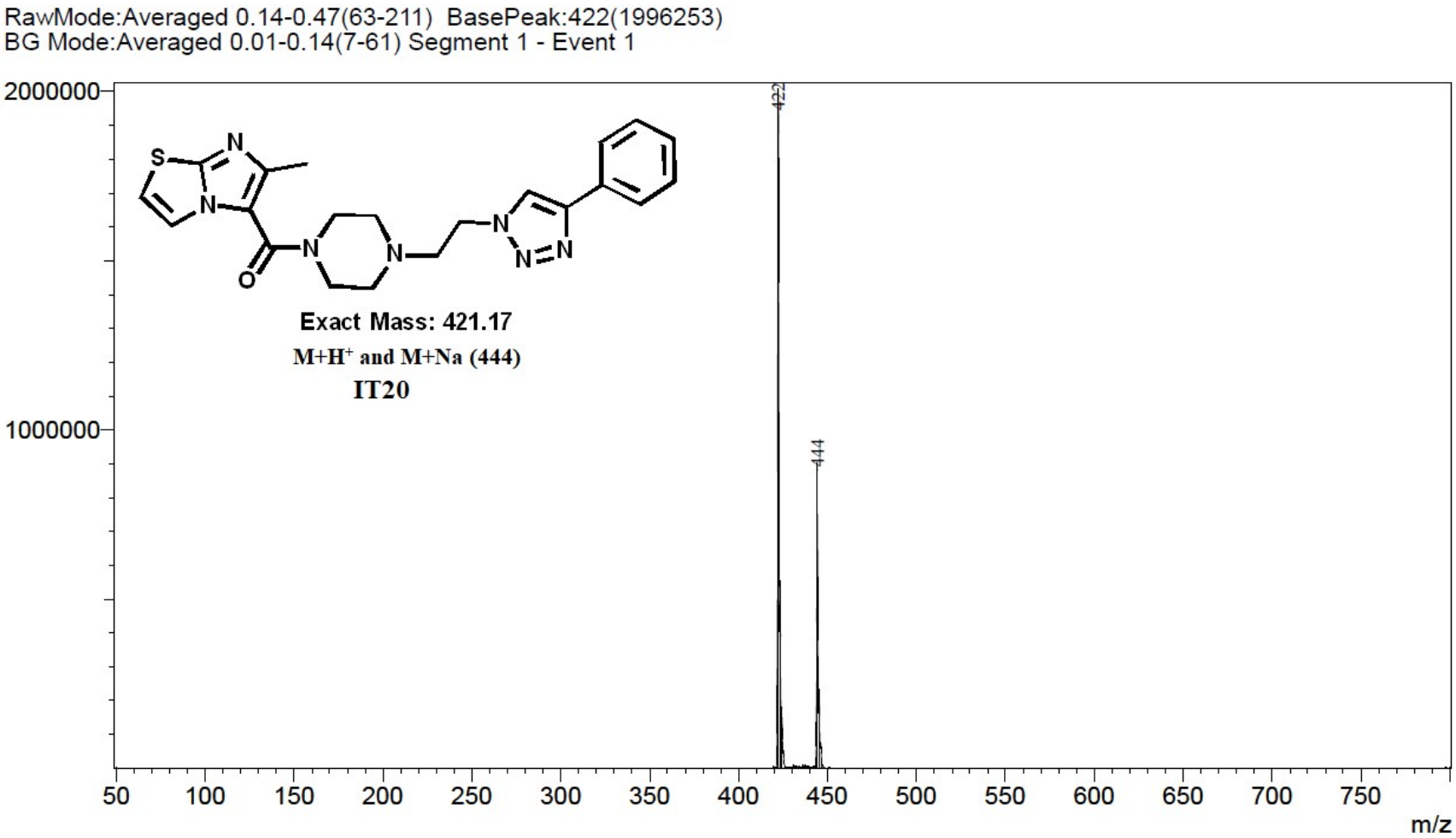

ESI MS spectrum of compound IT**20**

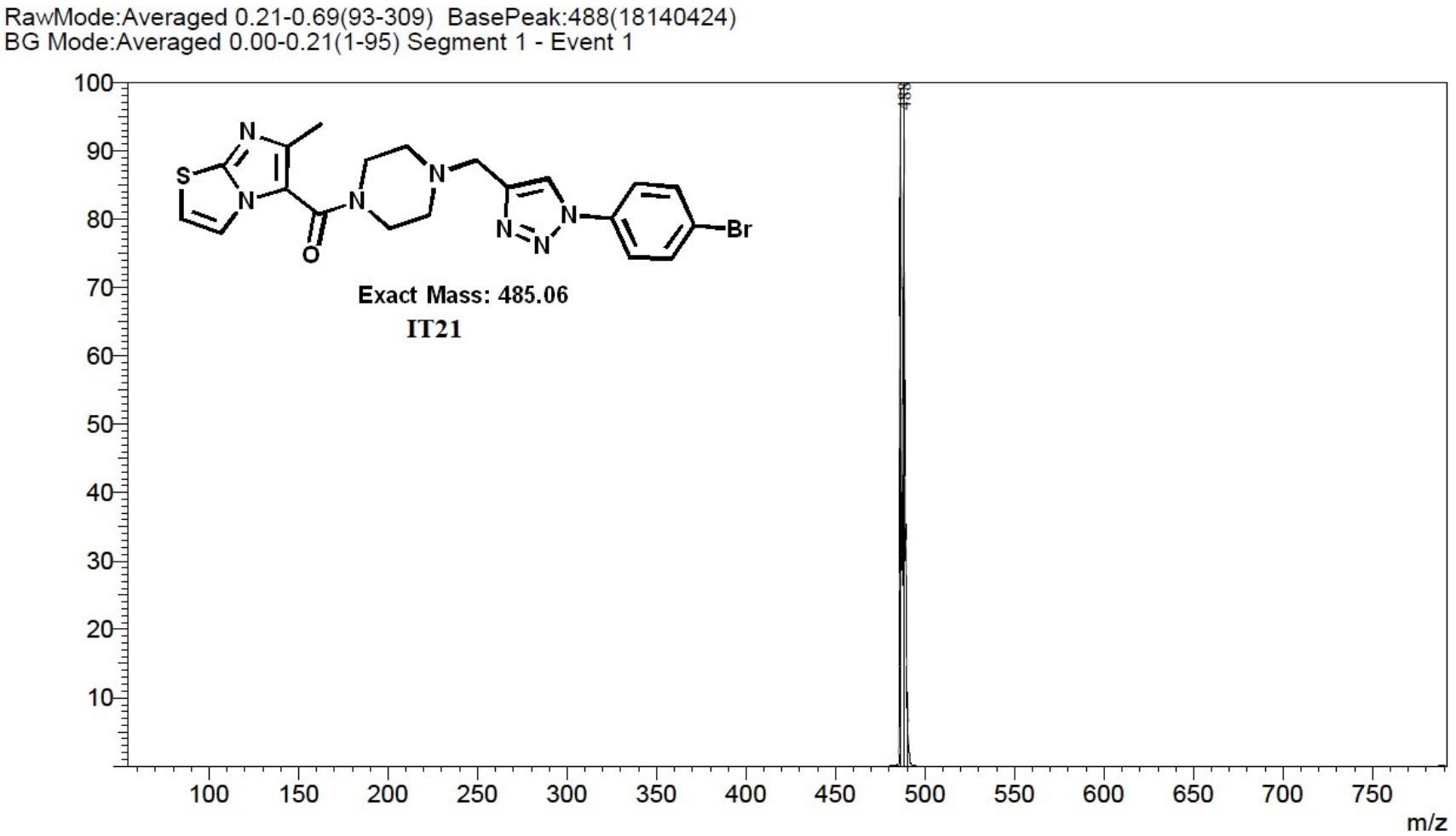

ESI MS spectrum of compound **IT21**

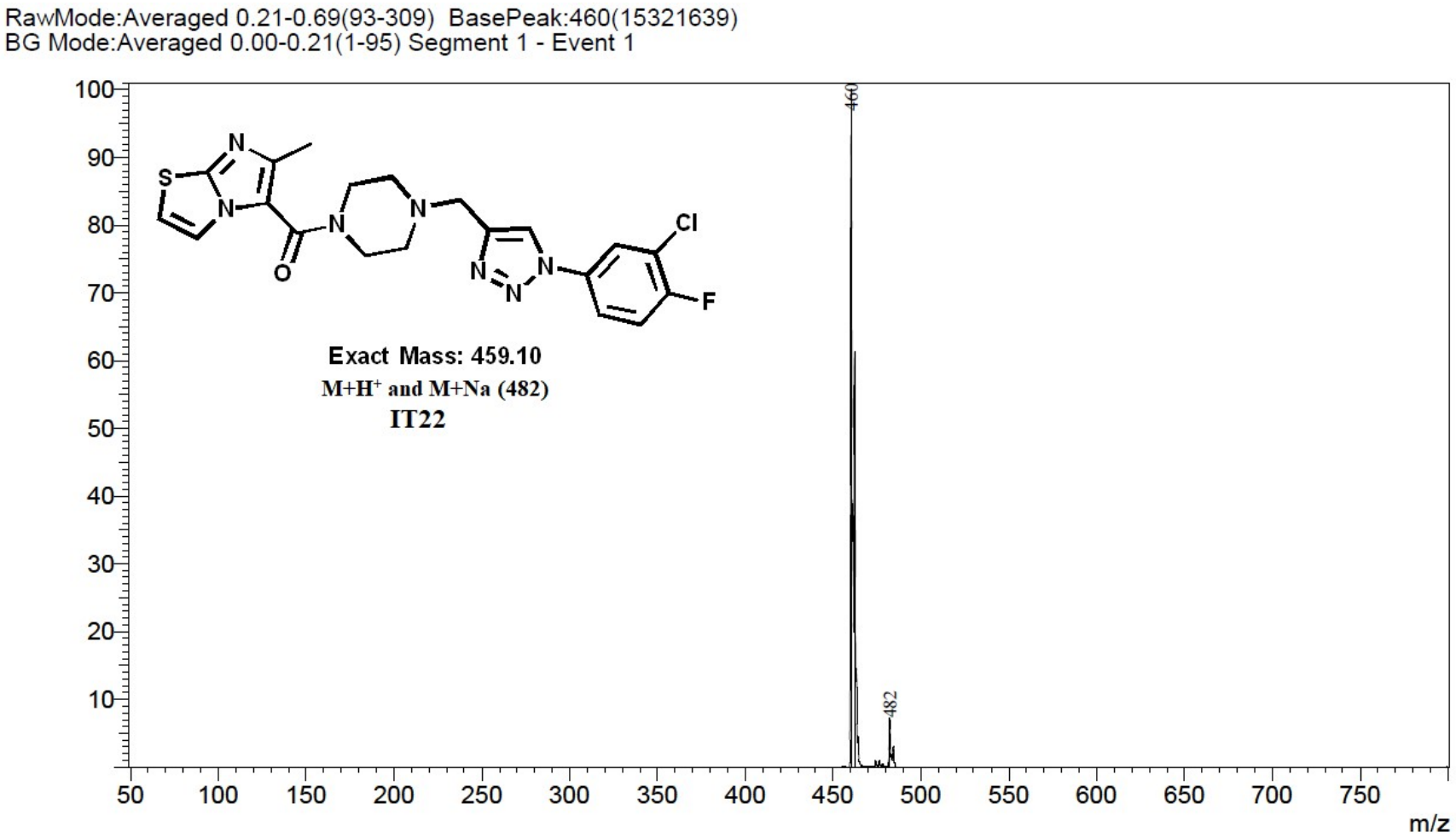

ESI MS spectrum of compound **IT22**

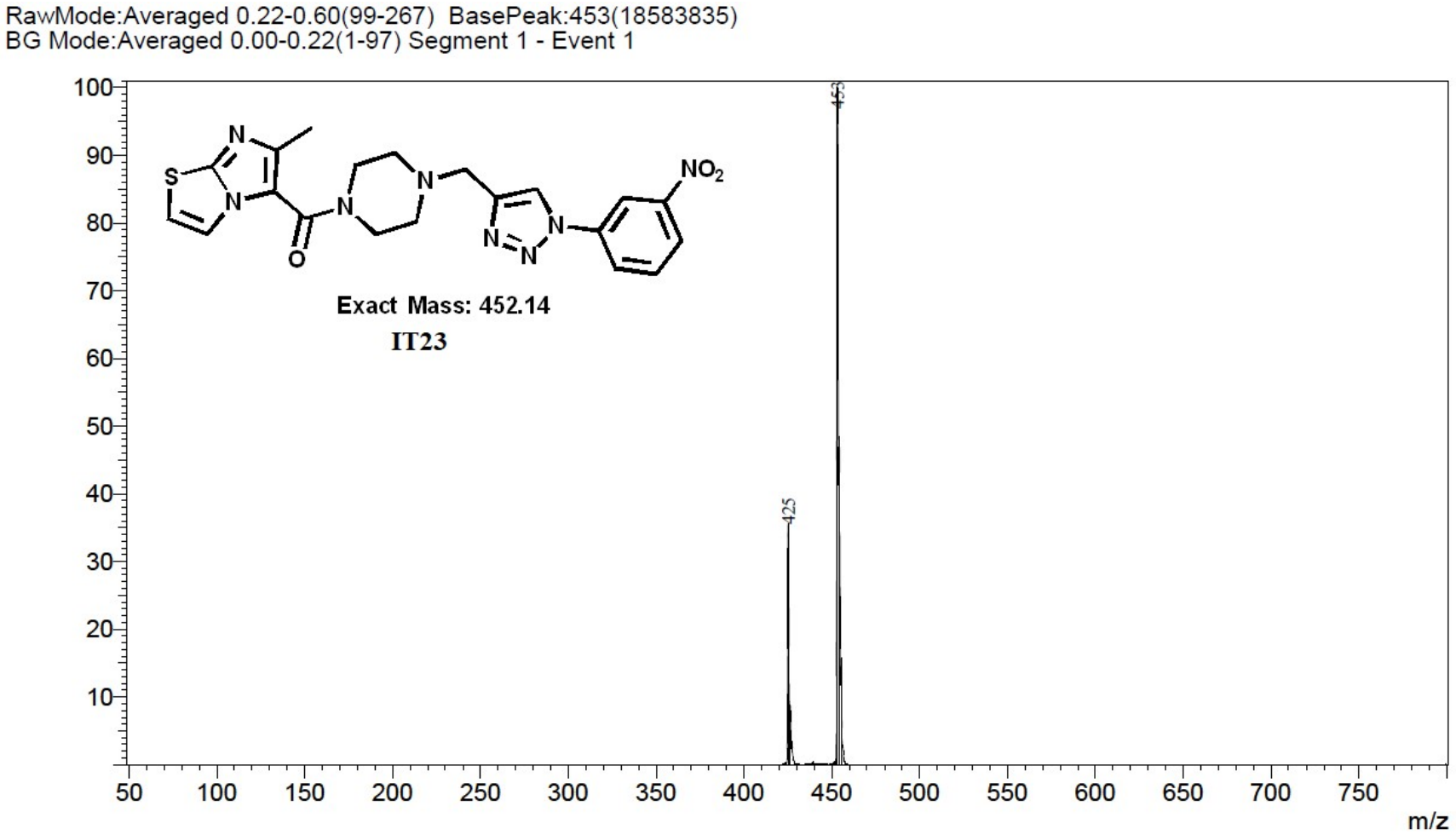

ESI MS spectrum of compound **IT23**

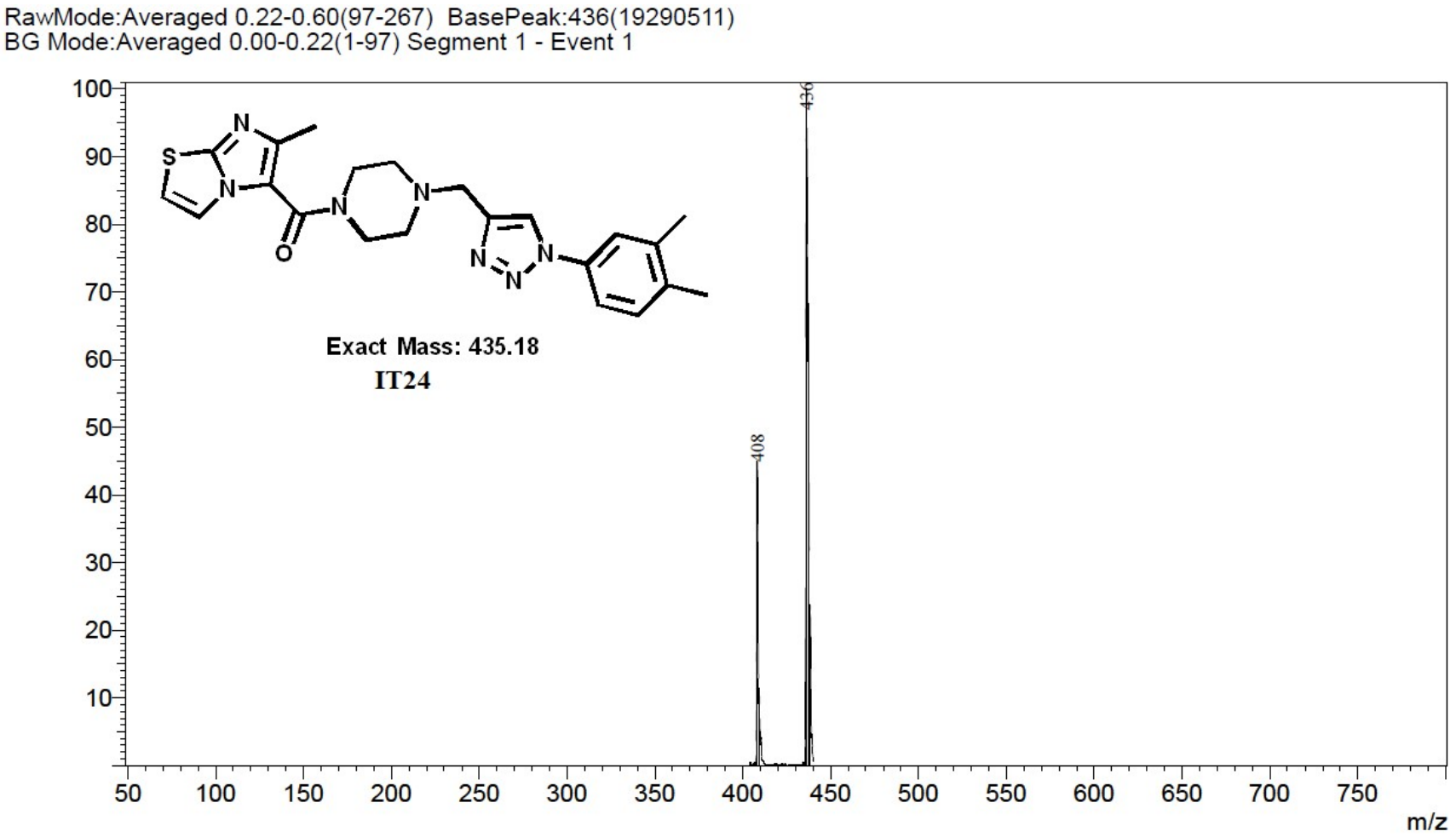

ESI MS spectrum of compound **IT24**

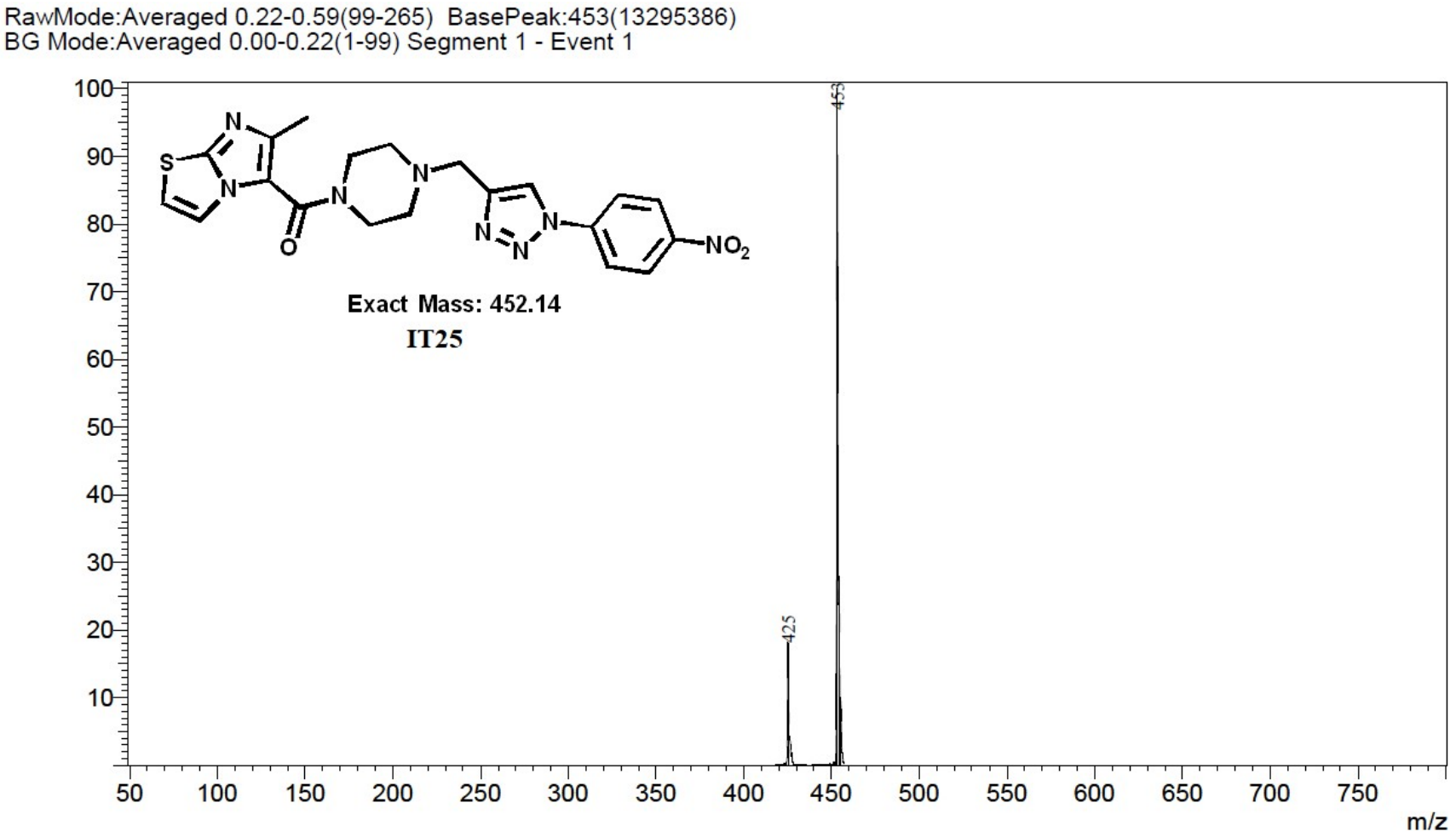

ESI MS spectrum of compound **IT25**

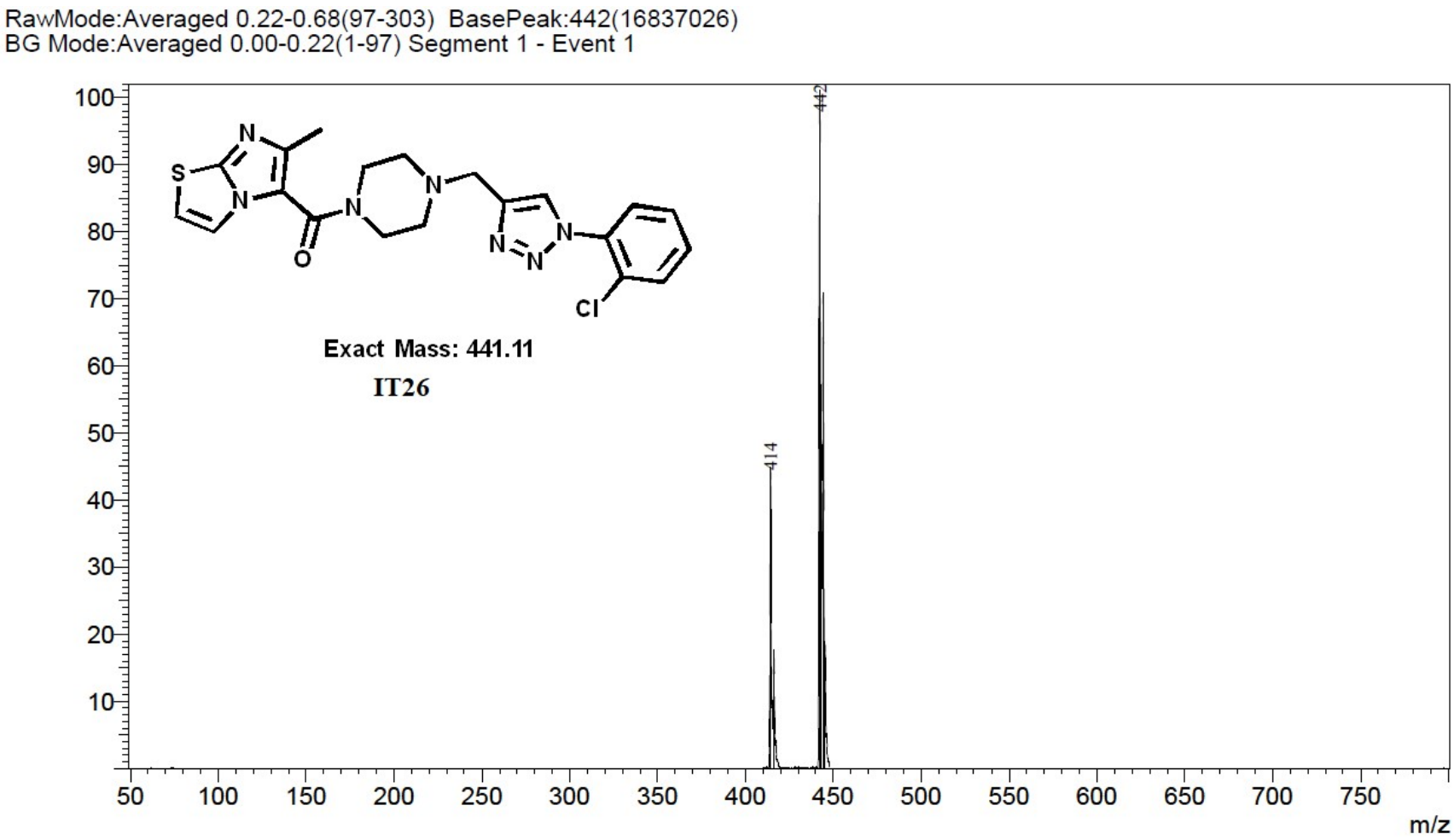

ESI MS spectrum of compound **IT26**

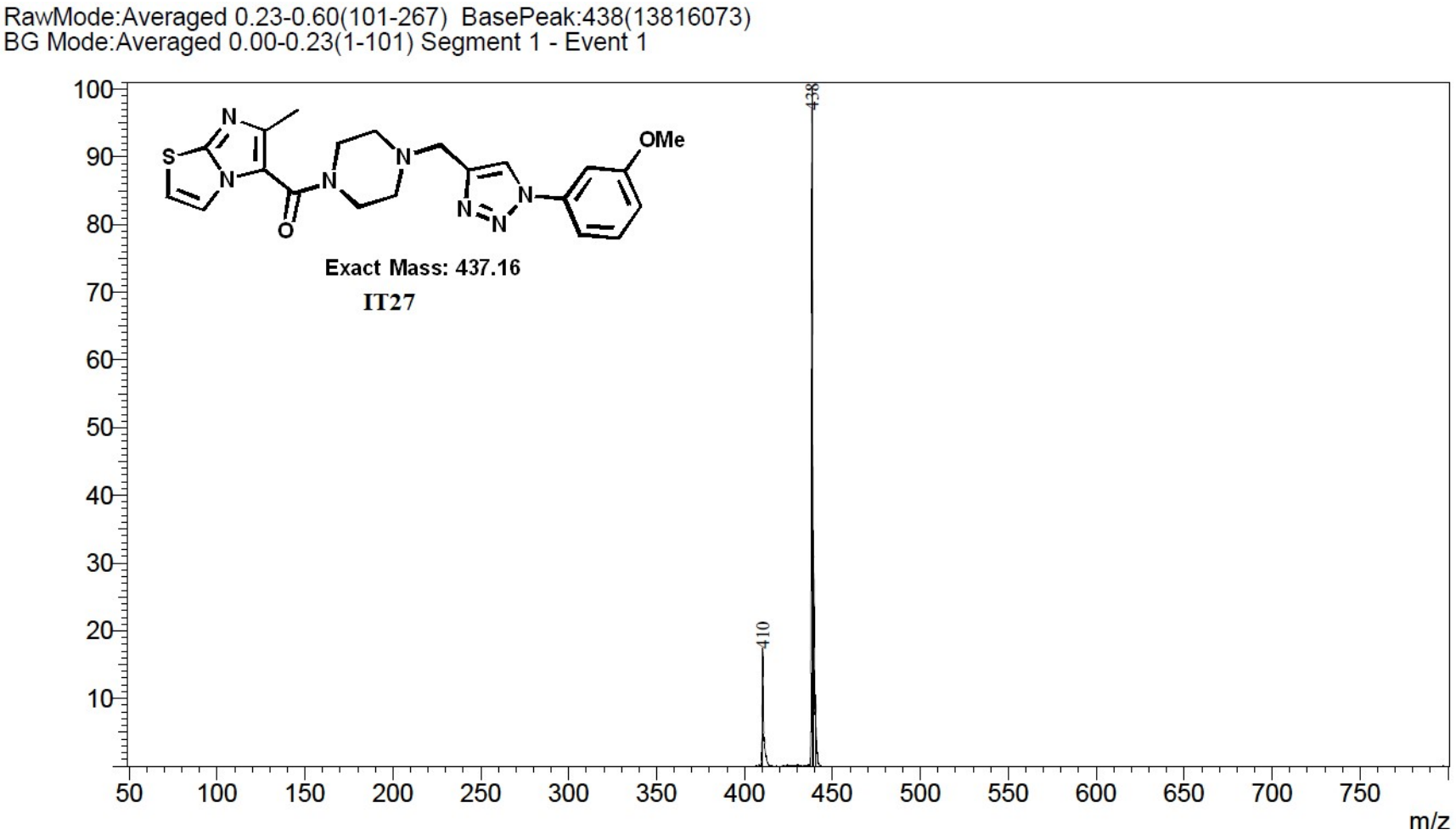

ESI MS spectrum of compound **IT27**

5.0. HPLC data of IT series compounds

==== Shimadzu LCsolution Analysis Report ====

C:\Chemistry\Dr. KVG\ADI\IT-06.lcd

Acquired by	: Admin
Sample Name	: IT-06
Tray#	: 1
Vail #	: 99
Injection Volume	: 5 uL
Data File Name	: IT-06
Method File Name	: ANVS-MB-Assay-RS.lcm
Batch File Name	: 25-06-2022.lcb
Report File Name	: Default.lcr

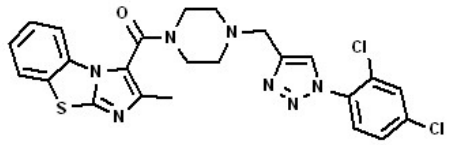

<Chromatogram>

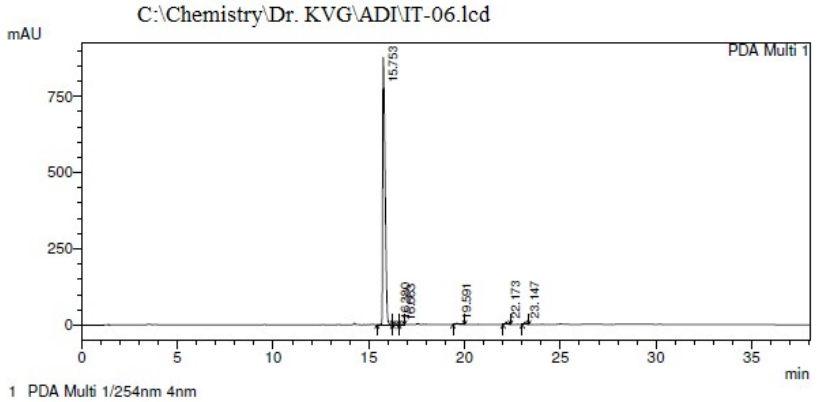

1 PDA Multi 1/254nm 4nm

PeakTable

PDA Ch1 254nm 4nm

Peak#	Ret. Time	Area	Height	Area %	Height %
1	15.753	7488139	876695	97.662	96.776
2	16.380	42579	6878	0.555	0.759
3	16.663	13206	1928	0.172	0.213
4	19.591	34343	5038	0.448	0.556
5	22.173	45768	8022	0.597	0.886
6	23.147	43361	7345	0.566	0.811
Total		7667396	905906	100.000	100.000

HPLC of IT06

==== Shimadzu LCsolution Analysis Report ====

C:\Chemistry\Dr. KVG\ADI\IT-08.lcd

Acquired by	: Admin
Sample Name	: IT-08.
Tray#	: 1
Vail #	: 96
Injection Volume	: 5 uL
Data File Name	: IT-08.lcd
Method File Name	: ANVS-MB-Assay-RS.lcm
Batch File Name	: 24-06-2022.lcb
Report File Name	: Default.lcr

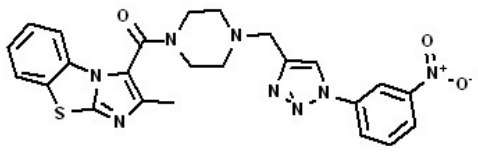

<Chromatogram>

C:\Chemistry\Dr. KVG\ADI\IT-08.lcd

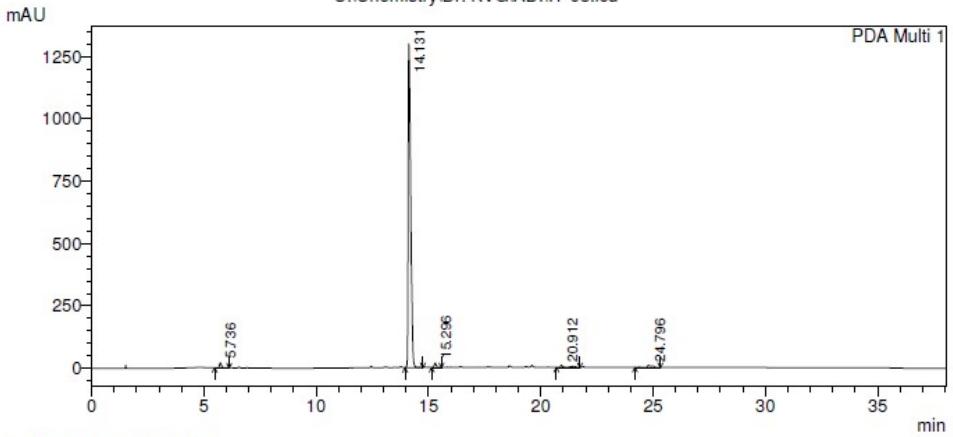

1 PDA Multi 1/254nm 4nm

PeakTable

PDA Ch1 254nm 4nm

Peak#	Ret. Time	Area	Height	Area %	Height %
1	5.736	123228	19759	1.174	1.459
2	14.131	9966168	1298582	94.966	95.910
3	15.296	110694	18025	1.055	1.331
4	20.912	145287	9130	1.384	0.674
5	24.796	149107	8464	1.421	0.625
Total		10494484	1353960	100.000	100.000

HPLC of IT08

==== Shimadzu LCsolution Analysis Report ====

C:\Chemistry\Dr. KVG\ IT-09.lcd

Acquired by	: Admin
Sample Name	: IT-09
Tray#	: 1
Vail #	: 100
Injection Volume	: 5 uL
Data File Name	: IT-09
Method File Name	: ANVS-MB-Assay-RS.lcm
Batch File Name	: 25-06-2022.lcb
Report File Name	: Default.lcr

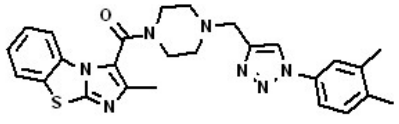

<Chromatogram>

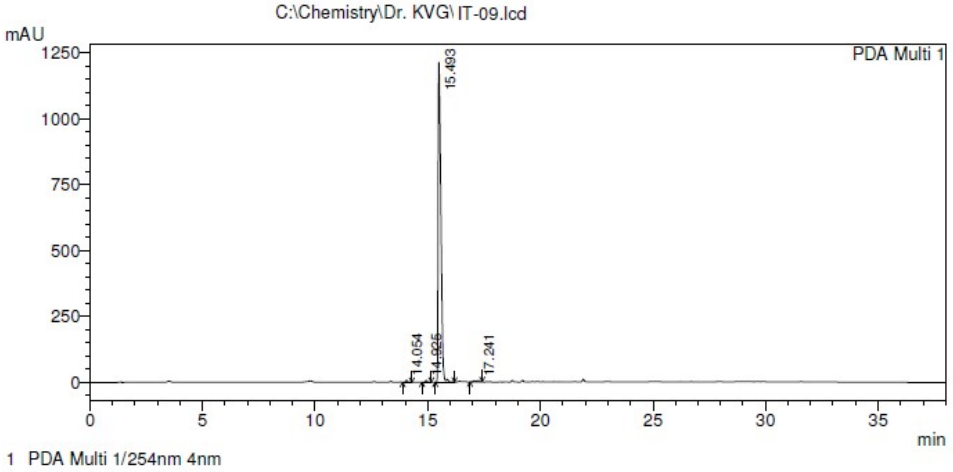

1 PDA Multi 1/254nm 4nm

PeakTable

PDA Ch1 254nm 4nm

Peak#	Ret. Time	Area	Height	Area %	Height %
1	14.054	45563	8146	0.437	0.662
2	14.925	34789	7044	0.333	0.572
3	15.493	10299792	1211463	98.718	98.391
4	17.241	53400	4622	0.512	0.375
Total		10433544	1231275	100.000	100.000

HPLC of IT09

==== Shimadzu LCsolution Analysis Report ====

C:\Chemistry\Dr. KVG\27-06-2022\IT-10.lcd

Acquired by	: Admin
Sample Name	: IT-10
Tray#	: 1
Vail #	: 97
Injection Volume	: 5 uL
Data File Name	: IT-10.lcd
Method File Name	: ANVS-MB-Assay-RS.lcm
Batch File Name	: 27-06-2022.lcb
Report File Name	: Default.lcr

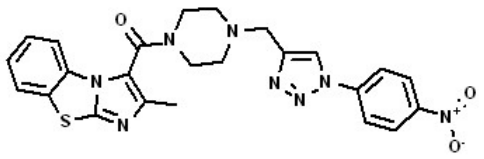

<Chromatogram>

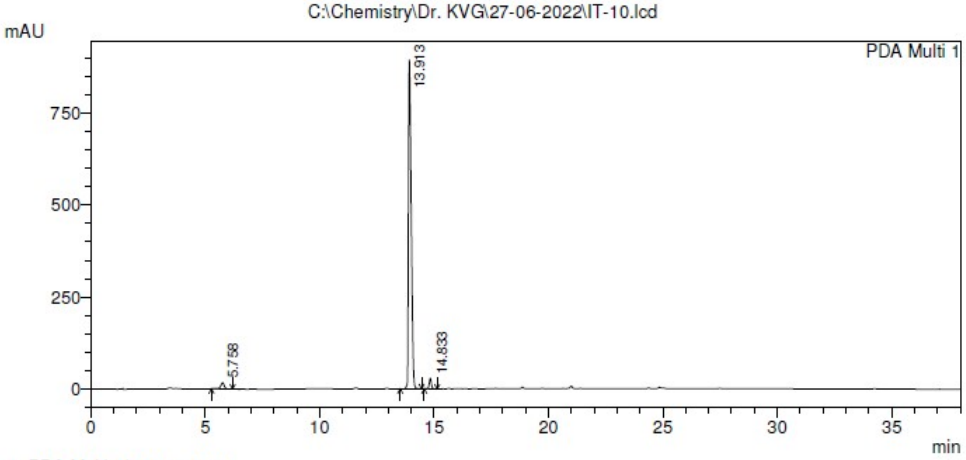

1 PDA Multi 1/254nm 4nm

PeakTable

PDA Ch1 254nm 4nm

Peak#	Ret. Time	Area	Height	Area %	Height %
1	5.758	185289	16790	2.308	1.787
2	13.913	7659112	894178	95.420	95.150
3	14.833	182344	28790	2.272	3.064
Total		8026744	939758	100.000	100.000

HPLC of IT10

==== Shimadzu LCsolution Analysis Report ====

C:\Chemistry\Dr. KVG\IT-12.lcd

Acquired by	: Admin
Sample Name	: IT-12
Tray#	: 1
Vail #	: 101
Injection Volume	: 5 uL
Data File Name	: IT-12
Method File Name	: ANVS-MB-Assay-RS.lcm
Batch File Name	: 25-06-2022.lcb
Report File Name	: Default.lcr

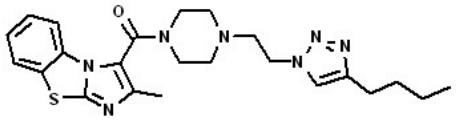

<Chromatogram>

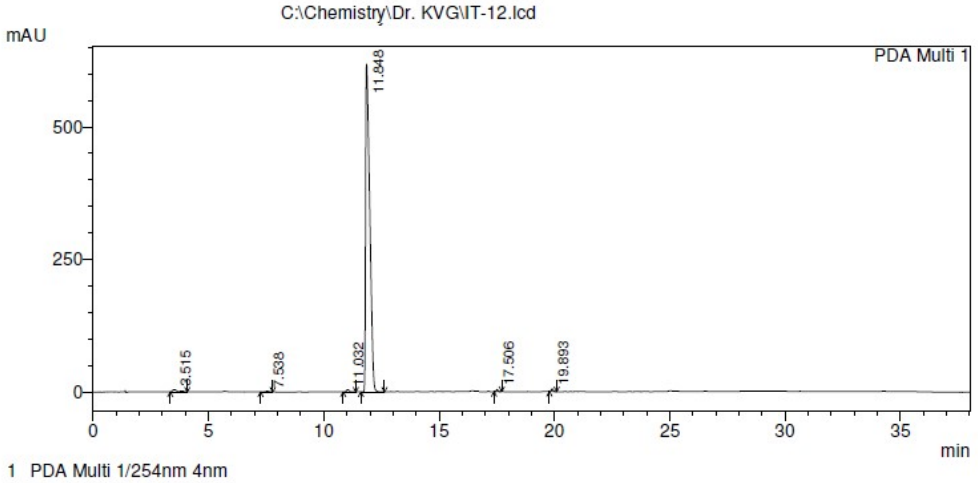

1 PDA Multi 1/254nm 4nm

PeakTable

PDA Ch1 254nm 4nm

Peak#	Ret. Time	Area	Height	Area %	Height %
1	3.515	77200	4215	0.970	0.662
2	7.538	20856	1348	0.262	0.212
3	11.032	37844	4200	0.476	0.660
4	11.848	7774317	617958	97.719	97.040
5	17.506	18597	3913	0.234	0.614
6	19.893	26948	5172	0.339	0.812
Total		7955761	636806	100.000	100.000

HPLC of IT12

==== Shimadzu LCsolution Analysis Report ====

C:\Chemistry\Dr. KVG\24-06-2022\IT-15.lcd

Acquired by	: Admin
Sample Name	: IT-15
Tray#	: 1
Vail #	: 94
Injection Volume	: 5 uL
Data File Name	: IT-15.lcd
Method File Name	: ANVS-MB-Assay-RS.lcm
Batch File Name	: 24-06-2022.lcb
Report File Name	: Default.lcr

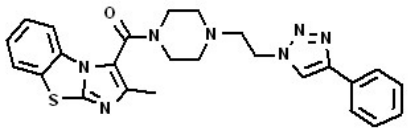

<Chromatogram>

C:\Chemistry\Dr. KVG\24-06-2022\IT-15.lcd

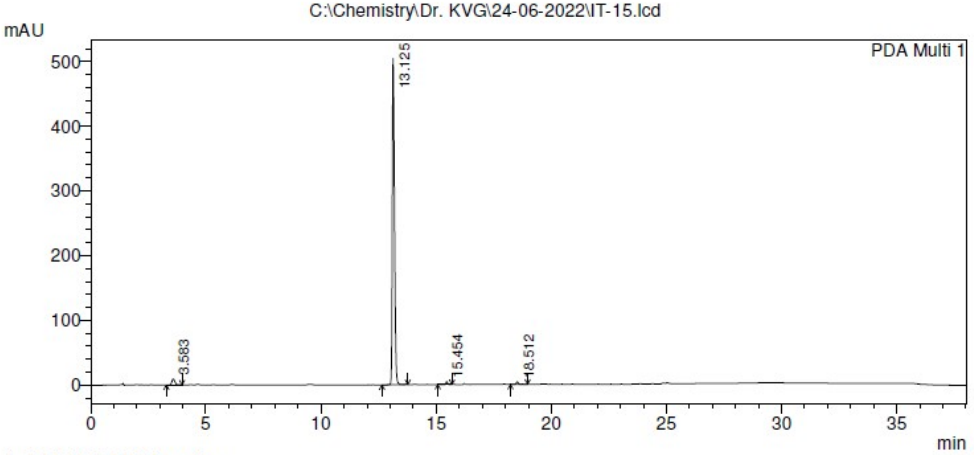

1 PDA Multi 1/254nm 4nm

PeakTable

PDA Ch1 254nm 4nm

Peak#	Ret. Time	Area	Height	Area %	Height %
1	3.583	82701	9228	2.372	1.767
2	13.125	3359097	504538	96.338	96.596
3	15.454	18539	4663	0.532	0.893
4	18.512	26442	3890	0.758	0.745
Total		3486780	522319	100.000	100.000

HPLC of IT15

==== Shimadzu LCsolution Analysis Report ====

C:\Chemistry\Dr. KVG\IT-17.lcd

Acquired by	: Admin
Sample Name	: IT-17
Tray#	: 1
Vail #	: 98
Injection Volume	: 5 uL
Data File Name	: IT-17
Method File Name	: ANVS-MB-Assay.RS-20.lcm
Batch File Name	: 25-06-2022.lcb
Report File Name	: Default.lcr

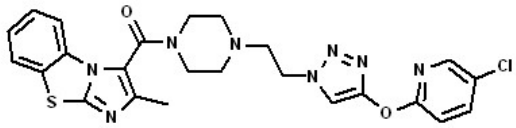

<Chromatogram>

C:\Chemistry\Dr. KVG\IT-17.lcd

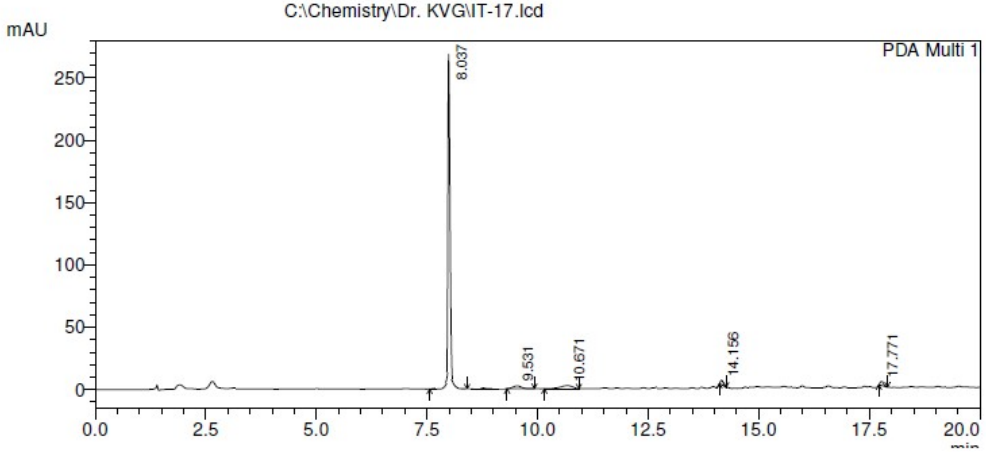

1 PDA Multi 1/254nm 4nm

PeakTable

PDA Ch1 254nm 4nm

Peak#	Ret. Time	Area	Height	Area %	Height %
1	8.037	5729115	264955	98.096	95.712
2	9.531	30302	2252	0.519	0.814
3	10.671	49026	2531	0.839	0.914
4	14.156	15212	3716	0.260	1.342
5	17.771	16673	3371	0.285	1.218
Total		5840329	276825	100.000	100.000

HPLC of IT17

==== Shimadzu LCsolution Analysis Report ====

C:\Chemistry\Dr. KVG\IT-18.lcd

Acquired by	: Admin
Sample Name	: IT-18
Tray#	: 1
Vail #	: 102
Injection Volume	: 5 uL
Data File Name	: IT-18
Method File Name	: ANVS-MB-Assay.RS-14.lcm
Batch File Name	: 25-06-2022.lcb
Report File Name	: Default.lcr

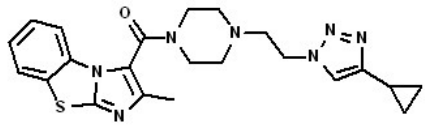

<Chromatogram>

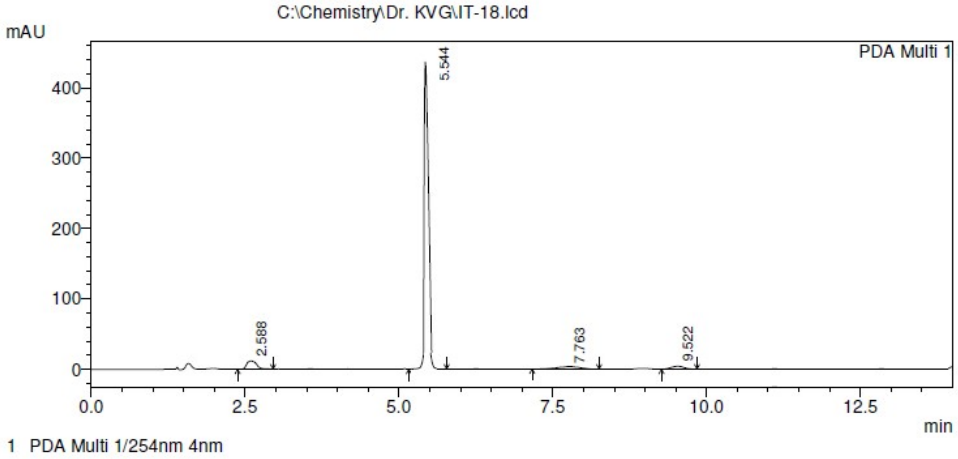

1 PDA Multi 1/254nm 4nm

PeakTable

PDA Ch1 254nm 4nm

Peak#	Ret. Time	Area	Height	Area %	Height %
1	2.588	130341	11524	1.642	2.510
2	5.544	7662715	440038	96.543	95.833
3	7.763	86077	3429	1.084	0.747
4	9.522	57982	4182	0.731	0.911
Total		7937116	459173	100.000	100.000

HPLC of IT18

References:

[1] D. Lagorce, L. Bouslama, J. Becot, M.A. Miteva, B.O. Villoutreix, FAF-Drugs4: Free ADME-tox filtering computations for chemical biology and early stages drug discovery Bioinformatics. 33 (2017) 3658–3660. https://doi.org/10.1093/bioinformatics/btx491.

[2] A. Daina, O. Michielin, V. Zoete, SwissADME: A free web tool to evaluate pharmacokinetics, drug-likeness and medicinal chemistry friendliness of small molecules Sci. Rep. 7 (2017) 1–13. https://doi.org/10.1038/srep42717.

[3] Schrödinger Release 2019-1: Maestro, Schrödinger, LLC, New York, NY, 2019, n.d.

[4] S.K. Burley, H.M. Berman, C. Bhikadiya, C. Bi, L. Chen, L. Di Costanzo, C. Christie, K. Dalenberg, J.M. Duarte, S. Dutta, Z. Feng, S. Ghosh, D.S. Goodsell, R.K. Green, V. Guranović, D. Guzenko, B.P. Hudson, T. Kalro, Y. Liang, R. Lowe, H. Namkoong, E. Peisach, I. Periskova, A. Prlić, C. Randle, A. Rose, P. Rose, R. Sala, M. Sekharan, C. Shao, L. Tan, Y.-P. Tao, Y. Valasatava, M. Voigt, J. Westbrook, J. Woo, H. Yang, J. Young, M. Zhuravleva, C. Zardecki, RCSB Protein Data Bank: biological macromolecular structures enabling research and education in fundamental biology, biomedicine, biotechnology and energy, Nucleic Acids Res. 47 (2019) D464–D474. https://doi.org/10.1093/nar/gky1004.

[5] A.W. Hung, H.L. Silvestre, S. Wen, A. Ciulli, T.L. Blundell, C. Abell, Application of Fragment Growing and Fragment Linking to the Discovery of Inhibitors of Mycobacterium tuberculosis Pantothenate Synthetase, Angew. Chemie Int. Ed. 48 (2009) 8452–8456. https://doi.org/10.1002/anie.200903821.

[6] Schrödinger Release 2020-4: Desmond Molecular Dynamics System, D. E. Shaw Research, New York, NY, 2020. Maestro-Desmond Interoperability Tools, Schrödinger, New York, NY, 2020., n.d.

[7] Schrödinger Release 2019-1: LigPrep, Schrödinger, LLC, New York, NY, 2019., (n.d.).

[8] Schrödinger Release 2019-1: Schrödinger Suite 2019-1 Protein Preparation Wizard; Epik, Schrödinger, LLC, New York, NY, 2019., (n.d.).

[9] P. Mark, L. Nilsson, Structure and dynamics of the TIP3P, SPC, and SPC/E water models at 298 K, J. Phys. Chem. A. 105 (2001) 9954–9960. https://doi.org/10.1021/jp003020w.

[10] W.L. Jorgensen, D.S. Maxwell, J. Tirado-Rives, Development and Testing of the OPLS All-Atom Force Field on Conformational Energetics and Properties of Organic Liquids, J. Am. Chem. Soc. 118 (1996) 11225–11236. https://doi.org/10.1021/ja9621760.

[11] M.T. and B.J.G.J.M. Berne, Reversible multiple time scale molecular dynamics, J. Phys. Chem. 97 (1993) 13429–13434. https://doi.org/10.1021/j100153a002.

[12] A. Cheng, K.M. Merz, Application of the Nosé−Hoover Chain Algorithm to the Study of Protein Dynamics, J. Phys. Chem. 100 (1996) 1927–1937. https://doi.org/10.1021/jp951968y.

[13] G. Kalibaeva, M. Ferrario, G. Ciccotti, Constant pressure-constant temperature molecular dynamics: A correct constrained NPT ensemble using the molecular virial, Mol. Phys. 101 (2003) 765–778. https://doi.org/10.1080/0026897021000044025.

[14] B.K. Kumar, Faheem, K.V.G.C. Sekhar, R. Ojha, V.K. Prajapati, A. Pai, S. Murugesan, Pharmacophore based virtual screening, molecular docking, molecular dynamics and MM-GBSA approach for identification of prospective SARS-CoV-2 inhibitor from natural product databases, J. Biomol. Struct. Dyn. 0 (2020) 1–24. https://doi.org/10.1080/07391102.2020.1824814.

[15] B. Karan Kumar, Faheem, R. Balana Fouce, E. Melcon-Fernandez, Y. Perez-Pertejo Yolanda, R.M. Reguera, N. Adinarayana, K.V.G. Chandra Sekhar, S. Vanaparthi, S. Murugesan, Design, synthesis and evaluation of novel β-carboline ester analogues as potential anti-leishmanial agents, J. Biomol. Struct. Dyn. 0 (2021) 1–16. https://doi.org/10.1080/07391102.2021.1973564.

[16] D. Cappoen, D. Forge, F. Vercammen, V. Mathys, M. Kiass, V. Roupie, R. Anthonissen, L. Verschaeve, J.J. Vanden Eynde, K. Huygen, Biological evaluation of bisbenzaldehydes against four Mycobacterium species, Eur. J. Med. Chem. 63 (2013) 731–738. https://doi.org/10.1016/j.ejmech.2013.03.023.

[17] E. Torfs, J. Vajs, M.B. de Macedo, F. Cools, B. Vanhoutte, Y. Gorbanev, A. Bogaerts, L. Verschaeve, G. Caljon, L. Maes, P. Delputte, P. Cos, J. Košmrlj, D. Cappoen, Synthesis and in vitro investigation of halogenated 1,3-bis(4-nitrophenyl)triazenide salts as antitubercular compounds, Chem. Biol. Drug Des. 91 (2018) 631–640. https://doi.org/10.1111/cbdd.13087.